Universiteit Utrecht

Graduate School of Natural Sciences

The fractional Langevin equation

Master Thesis

Robin C. Verstraten

Theoretical Physics & Mathematical Sciences

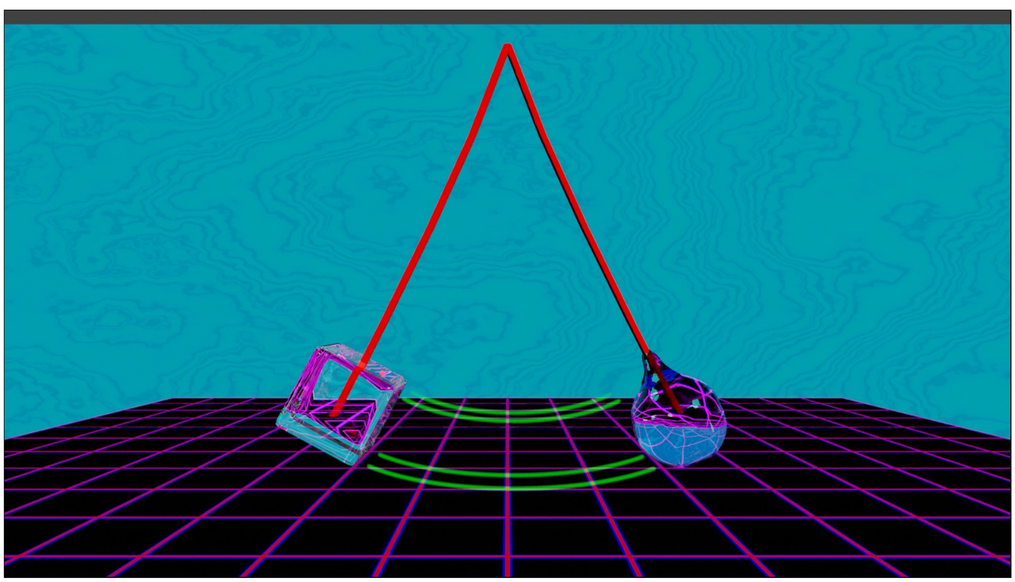

Supervisors:

Prof. Dr. Cristiane de Morais Smith, ITP Utrecht;

Dr. Paul A. Zegeling, UU Mathematics Dep;

Msc. Rodrigo F. Ozela, ITP Utrecht.

13th July 2020

Abstract

We begin with an overview of fractional derivatives, which have many different definitions, not all of which are equivalent. For some of the most commonly used definitions, we present a few properties and techniques for solving fractional differential equations. Furthermore, we show some of the key differences when solving identical equations using a different definition. There are already applications of fractional derivatives, but each application requires a critical assessment for which definition is most suitable. We show a new application of fractional derivatives in the field of glasses, making use of Caputo fractional derivatives. An analytical solution of the fractional Langevin equation is obtained, where the first-order friction term is replaced by a Caputo fractional derivative of order s. Then, we show that for $0 < s < 0.1$, the ground state of the fractional Langevin solutions exhibits emergent periodic glassy behaviour, thus characterising the recently conjectured time glass. Finally, we present a semi-classical microscopic model, which, in the low-temperature limit, is effectively described by the fractional Langevin equation, thus establishing the link between sub-ohmic open systems and fractional derivative equations.

Acknowledgements

I would like to thank my supervisors Prof. Dr. Cristiane Morais Smith and Dr. Paul Zegeling for all their support. They asked the critical questions and inspired me to dive into this thesis and make it my own. I also want to thank Rodrigo Ozela for always being there for me whenever I needed help or improvements. In particular I would like to thank Cristiane and Ozela for the support and work they have done to make our paper about time glass. I have leaned more than I would have ever imagined, being pushed into unknown territory (Ozela when Cristiane suggested me as a speaker for the WQC seminar: “She has just thrown you into fire”) and helping me improve my first attempts, always motivating to push further even after the setbacks. I would also like to thank Cristiane for the countless video talks that she organised with other experts in the field, including Nobel laureate Frank Wilczek, who conjectured time glasses and said he would be honoured if we called our material a time glass. I have leaned so much from you all!

I would also like to thank my fellow master students, particularly those in the master room as long as it lasted. Unfortunately we would not finish our theses together due to the corona-virus outbreak, but they were a tremendous motivator to manage hard work and a healthy amount of breaks. Fortunately, the cats from home were keen to take over this support, and friends still kept in touch thanks to the internet. My best friends even visited several times, keeping a safe distance and providing a healthy dose of sanity in these crazy times. I also want to thank my fellow student and good friend Kevin for being so kind to proofread my thesis and listening to all my messages.

Last but not least, I am grateful to my parents — my dad from Germany and my mom at home. Without you I would not have made it to university, you really gave it your all and we got there despite everyone’s doubt. All the way from primary- to high-school, you helped me to overcome my weaknesses and have allowed my strengths to shine. From the bottom of my heart, thank you.

Contents

Introduction

After Newton's *Principia Mathematica* (1687) and the simultaneous work of Leibniz [1], laying the foundations of the modern Calculus, Leibniz first proposed the idea of fractional calculus in a letter to l'Hôpital in 1695 [2]. As natural as it sounded, they did not manage to give a mathematical foundation. Euler only came so far as introducing the Gamma function in 1738 [3], and only in 1822 came the first mathematical proposal by Fourier [4], after which Liouville laid the proper foundations in 1832 [5][1]. In 1847, Riemann managed to encapsulate Liouville's results into a new formulation using ordinary integrals [8]. Finally, Grünwald understood the deep relation to integrals only in 1867, 172 years after Leibniz's first proposal [9]. Another century passed before Caputo found new applications using his newly found definition in 1969 [10]. From here, many more mathematicians picked up interest in the topic, and more and more applications are still being found today [11–14].

An even older problem is the theoretical description of glasses. Though glasses have been used for many centuries, the microscopic states have been puzzling researchers in condensed matter physics ever since [15]. Under the microscope, researchers have great difficulty to distinguish a glass from a liquid because the atoms show a random structure [16]. As we can simply see with the eye that glass is much more solid than liquid like, we therefore need a theory which is microscopically liquid based, yet provides an overall solid structure. One of these theories uses many hard spheres [17]: At low density, spheres are free to move around as Brownian motion and thus form a liquid. However, at high density, the in principle free to move spheres are prohibited from moving past its neighbours as there is no space left between them, thus effectively caging all spheres in their place. More recently, the Gardner phase [18] was found to occur in this hard sphere model when the density is increased even further [19]. In doing so, the spheres show collective behaviour where a sphere is not only moving inside its own cage, but the cage of neighbouring spheres begins to move as a collective particle inside an even larger cage of neighbours. This caging has been shown to occur in a fractal manner [20], which is a key property of the Gardner phase.

Another recent example of such collective behaviour has been found in the so called time crystal. This is a phase in which the ground state shows an emergent periodicity in time, similar to how an ordinary crystal shows emergent periodicity in space. These phases do require some sort of external energy in the form of either a thermal bath or a driving force, as eternal movement without energy is still impossible. These time crystals were first conjectured by Wilczek [21], and have already been observed [22] and with this success Wilczek [23] also proposed several other types of time materials, including time glass.

In this thesis, we aim to provide a comprehensive introduction to fractional calculus, including many comparisons between (and properties of) some of the most commonly used definitions. After a summary for physicists, we show some of the key solving methods and differences in solutions when choosing a particular definition for an application. After a short introduction to Brownian motion, glasses, time crystals, and an extensive introduction to the Caldeira-Leggett model, we show a new application in the field of glasses with the emergence of a time glass from the fractional Langevin equation with white noise, including a generalisation of the Caldeira-Leggett model to show the connection of a two-level systems bath to the fractional Langevin equation. We finish with an overview of several existing applications in physics, which can all be described by a single general equation, which we call the fractional-kinetics Langevin equation.

[1] Only recently [6], it was understood that Abel was actually already working on Caputo derivatives and Riemann-Liouville integrals in his first paper in 1823 [7], where he showed these two operators are inverses of each other. However, he (and his then small audience) did not realise that he was working with fractional derivatives.

1 An overview of fractional derivatives

There are many definitions of fractional derivatives [24]. This occurs because it is an extension of classical derivatives with not enough constraints to only have one logical definition. Some of them are equivalent, but some are not. In this chapter, we will give an overview of the most commonly used definitions of fractional derivatives, their properties, which are equivalent and which are not, and consider which definitions are the most physical and what applications they are most suited for. Definitions are based on Hilfer et al. [2] and Podlubny [25], although there are many other good sources such as Refs. [13, 14, 26–30].

1.1 Mathematical tools

We start with some tools that will be used for defining fractional derivatives.

Definition 1.1.1. The *(Euler-)Gamma function* is defined as $\Gamma(z) = \int_0^\infty e^{-t}t^{z-1}\,dt$ with $Re(z) > 0$.

In fact, one can even enter complex numbers as seen in Figure 1, and with an analytical extension the Gamma function can be defined as a meromorphic function on the complex plane. The poles of this function lie at $z = 0, -1, -2, \ldots$.

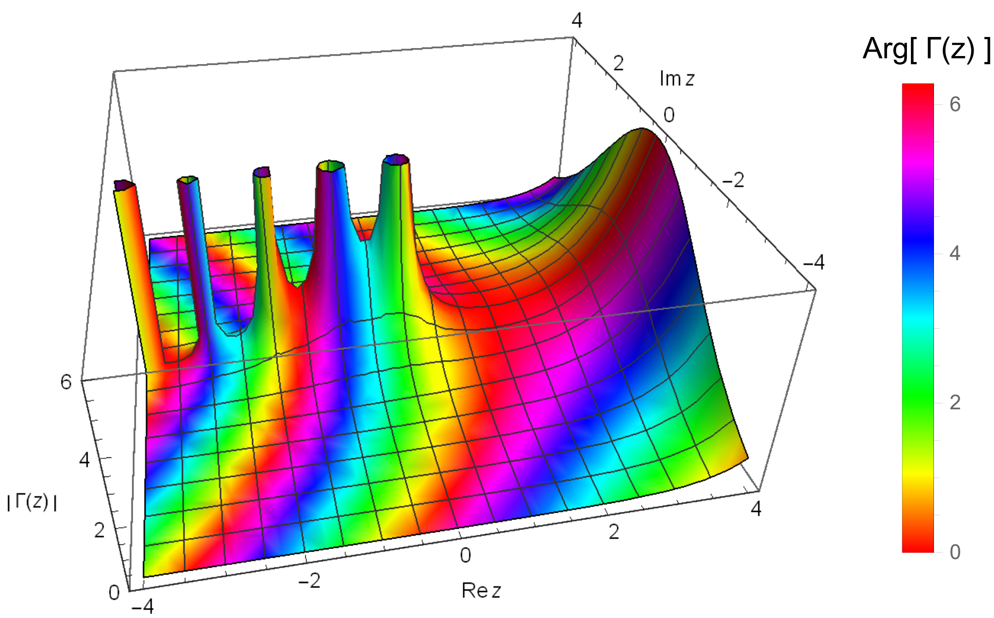

Figure 1: A plot of $\Gamma(z)$ in the complex plane, where the colour indicates the complex phase $\arg[\Gamma(z)]$.

Lemma 1.1.2. *The Gamma function satisfies* $\Gamma(z+1) = z\Gamma(z)$.

Proof. Integration by parts gives

$$\Gamma(z+1) = \int_0^\infty e^{-t}t^z\,dt = [-e^{-t}t^z]_{t=0}^{t=\infty} + z\int_0^\infty e^{-t}t^{z-1}\,dt = z\Gamma(z).$$

□

Since $\Gamma(1) = \int_0^\infty e^{-t}\, dt = [-e^{-t}]_{t=0}^{t=\infty} = 1$, A simple consequence of this Lemma is that for $n \in \mathbb{N}$

$$\Gamma(n+1) = n!$$

Accordingly, the Gamma function is often used as the generalisation of the factorial for integers.

Definition 1.1.3. The *Beta function* is defined by

$$B(z,w) = \int_0^1 \tau^{z-1}(1-\tau)^{w-1}\, d\tau \qquad (Re(z) > 0, \quad Re(w) > 0).$$

The Beta function can also be extended to negative values of z and w, although with many poles, and a plot of this extension is shown in Figure 2.

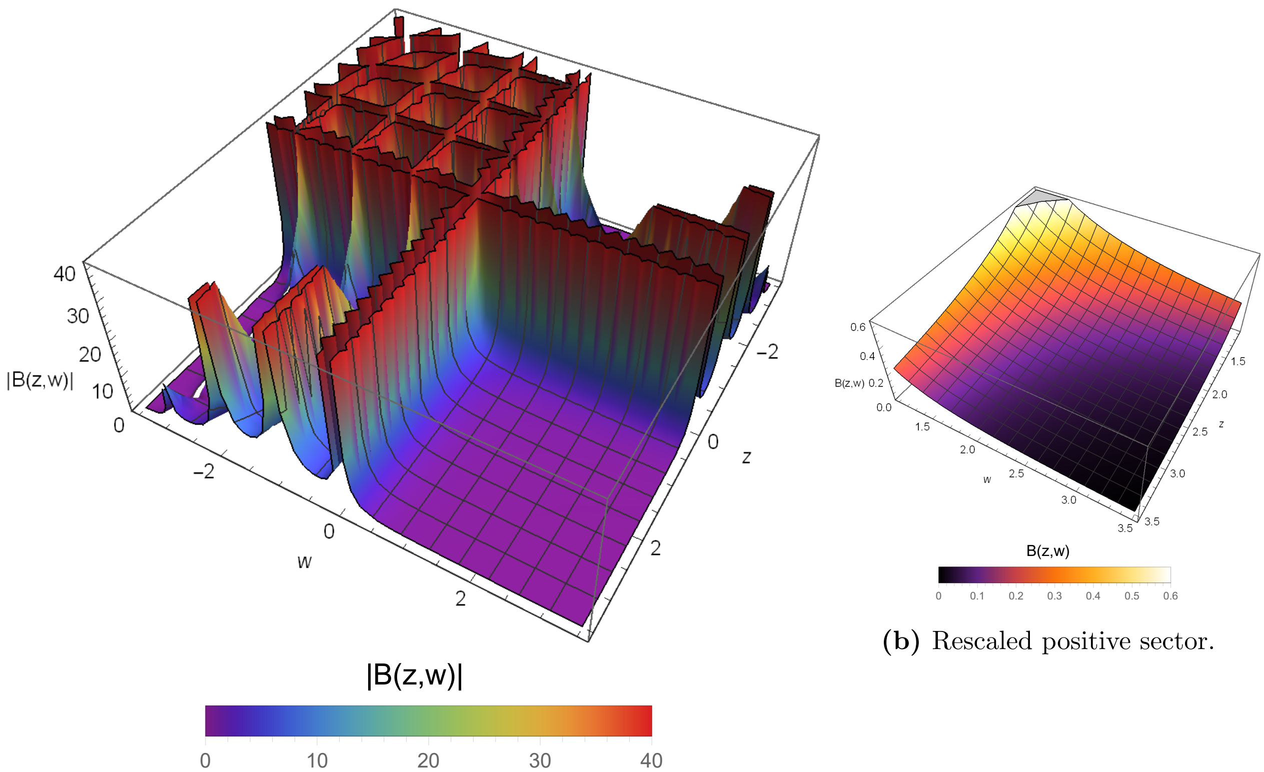

(a) Absolute value of $B(z,w)$, centred at (0,0).

(b) Rescaled positive sector.

Figure 2: A plot of the Beta function extension with colour indicating height. All the poles lie at points where either z or $w \in \{0, -1, -2, ...\}$. Without the absolute value, each alternating valley on the negative side will be positive and negative, similar to the Gamma function for negative real values.

The Beta function is defined to have a related structure to the Gamma function and, from this structure, we can derive the following Lemma.

Lemma 1.1.4. *For $Re(z) > 0$ and $Re(w) > 0$, the following property holds:*

$$B(z,w) = \frac{\Gamma(z)\Gamma(w)}{\Gamma(z+w)}.$$

Proof. We make a change of basis in the double integral $\Gamma(z)\Gamma(w) = \int_0^\infty \int_0^\infty e^{-(t+s)} t^{z-1} s^{w-1}\, dt\, ds$. Set $t = xy$ and $s = x(1-y)$, then the boundary conditions become $0 < x < \infty$ and $0 < y < 1$. The Jacobian of this transformation is $J = \det \begin{vmatrix} y & x \\ 1-y & -x \end{vmatrix} = -xy - x + xy = -x$, or $|J| = x$, which gives

$$\begin{aligned}\Gamma(z)\Gamma(w) &= \int_0^1 \int_0^\infty e^{-x}(xy)^{z-1}[x(1-y)]^{w-1} x\, dx\, dy \\ &= \int_0^\infty e^{-x} x^{z+w-1}\, dx \int_0^1 y^{z-1}(1-y)^{w-1}\, dy \\ &= \Gamma(z+w)B(z,w).\end{aligned}$$

□

This Lemma also implies that $B(w,z) = B(z,w)$. Although the above calculation is only valid for positive values of z and w, we can still use it to interpret the many poles in Figure 2. As the formula with Gamma functions suggests that we would have poles whenever z or w is a negative integer.

Another important function in classical derivatives is the exponential function $e^x = \sum_{k=o}^\infty \frac{x^k}{k!}$. A generalisation to a similar function for fractional derivatives is the following.

Definition 1.1.5. The *one parameter Mittag-Leffler function* is defined by

$$E_\alpha(z) = \sum_{k=0}^\infty \frac{z^k}{\Gamma(\alpha k + 1)}.$$

The two parameter Mittag-Leffler function is defined by

$$E_{\alpha,\beta}(z) = \sum_{k=0}^\infty \frac{z^k}{\Gamma(\alpha k + \beta)}.$$

Observe that $E_\alpha(z) = E_{\alpha,1}(z)$ and that $E_1(z) = E_{1,1}(z) = e^z$. Some examples of Mittag-Leffler functions for different values of α and β have been plot in Figure 3. Notice that $E_{\alpha,\beta}(0) = \frac{1}{\Gamma(\beta)}$ and how $E_2(t)$ shows oscillating behaviour for negative t.

Another important result for us is the Leibniz integral rule:

Theorem 1.1.6. *(Leibniz integral rule, [31]) The derivative of an integral with variables in both the integral and in the boundary terms is given by:*

$$\frac{d}{dx}\left(\int_{a(x)}^{b(x)} f(x,t)dt\right) = f(x,b(x)) \cdot \frac{d}{dx}b(x) - f(x,a(x)) \cdot \frac{d}{dx}a(x) + \int_{a(x)}^{b(x)} \frac{\partial}{\partial x} f(x,t)dt. \quad (1.1)$$

1.1.1 Fourier transforms

Often used in physics, the Fourier transform is a useful concept in analysing functions. Also for Partial Differential Equations (PDE's), Fourier transforms can play an important role in constructing solutions. A natural question to ask then, is how Fourier transforms interact with (fractional)

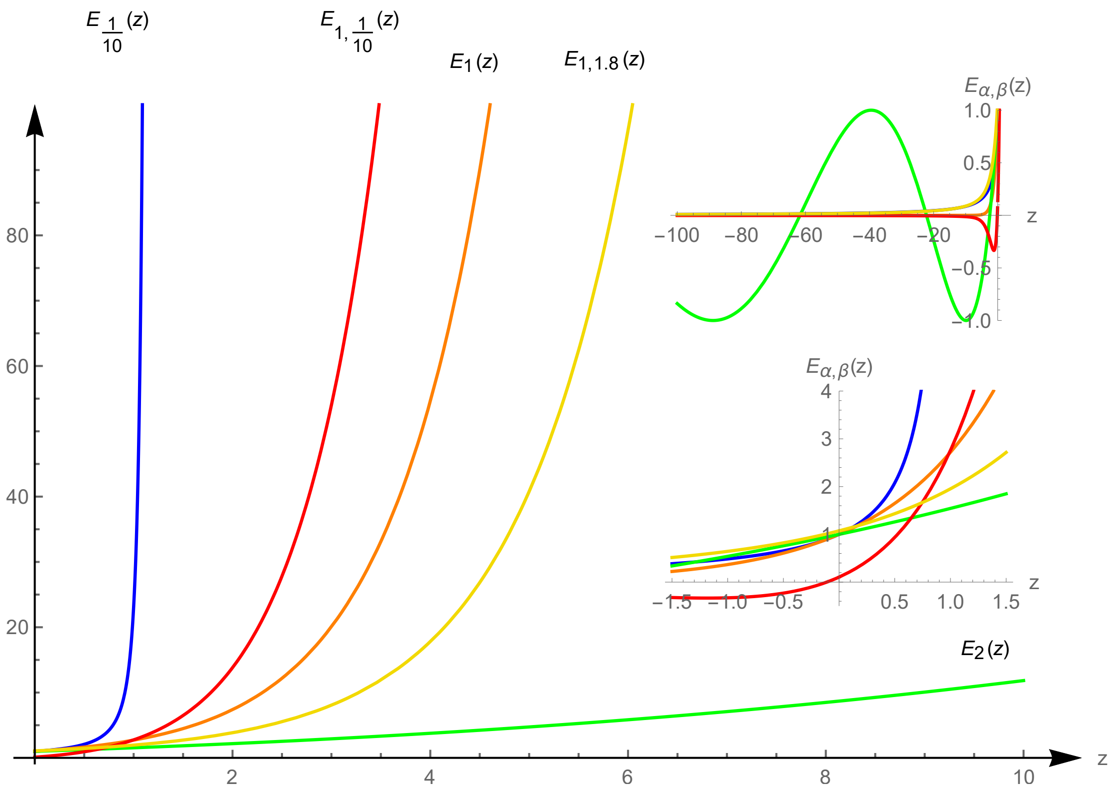

Figure 3: A plot of some Mittag-Leffler functions of different parameters and in different regions. Upper inset: A zoom-in of the negative z values, some values show oscillations. Lower inset: A zoom-in of the region around $z = 0$.

derivatives. For either a periodic function or a function $f(t) \in L^2(\mathbb{R})$, where

$$L^2(\mathbb{R}) = \left\{ f(x) \mid \left(\int_{-\infty}^{\infty} |f(x)|^2 \, dx \right)^{1/2} < \infty \right\},$$

we define the Fourier transform[2] as

$$f(\omega) = \frac{1}{2\pi} \int_{-\infty}^{\infty} f(t) e^{-i\omega t} \, dt. \tag{1.2}$$

Its inverse Fourier transform is then defined as

$$f(t) = \int_{-\infty}^{\infty} f(\omega) e^{i\omega t} \, d\omega. \tag{1.3}$$

[2]There are several conventions, but for our purposes, of combining derivatives with Fourier transforms, the one used here will be the most convenient.

Indeed, checking if this is the inverse transform, we find

$$\begin{aligned}\int_{-\infty}^{\infty} f(\omega)e^{i\omega t}\, d\omega &= \frac{1}{2\pi}\int_{-\infty}^{\infty}\int_{-\infty}^{\infty} f(t')e^{-i\omega t'}\, dt' e^{i\omega t}\, d\omega \\ &= \frac{1}{2\pi}\int_{-\infty}^{\infty}\int_{-\infty}^{\infty} f(t')e^{i\omega(t-t')}\, dt'\, d\omega \\ &= \int_{-\infty}^{\infty} f(t')\delta(t-t')\, dt' \\ &= f(t),\end{aligned}$$

where we used that

$$\frac{1}{2\pi}\int_{-\infty}^{\infty} e^{i\omega(t-t')}\, d\omega = \delta(t-t'). \tag{1.4}$$

Let us now see how derivatives interact with these Fourier transforms. Let $n \in \mathbb{N}$, then

$$\frac{d^n}{dt^n} f(t) = \frac{d^n}{dt^n}\int_{-\infty}^{\infty} f(\omega)e^{i\omega t}\, d\omega = \int_{-\infty}^{\infty} (i\omega)^n f(\omega)e^{i\omega t}\, d\omega$$

and we find that $f^{(n)}(\omega) = (i\omega)^n f(\omega)$. Since this notation can sometimes be a bit confusing, we will also denote the Fourier transform as $f(\omega) = \mathcal{F}\left(f(t);\omega\right)$ and the inverse Fourier transform as $f(t) = \mathcal{F}^{-1}\left(f(\omega);t\right)$. In this notation, we see that

$$\mathcal{F}\left(\frac{d^n}{dt^n} f(t);\omega\right) = (i\omega)^n \mathcal{F}\left(f(t);\omega\right). \tag{1.5}$$

We can also do the above for an n-fold integral $\int_a^t \int_a^{t_1} \dots \int_a^{t_{n-1}} f(t_n)\, dt_n \dots dt_2\, dt_1$, and it is quickly seen that this gives

$$\mathcal{F}\left(\int_a^t \int_a^{t_1} \dots \int_a^{t_{n-1}} f(t_n)\, dt_n \dots dt_2\, dt_1;\omega\right) = (i\omega)^{-n} \mathcal{F}\left(f(t);\omega\right). \tag{1.6}$$

1.1.2 Laplace transforms

Definition 1.1.7. The *Laplace transform* of a function $f(t)$ defined on $[0,\infty)$, denoted by either $F(s)$ or $\mathcal{L}\left(f(t);s\right)$, with $s \in \mathbb{C}$, is given by

$$F(s) = \mathcal{L}\left(f(t);s\right) = \int_0^{\infty} f(t)e^{-st}\, dt$$

And the *inverse Laplace transform* is given by

$$f(t) = \mathcal{L}^{-1}\left(F(s);t\right) = \int_{c-i\infty}^{c+i\infty} F(s)e^{st}\, ds,$$

where $c \in \mathbb{R}$ is chosen such that all singularities of $F(s)$ lie to the left of the line $Re(s) = c$.

Example 1.1.8. Let $f(t) = t^a$ for some $a \in \mathbb{R}$, then

$$\mathcal{L}\left(t^a;s\right) = \int_0^{\infty} t^a e^{-st}\, dt = s^{-(a+1)}\int_0^{\infty} t^a e^{-t}\, dt = s^{-(a+1)}\Gamma(a+1).$$

$\triangle$

The Laplace transformation is one-to-one if $f(t)$ is continuous. As already mentioned, there may be values of s for which $F(s)$ has a singularity, i.e. the integral is not convergent, but these are, in fact, the most important points for the inverse transform. The inverse transform can be tricky to work with. However, one can often use a few basic transformation tables to see what it should be thanks to many properties of the Laplace transform.

Definition 1.1.9. A *convolution* of two functions f and g is given by

$$f(t) * g(t) = \int_0^t f(t-\tau)g(\tau)\, d\tau.$$

Lemma 1.1.10. *Let f and g be two functions and suppose $F(s)$ and $G(s)$ both exist, then*

$$\mathcal{L}\left(f(t) * g(t); s\right) = F(s)G(s). \tag{1.7}$$

Proof. A direct calculation of Equation (1.7) gives

$$\begin{aligned}
\mathcal{L}\left(f(t) * g(t); s\right) &= \int_0^\infty f(t) * g(t) e^{-st}\, dt \\
&= \int_0^\infty \int_0^t f(t-\tau)g(\tau)e^{-st}\, d\tau\, dt \\
&= \int_0^\infty \int_\tau^\infty f(t-\tau)g(\tau)e^{-st}\, dt\, d\tau \\
[\text{set } t = \xi + \tau] \quad &= \int_0^\infty \int_0^\infty f(\xi)g(\tau)e^{-s(\xi+\tau)}\, d\xi\, d\tau \\
&= \int_0^\infty f(\xi)e^{-s\xi}\, d\xi \int_0^\infty g(\tau)e^{-s\tau}\, d\tau \\
&= F(s)G(s).
\end{aligned}$$

□

We show some basic and more advanced example transformations.

Example 1.1.11. Let $n \in \mathbb{N}$, then, assuming the integrals exist, repeated integration by parts gives

$$\begin{aligned}
\mathcal{L}\left(\frac{d^n}{dt^n} f(t); s\right) &= \int_0^\infty \frac{d^n f(t)}{dt^n} e^{-st}\, dt \\
&= -f^{(n-1)}(0) + s\int_0^\infty \frac{d^{n-1} f(t)}{dt^{n-1}} e^{-st}\, dt \\
&= -f^{(n-1)}(0) - sf^{(n-2)}(0) + s^2 \int_0^\infty \frac{d^{n-2} f(t)}{dt^{n-2}} e^{-st}\, dt \\
&= \dots \\
&= s^n F(s) - \sum_{k=0}^{n-1} s^{n-1-k} f^{(k)}(0).
\end{aligned}$$

△

Example 1.1.12. Observe that

$$\mathcal{L}\left(-tf(t);s\right) = \int_0^\infty -tf(t)e^{-st}\,dt = \frac{d}{ds}\int_0^\infty f(t)e^{-st}\,dt = \frac{d}{ds}\mathcal{L}\left(f(t);s\right)$$

and that this relation can be generalised to

$$\mathcal{L}\left((-t)^n f(t);s\right) = \frac{d^n}{ds^n}\mathcal{L}\left(f(t);s\right).$$

△

Example 1.1.13. Recall the two parameter Mittag-Leffler function $E_{\alpha,\beta}(t) = \sum_{k=0}^\infty \frac{t^k}{\Gamma(\alpha k+\beta)}$. We can compute its Laplace transform as

$$\begin{aligned}\mathcal{L}\left(E_{\alpha,\beta}(t);s\right) &= \int_0^\infty \sum_{k=0}^\infty \frac{t^k}{\Gamma(\alpha k+\beta)}e^{-st}\,dt = \sum_{k=0}^\infty \frac{1}{\Gamma(\alpha k+\beta)}\int_0^\infty t^k e^{-st}\,dt \\ &= \sum_{k=0}^\infty \frac{(-1)^k}{\Gamma(\alpha k+\beta)}\frac{d^k}{ds^k}\mathcal{L}\left(1;s\right) = \sum_{k=0}^\infty \frac{(-1)^k}{\Gamma(\alpha k+\beta)}\frac{d^k}{ds^k}s^{-1} \\ &= \sum_{k=0}^\infty \frac{\Gamma(k+1)}{\Gamma(\alpha k+\beta)}s^{-k},\end{aligned}$$

where we used that

$$\mathcal{L}\left(1;s\right) = \int_0^\infty e^{-st}\,dt = \left[\frac{-1}{s}e^{-st}\right]_{t=0}^\infty = \frac{1}{s}.$$

△

Example 1.1.14. Following a calculation along the lines of Kisela [32, p.11], it is possible to find a formula whose Laplace transform gives a more general fraction than simply $\frac{1}{s}$. This will be very useful when trying to transform back solutions of fractional differential equations obtained with Laplace transforms. For $m \in \mathbb{N}$ and $-1 < t < 1$, we see that

$$\begin{aligned}\frac{m!}{(1-t)^{m+1}} &= \frac{d^m}{dt^m}\frac{1}{1-t} = \frac{d^m}{dt^m}\sum_{k=0}^\infty t^k = \sum_{k=0}^\infty \frac{d^m}{dt^m}t^k = \sum_{k=m}^\infty \frac{k!}{(k-m)!}t^{k-m} \\ \text{[shift } k\to k+m\text{]} \qquad &= \sum_{k=0}^\infty \frac{(k+m)!}{k!}t^k.\end{aligned}$$

Next, consider the m^{th} integer order derivative of the Mittag-Leffler function:

$$E_{\alpha,\beta}^{(m)}(t) = \frac{d^m}{dt^m}\sum_{k=0}^\infty \frac{t^k}{\Gamma(\alpha k+\beta)} = \sum_{k=m}^\infty \frac{k!\,t^{k-m}}{(k-m)!\,\Gamma(\alpha k+\beta)} = \sum_{k=0}^\infty \frac{(k+m)!}{k!}\frac{t^k}{\Gamma(\alpha k+\alpha m+\beta)}$$

and consider this as an independent function, in the sense that $E_{\alpha,\beta}^{(m)}(f(t)) = E_{\alpha,\beta}^{(m)}(\xi)\Big|_{\xi=f(t)}$, so that we do not get extra terms from the derivative of a composition, such as with $f(g(t))$. Let $\alpha,\beta > 0$,

$a \in \mathbb{R}$, $m \in \mathbb{N}$, and $|a| < Re(s^\alpha)$, then we get the following Laplace transform:

$$\begin{aligned}
\mathcal{L}\left(t^{\alpha m+\beta-1}E^{(m)}_{\alpha,\beta}(at^\alpha); s\right) &= \mathcal{L}\left(t^{\alpha m+\beta-1}\sum_{k=0}^{\infty}\frac{(k+m)!}{k!}\frac{(at^\alpha)^k}{\Gamma(\alpha k+\alpha m+\beta)}; s\right) \\
&= \sum_{k=0}^{\infty}\frac{(k+m)!}{k!}\frac{a^k}{\Gamma(\alpha k+\alpha m+\beta)}\mathcal{L}\left(t^{\alpha m+\beta-1+\alpha k}; s\right) \\
&= \sum_{k=0}^{\infty}\frac{(k+m)!}{k!}\frac{a^k\Gamma(\alpha m+\beta+\alpha k)}{\Gamma(\alpha k+\alpha m+\beta)}s^{-(\alpha m+\beta+\alpha k)} = \sum_{k=0}^{\infty}\frac{(k+m)!}{k!}\frac{a^k}{s^{\alpha m+\beta+\alpha k}} \\
&= s^{-\alpha m-\beta}\sum_{k=0}^{\infty}\frac{(k+m)!}{k!}\left(\frac{a}{s^\alpha}\right)^k = \frac{m!\, s^{-\alpha m-\beta}}{(1-a/s^\alpha)^{m+1}} = \frac{m!\, s^{\alpha-\beta}}{(s^\alpha-a)^{m+1}}.
\end{aligned}$$

Although this is still far from a general fraction, this will often be useful in two-term fractional differential equations. △

1.2 Riemann-Liouville fractional derivative

In order to generalise the order of derivatives and integrals we should first find some structure in ordinary integrals and derivatives. We can then look for places where a generalisation could make sense. We will mostly focus on functions which depend on a time t.

Remark 1.2.1. Let $n \in \mathbb{N}$. Then, taking the n^{th} integral of a function f, we find

$$(I^n_{a+}f)(t) = \int_a^t\int_a^{t_1}\cdots\int_a^{t_{n-1}} f(t_n)\, dt_n \ldots dt_2\, dt_1 = \frac{1}{(n-1)!}\int_a^t (t-\tau)^{n-1}f(\tau)\, d\tau.$$

The subscript $a+$ indicates that the integral has a as its lower limit. This equality may be proven by induction. This formula can be used to define a fractional integral.

Definition 1.2.2. Let $\alpha > 0$. Then, we define the *Riemann-Liouville fractional integral* of order α with lower limit $a < t$ to be

$${}^{RL}_{a+}\mathbf{D}^{-\alpha}_t f(t) = \frac{1}{\Gamma(\alpha)}\int_a^t (t-\tau)^{\alpha-1}f(\tau)\, d\tau$$

and the Riemann-Liouville fractional integral of order α with upper limit $b > t$ to be

$${}^{RL}_{b-}\mathbf{D}^{-\alpha}_t f(t) = \frac{1}{\Gamma(\alpha)}\int_t^b (t-\tau)^{\alpha-1}f(\tau)\, d\tau.$$

Definition 1.2.3. Let $-\infty \le a < t < b \le \infty$. The *Riemann-Liouville fractional derivative* of order $\alpha \ge 0$ is defined to be

$$\begin{aligned}
{}^{RL}_{a+}\mathbf{D}^{\alpha}_t f(t) &= \frac{d^n}{dt^n}\,{}^{RL}_{a+}\mathbf{D}^{\alpha-n}_t f(t) = \frac{d^n}{dt^n}\frac{1}{\Gamma(n-\alpha)}\int_a^t (t-\tau)^{n-\alpha-1}f(\tau)\, d\tau, \\
{}^{RL}_{b-}\mathbf{D}^{\alpha}_t f(t) &= (-1)^n\frac{d^n}{dt^n}\,{}^{RL}_{b-}\mathbf{D}^{\alpha-n}_t f(t) = \frac{d^n}{dt^n}\frac{(-1)^n}{\Gamma(n-\alpha)}\int_t^b (t-\tau)^{n-\alpha-1}f(\tau)\, d\tau,
\end{aligned}$$

where n is an integer such that $n-1 \le \alpha < n$.[3]

[3] For non-integer α, this is just the ceiling, but for integer α we have $n = \alpha + 1$.

Note that $\alpha = 0$ simply gives the identity operator. An equivalent definition would be to let $m \in \mathbb{Z}$ such that $m \leq \alpha < m+1$ and to have

$$
\begin{aligned}
{}^{RL}_{a+}\mathbf{D}^{\alpha}_{t} f(t) &= \frac{d^{m+1}}{dt^{m+1}} {}^{RL}_{a+}\mathbf{D}^{\alpha-m-1}_{t} f(t) = \frac{d^{m+1}}{dt^{m+1}} \frac{1}{\Gamma(m-\alpha+1)} \int_a^t (t-\tau)^{m-\alpha} f(\tau)\, d\tau, \\
{}^{RL}_{b-}\mathbf{D}^{\alpha}_{t} f(t) &= (-1)^{m+1} \frac{d^{m+1}}{dt^{m+1}} {}^{RL}_{b-}\mathbf{D}^{\alpha-m-1}_{t} f(t) = \frac{d^{m+1}}{dt^{m+1}} \frac{(-1)^{m+1}}{\Gamma(m-\alpha+1)} \int_t^b (t-\tau)^{m-\alpha} f(\tau)\, d\tau.
\end{aligned}
$$

What we are doing in this definition comes down to generalising integrals, and then defining the fractional derivatives by integrating the smallest amount such that we are an integer amount of n integrals away from the α^{th} derivative and then applying n derivatives to get to the correct order α.

Remark 1.2.4. There are many notations used for fractional derivatives. We will mostly follow the notation of Podlubny [25], which is ${}^{RL}_{a}\mathbf{D}^{\alpha}_{t} f(t)$, where $\alpha < 0$ is interpreted as an integral and $\alpha > 0$ as a derivative. We also omit the $+$ and $-$ from the notation for convenience, but you should be aware of whether or not a is bigger than t.

Example 1.2.5. Let us try our definition on a simple power function $f(t) = (t-a)^{\nu}$. Then, for $\alpha > 0$, we obtain

$$
\begin{aligned}
{}^{RL}_{a}\mathbf{D}^{-\alpha}_{t} f(t) &= \frac{1}{\Gamma(\alpha)} \int_a^t (t-\tau)^{\alpha-1} (\tau-a)^{\nu}\, d\tau \\
[\text{set } \tau = a + z(t-a)\,] \quad &= \frac{1}{\Gamma(\alpha)} \int_0^1 [(1-z)(t-a)]^{\alpha-1} [z(t-a)]^{\nu} (t-a)\, dz \\
&= \frac{1}{\Gamma(\alpha)} (t-a)^{\nu+\alpha} \int_0^1 (1-z)^{\alpha-1} (z)^{\nu}\, dz \\
&= \frac{1}{\Gamma(\alpha)} (t-a)^{\nu+\alpha} B(\alpha, \nu+1) \\
&= \frac{\Gamma(\nu+1)}{\Gamma(\nu+\alpha+1)} (t-a)^{\nu+\alpha}.
\end{aligned}
$$

Similarly, for $\alpha > 0$ and say $n-1 \leq \alpha < n$, we obtain

$$
\begin{aligned}
{}^{RL}_{a}\mathbf{D}^{\alpha}_{t} f(t) &= \frac{d^n}{dt^n} \frac{1}{\Gamma(n-\alpha)} \int_a^t (t-\tau)^{n-\alpha-1} (\tau-a)^{\nu}\, d\tau \\
[\text{set } \tau = a + z(t-a)\,] \quad &= \frac{d^n}{dt^n} \frac{1}{\Gamma(n-\alpha)} \int_0^1 [(1-z)(t-a)]^{n-\alpha-1} [z(t-a)]^{\nu} (t-a)\, dz \\
&= \frac{d^n}{dt^n} (t-a)^{n+\nu-\alpha} \frac{1}{\Gamma(n-\alpha)} \int_0^1 (1-z)^{n-\alpha-1} z^{\nu}\, dz \\
&= \frac{d^n}{dt^n} (t-a)^{n+\nu-\alpha} \frac{1}{\Gamma(n-\alpha)} B(n-\alpha, \nu+1) \\
&= \frac{\Gamma(n+\nu-\alpha+1)}{\Gamma(\nu-\alpha+1)} (t-a)^{\nu-\alpha} \frac{\Gamma(n-\alpha)\Gamma(\nu+1)}{\Gamma(n-\alpha)\Gamma(n-\alpha+\nu+1)} \\
&= \frac{\Gamma(\nu+1)}{\Gamma(\nu-\alpha+1)} (t-a)^{\nu-\alpha}.
\end{aligned}
$$

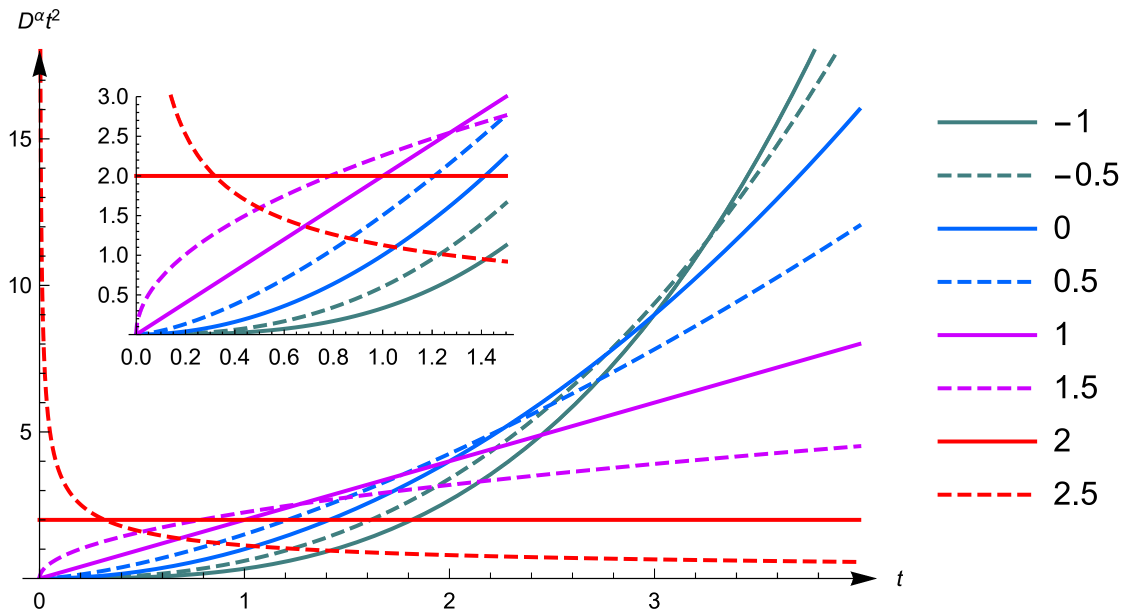

Figure 4: A plot of ${}^{RL}_{0}\mathbf{D}^{\alpha}_{t}\ t^2$ for α as indicated in the legend. Dashed lines are ordinary integer derivatives and integrals, while the full lines are of fractional order. Notice how the different orders cross each other and how the fractional orders fit between the integer orders. Inset: Zoom-in on the small t values.

Observe that these extensions of integer derivatives of an exponent are in line with using $\Gamma(z+1) = z!$ for $z \in \mathbb{N}$ as the extension of the factorial. Visually, they also seem to have a natural place in Figure 4 compared to the integer order derivatives, with the exception of $\alpha = 2.5$ where one would, perhaps intuitively, expect the zero function as it is a higher order derivative than the power of t. △

Example 1.2.6. Suppose that $f(t) = e^{\omega(t-a)}$, then

$$\begin{aligned}
{}^{RL}_{a}\mathbf{D}^{\alpha}_{t} e^{\omega(t-a)} &= {}^{RL}_{a}\mathbf{D}^{\alpha}_{t} \sum_{k=0}^{\infty} \frac{(\omega(t-a))^k}{k!} \\
&= \sum_{k=0}^{\infty} \frac{\omega^k}{\Gamma(k+1)}\, {}^{RL}_{a}\mathbf{D}^{\alpha}_{t} (t-a)^k \\
&= \sum_{k=0}^{\infty} \frac{\omega^k}{\Gamma(k+1)} \frac{\Gamma(k+1)}{\Gamma(k-\alpha+1)} (t-a)^{k-\alpha} \\
&= (t-a)^{-\alpha} \sum_{k=0}^{\infty} \frac{(\omega(t-a))^k}{\Gamma(k-\alpha+1)} \\
&= (t-a)^{-\alpha} E_{1,1-\alpha}(\omega(t-a)).
\end{aligned}$$

This might look different from what one could expect of a classical derivative with $\frac{d^n}{dt^n} e^{\omega(t-a)} = \omega^n e^{\omega(t-a)}$ for integer n. However, if we assume $\alpha \in \mathbb{Z}$ then we can shift the sum in the Mittag-Leffler function to recover the ordinary integer derivative. △

There are some fundamental properties that we would like derivatives to have; for example, we want

$$\frac{d^n}{dt^n}\left(\frac{d^m f(t)}{dt^m}\right) = \frac{d^m}{dt^m}\left(\frac{d^n f(t)}{dt^n}\right) = \frac{d^{n+m} f(t)}{dt^{n+m}}, \tag{1.8}$$

the additivity property of derivatives. This is not true if we want to have this property hold for integrals too, as we get extra polynomials in the boundary terms, in the sense that $\int_a^x f'(y)\, dy = f(x) - f(a)$. Let us investigate in what sense the fractional orders are additive.

Consider $n \in \mathbb{Z}$ positive, $k \in \mathbb{Z}$ and $0 < \alpha \leq 1$, then by definition we have

$$\frac{d^n}{dt^n}\, {}^{RL}_{\ a}\mathbf{D}_t^{k-\alpha} f(t) = \frac{1}{\Gamma(\alpha)} \frac{d^{n+k}}{dt^{n+k}} \int_a^t (t-\tau)^{\alpha-1} f(\tau)\, d\tau.$$

Denoting $p = k - \alpha$, we then find that

$$\frac{d^n}{dt^n}\, {}^{RL}_{\ a}\mathbf{D}_t^{p} f(t) = {}^{RL}_{\ a}\mathbf{D}_t^{p+n} f(t).$$

Lemma 1.2.7. *Suppose that $0 \leq m \leq p < m+1$, then*

$$\begin{aligned} {}^{RL}_{\ a}\mathbf{D}_t^{p} f(t) &= \sum_{k=0}^{m} \frac{f^{(k)}(a)(t-a)^{k-p}}{\Gamma(k-p+1)} + \frac{1}{\Gamma(m-p+1)} \int_a^t (t-\tau)^{m-p} f^{(m+1)}(\tau)\, d\tau \\ &= \sum_{k=0}^{m} \frac{f^{(k)}(a)(t-a)^{k-p}}{\Gamma(k-p+1)} + {}^{RL}_{\ a}\mathbf{D}_t^{p-m-1} f^{(m+1)}(t), \end{aligned}$$

where the second line is just entering the definition because $p - m - 1 < 0$.

Proof. Repeated integration by parts and differentiation gives

$$\begin{aligned} {}^{RL}_{\ a}\mathbf{D}_t^{p} f(t) &= \frac{d^{m+1}}{dt^{m+1}} \frac{1}{\Gamma(m-p+1)} \int_a^t (t-\tau)^{m-p} f(\tau)\, d\tau \\ &= \frac{d^{m}}{dt^{m}} \frac{1}{\Gamma(m-p+1)} \int_a^t (m-p)(t-\tau)^{m-p-1} f(\tau)\, d\tau \\ &= \frac{d^{m}}{dt^{m}} \frac{1}{\Gamma(m-p+1)} \left(\left[-(t-\tau)^{m-p} f(\tau)\right]_{\tau=a}^{t} - \int_a^t -(t-\tau)^{m-p} f^{(1)}(\tau)\, d\tau \right) \\ &= \frac{d^{m}}{dt^{m}} \frac{1}{\Gamma(m-p+1)} \left((t-a)^{m-p} f(a) + \int_a^t (t-\tau)^{m-p} f^{(1)}(\tau)\, d\tau \right) \\ &= \dots \end{aligned}$$

(keeping the boundary term and repeating the steps above m times with the integral)

$$\begin{aligned} &= \dots \\ &= \frac{1}{\Gamma(m-p+1)} \left(\sum_{k=0}^{m} \frac{d^{m-k}}{dt^{m-k}} (t-a)^{m-p} f^{(k)}(a) + \int_a^t (t-\tau)^{m-p} f^{(m+1)}(\tau)\, d\tau \right) \end{aligned}$$

The terms in the summation can now be calculated directly, namely

$$\frac{d^{m-k}}{dt^{m-k}} (t-a)^{m-p} f^{(k)}(a) = \frac{\Gamma(m-p+1)}{\Gamma(k-p+1)} (t-a)^{k-p} f^{(k)}(a).$$

Hence,

$$
\begin{aligned}
{}_a^{RL}\mathbf{D}_t^p f(t) &= \frac{1}{\Gamma(m-p+1)}\left(\sum_{k=0}^{m}\frac{d^{m-k}}{dt^{m-k}}(t-a)^{m-p}f^{(k)}(a)+\int_a^t (t-\tau)^{m-p}f^{(m+1)}(\tau)\,d\tau\right)\\
&= \frac{1}{\Gamma(m-p+1)}\left(\sum_{k=0}^{m}\frac{\Gamma(m-p+1)(t-a)^{k-p}f^{(k)}(a)}{\Gamma(k-p+1)}+\int_a^t (t-\tau)^{m-p}f^{(m+1)}(\tau)\,d\tau\right)\\
&= \sum_{k=0}^{m}\frac{(t-a)^{k-p}f^{(k)}(a)}{\Gamma(k-p+1)}+\frac{1}{\Gamma(m-p+1)}\int_a^t (t-\tau)^{m-p}f^{(m+1)}(\tau)\,d\tau.
\end{aligned}
$$

□

Let us try to apply the above Lemma to some simple cases.

Example 1.2.8. Suppose $m = p = 1$, then

$$
\begin{aligned}
{}_a^{RL}\mathbf{D}_t^1 f(t) &= \frac{f^{(0)}(a)(t-a)^{-1}}{\Gamma(0)}+\frac{f^{(1)}(a)(t-a)^{0}}{\Gamma(1)}+{}_a^{RL}\mathbf{D}_t^{-1}f^{(2)}(t)\\
&= 0+f^{(1)}(a)+\frac{1}{\Gamma(1)}\int_a^t (t-\tau)^0 f^{(2)}(\tau)\,d\tau\\
&= f^{(1)}(a)+f^{(1)}(t)-f^{(1)}(a)=f^{(1)}(t),
\end{aligned}
$$

where we note that $\Gamma(0) = \infty$ causes the first fraction to vanish. △

Example 1.2.9. Suppose now that $m = p = 2$ then we have

$$
\begin{aligned}
{}_a^{RL}\mathbf{D}_t^2 f(t) &= \frac{f^{(0)}(a)(t-a)^{-2}}{\Gamma(-1)}+\frac{f^{(1)}(a)(t-a)^{-1}}{\Gamma(0)}+\frac{f^{(2)}(a)(t-a)^{0}}{\Gamma(1)}+{}_a^{RL}\mathbf{D}_t^{-1}f^{(3)}(t)\\
&= 0+0+f^{(2)}(a)+\frac{1}{\Gamma(1)}\int_a^t (t-\tau)^0 f^{(3)}(\tau)\,d\tau\\
&= f^{(2)}(a)+f^{(2)}(t)-f^{(2)}(a)=f^{(2)}(t).
\end{aligned}
$$

△

It is quite remarkable how these formulas seem to work out, but for non-integer p the first m terms will remain.

Example 1.2.10. Take $m = 0$ and $p = 1/2$, then we get

$$
{}_a^{RL}\mathbf{D}_t^{1/2} f(t) = \frac{f(a)}{\sqrt{\pi(t-a)}}+{}_a^{RL}\mathbf{D}_t^{-1/2}f^{(1)}(t).
$$

△

Example 1.2.11. Take $m = 3$ and $p = \pi$, then we get

$$
\begin{aligned}
{}_a^{RL}\mathbf{D}_t^{\pi} f(t) &= \frac{f(a)(t-a)^{-\pi}}{\Gamma(1-\pi)}+\frac{f^{(1)}(a)(t-a)^{1-\pi}}{\Gamma(2-\pi)}+\frac{f^{(2)}(a)(t-a)^{2-\pi}}{\Gamma(3-\pi)}\\
&\quad+\frac{f^{(3)}(a)(t-a)^{3-\pi}}{\Gamma(4-\pi)}+{}_a^{RL}\mathbf{D}_t^{\pi-4}f^{(4)}(t).
\end{aligned}
$$

△

Lemma 1.2.12. *For $p > 0$ we have* $\lim_{p\to 0} {}^{RL}_{a}\mathbf{D}_t^{-p} f(t) = f(t)$.

Proof. Integration by parts gives

$$\begin{aligned}
{}^{RL}_{a}\mathbf{D}_t^{-p} f(t) &= \frac{1}{\Gamma(p)} \int_a^t (t-\tau)^{p-1} f(\tau)\, d\tau \\
&= \frac{1}{\Gamma(p)} \left(\left[\frac{-1}{p}(t-\tau)^p f(\tau) \right]_{\tau=a}^{t} - \int_a^t \frac{-1}{p}(t-\tau)^p f'(\tau)\, d\tau \right) \\
&= \frac{1}{p\Gamma(p)} \left((t-a)^p f(a) + \int_a^t (t-\tau)^p f'(\tau)\, d\tau \right) \\
&= \frac{1}{\Gamma(p+1)} \left((t-a)^p f(a) + \int_a^t (t-\tau)^p f'(\tau)\, d\tau \right)
\end{aligned}$$

and, taking the limit now, gives

$$\begin{aligned}
\lim_{p\to 0} {}^{RL}_{a}\mathbf{D}_t^{-p} f(t) &= \lim_{p\to 0} \frac{1}{\Gamma(p+1)} \left((t-a)^p f(a) + \int_a^t (t-\tau)^p f'(\tau)\, d\tau \right) \\
&= f(a) + \int_a^t f'(\tau)\, d\tau = f(t).
\end{aligned}$$

$\square$

Lemma 1.2.13. *Suppose $p < 0$, then* ${}^{RL}_{a}\mathbf{D}_t^{q}\left({}^{RL}_{a}\mathbf{D}_t^{p} f(t)\right) = {}^{RL}_{a}\mathbf{D}_t^{p+q} f(t)$ *for any $q \in \mathbb{R}$.*

Proof. Remark that $q = 0$ is trivial. Next, take $q < 0$, then

$$\begin{aligned}
{}^{RL}_{a}\mathbf{D}_t^{q}\left({}^{RL}_{a}\mathbf{D}_t^{p} f(t)\right) &= \frac{1}{\Gamma(-q)} \int_a^t (t-\tau)^{-q-1} \left({}^{RL}_{a}\mathbf{D}_t^{p} f(\tau)\right) d\tau \\
&= \frac{1}{\Gamma(-q)\Gamma(-p)} \int_a^t (t-\tau)^{-q-1} \int_a^\tau (\tau-\xi)^{-p-1} f(\xi)\, d\xi\, d\tau \\
&= \frac{1}{\Gamma(-q)\Gamma(-p)} \int_a^t \int_\xi^t (t-\tau)^{-q-1} (\tau-\xi)^{-p-1} f(\xi)\, d\tau\, d\xi \\
\text{[substitute } \tau = \xi + z(t-\xi)] \quad &= \frac{1}{\Gamma(-q)\Gamma(-p)} \int_a^t (t-\xi)^{-p-q-1} f(\xi) \int_0^1 (1-z)^{-q-1} z^{-p-1}\, dz\, d\xi \\
&= \frac{B(-p,-q)}{\Gamma(-q)\Gamma(-p)} \int_a^t (t-\xi)^{-p-q-1} f(\xi)\, d\xi \\
&= \frac{1}{\Gamma(-p-q)} \int_a^t (t-\xi)^{-p-q-1} f(\xi)\, d\xi \\
&= {}^{RL}_{a}\mathbf{D}_t^{p+q} f(t).
\end{aligned}$$

Now, consider $q > 0$ and suppose that $0 < n \le q < n+1$ with n an integer. Then, we see that $q = (n+1) + (q-n-1)$ with $q-n-1 < 0$. Hence, it follows that

$$\begin{aligned}
{}^{RL}_{a}\mathbf{D}_t^{q}({}^{RL}_{a}\mathbf{D}_t^{p} f(t)) &= \frac{d^{n+1}}{dt^{n+1}} \left({}^{RL}_{a}\mathbf{D}_t^{q-n-1} ({}^{RL}_{a}\mathbf{D}_t^{p} f(t)) \right) \\
&= \frac{d^{n+1}}{dt^{n+1}} \left({}^{RL}_{a}\mathbf{D}_t^{p+q-n-1} f(t) \right) = {}^{RL}_{a}\mathbf{D}_t^{p+q} f(t).
\end{aligned}$$

$\square$

A consequence of this Lemma is that, for $p > 0$, we have ${}^{RL}_{a}\mathbf{D}^{p}_{t}({}^{RL}_{a}\mathbf{D}^{-p}_{t}f(t)) = f(t)$.

Lemma 1.2.14. *Let $n \in \mathbb{Z}$ positive and $p > 0$, then*

$$ {}^{RL}_{a}\mathbf{D}^{p}_{t}f^{(n)}(t) = {}^{RL}_{a}\mathbf{D}^{p+n}_{t}f(t) + \sum_{k=0}^{n-1}\frac{f^{(k)}(a)(t-a)^{k-p-n}}{\Gamma(k-p-n+1)}. $$

Proof. Let $m \le p < m+1$ then, using Lemma 1.2.7, we have

$$ {}^{RL}_{a}\mathbf{D}^{p}_{t}f^{(n)}(t) = \sum_{k=0}^{m}\frac{f^{(k+n)}(a)(t-a)^{k-p}}{\Gamma(k-p+1)} + {}^{RL}_{a}\mathbf{D}^{p-m-1}_{t}f^{(n+m+1)}(t). $$

Now, since $m+n \le p+n < m+n+1$, we have

$$ \begin{aligned} {}^{RL}_{a}\mathbf{D}^{p+n}_{t}f(t) &= \sum_{k=0}^{m+n}\frac{f^{(k)}(a)(t-a)^{k-p-n}}{\Gamma(k-p-n+1)} + {}^{RL}_{a}\mathbf{D}^{p-m-1}_{t}f^{(n+m+1)}(t) \\ \text{[relabelling } k=l+n] \quad &= \sum_{l=-n}^{m}\frac{f^{(l+n)}(a)(t-a)^{l-p}}{\Gamma(l-p+1)} + {}^{RL}_{a}\mathbf{D}^{p-m-1}_{t}f^{(n+m+1)}(t). \end{aligned} $$

Hence,

$$ \begin{aligned} {}^{RL}_{a}\mathbf{D}^{p}_{t}f^{(n)}(t) &= \sum_{k=0}^{m}\frac{f^{(k+n)}(a)(t-a)^{k-p}}{\Gamma(k-p+1)} + {}^{RL}_{a}\mathbf{D}^{p-m-1}_{t}f^{(n+m+1)}(t) \\ &= {}^{RL}_{a}\mathbf{D}^{p+n}_{t}f(t) + \sum_{l=-n}^{-1}\frac{f^{(l+n)}(a)(t-a)^{l-p}}{\Gamma(l-p+1)} \\ \text{[relabelling } k=n-l] \quad &= {}^{RL}_{a}\mathbf{D}^{p+n}_{t}f(t) + \sum_{k=0}^{n-1}\frac{f^{(k)}(a)(t-a)^{k-p-n}}{\Gamma(k-p-n+1)}. \end{aligned} $$

□

Lemma 1.2.15. *Let $p > 0$ and $k-1 \le p < k$, then*

$$ {}^{RL}_{a}\mathbf{D}^{-p}_{t}\,{}^{RL}_{a}\mathbf{D}^{p}_{t}f(t) = f(t) - \sum_{j=1}^{k}\left({}^{RL}_{a}\mathbf{D}^{p-j}_{t}f\right)(a)\frac{(t-a)^{p-j}}{\Gamma(p-j+1)}. $$

Proof. Integrating by parts and using the additivity of orders when the right derivative has negative order, we find

$$
\begin{aligned}
{}^{RL}_{a}\mathbf{D}_t^{-p}\,{}^{RL}_{a}\mathbf{D}_t^{p} f(t) &= \frac{d}{dt}\,{}^{RL}_{a}\mathbf{D}_t^{-p-1}\,{}^{RL}_{a}\mathbf{D}_t^{p} f(t)\\
&= \frac{d}{dt}\left[\frac{1}{\Gamma(p+1)}\int_a^t (t-\tau)^p\ {}^{RL}{}_{a}\mathbf{D}_{\tau}{}^{p} f(\tau)\,d\tau\right]\\
&= \frac{d}{dt}\left[\frac{1}{\Gamma(p+1)}\int_a^t (t-\tau)^p\ \frac{d^k}{d\tau^k}{}^{RL}{}_{a}\mathbf{D}_{\tau}{}^{p-k} f(\tau)\,d\tau\right]\\
&= \frac{d}{dt}\left[\frac{(-1)^k}{\Gamma(p+1)}\int_a^t \left(\frac{d^k}{d\tau^k}(t-\tau)^p\right)\ {}^{RL}{}_{a}\mathbf{D}_{\tau}{}^{p-k} f(\tau)\,d\tau\right.\\
&\qquad \left. - \sum_{j=1}^{k}\left(\frac{d^{k-j}}{dt^{k-j}}\,{}^{RL}_{a}\mathbf{D}_t^{p-k} f\right)(a)\ \frac{(t-a)^{p-j+1}}{\Gamma(2+p-j)}\right]\\
&= \frac{d}{dt}\left[\frac{1}{\Gamma(p-k+1)}\int_a^t (t-\tau)^{p-k}\ {}^{RL}{}_{a}\mathbf{D}_{\tau}{}^{p-k} f(\tau)\,d\tau\right.\\
&\qquad \left. - \sum_{j=1}^{k}\left({}^{RL}_{a}\mathbf{D}_t^{p-j} f\right)(a)\ \frac{(t-a)^{p-j+1}}{\Gamma(2+p-j)}\right]\\
&= \frac{d}{dt}\left[{}^{RL}_{a}\mathbf{D}_t^{-(p-k+1)}\,{}^{RL}_{a}\mathbf{D}_t^{p-k} f(t) - \sum_{j=1}^{k}\left({}^{RL}_{a}\mathbf{D}_t^{p-j} f\right)(a)\ \frac{(t-a)^{p-j+1}}{\Gamma(2+p-j)}\right]\\
&= \frac{d}{dt}\left[{}^{RL}_{a}\mathbf{D}_t^{-1} f(t) - \sum_{j=1}^{k}\left({}^{RL}_{a}\mathbf{D}_t^{p-j} f\right)(a)\ \frac{(t-a)^{p-j+1}}{\Gamma(2+p-j)}\right]\\
&= f(t) - \sum_{j=1}^{k}\left({}^{RL}_{a}\mathbf{D}_t^{p-j} f\right)(a)\ \frac{(t-a)^{p-j}}{\Gamma(1+p-j)}.
\end{aligned}
$$

□

Lemma 1.2.16. *For $p, q > 0$ and $k-1 \leq q < k$ we have*

$$
{}^{RL}_{a}\mathbf{D}_t^{-p}\,{}^{RL}_{a}\mathbf{D}_t^{q} f(t) = {}^{RL}_{a}\mathbf{D}_t^{q-p} f(t) - \sum_{j=1}^{k}\left({}^{RL}_{a}\mathbf{D}_t^{q-j} f\right)(a)\frac{(t-a)^{p-j}}{\Gamma(p-j+1)}.
$$

Proof. We have

$$
\begin{aligned}
{}^{RL}_{a}\mathbf{D}_t^{-p}\,{}^{RL}_{a}\mathbf{D}_t^{q} f(t) &= {}^{RL}_{a}\mathbf{D}_t^{q-p}\,{}^{RL}_{a}\mathbf{D}_t^{-q}\,{}^{RL}_{a}\mathbf{D}_t^{q} f(t)\\
&= {}^{RL}_{a}\mathbf{D}_t^{q-p}\left[f(t) - \sum_{j=1}^{k}\left({}^{RL}_{a}\mathbf{D}_t^{q-j} f\right)(a)\ \frac{(t-a)^{q-j}}{\Gamma(1+q-j)}\right]\\
&= {}^{RL}_{a}\mathbf{D}_t^{q-p} f(t) - \sum_{j=1}^{k}\left({}^{RL}_{a}\mathbf{D}_t^{q-j} f\right)(a)\ \frac{(t-a)^{p-j}}{\Gamma(1+p-j)}.
\end{aligned}
$$

□

Lemma 1.2.17. *Take $p, q > 0$ and let $n, m \in \mathbb{Z}$ be such that $n-1 \le q < n$ and $m-1 \le p < m$. Then*

$$ {}^{RL}_{a}\mathbf{D}^{p}_{t}\, {}^{RL}_{a}\mathbf{D}^{q}_{t} f(t) = {}^{RL}_{a}\mathbf{D}^{p+q}_{t} f(t) + \sum_{j=1}^{n} \left({}^{RL}_{a}\mathbf{D}^{q-j}_{t} f \right)(a) \frac{(t-a)^{-p-j}}{\Gamma(-p-j+1)}. $$

Proof. Since $p = (p-n)+n$, with $p-n<0$, and applying Lemma 1.2.16, we have

$$ \begin{aligned} {}^{RL}_{a}\mathbf{D}^{p}_{t}\, {}^{RL}_{a}\mathbf{D}^{q}_{t} f(t) &= \frac{d^m}{dt^m}\, {}^{RL}_{a}\mathbf{D}^{p-m}_{t} ({}^{RL}_{a}\mathbf{D}^{q}_{t} f(t)) \\ &= \frac{d^m}{dt^m} \left({}^{RL}_{a}\mathbf{D}^{p+q-m}_{t} f(t) - \sum_{j=1}^{n} \left({}^{RL}_{a}\mathbf{D}^{q-j}_{t} f \right)(a) \frac{(t-a)^{m-p-j}}{\Gamma(1+m-p-j)} \right) \\ &= \frac{d^m}{dt^m} \left({}^{RL}_{a}\mathbf{D}^{p+q-m}_{t} f(t) - \sum_{j=1}^{n} \left({}^{RL}_{a}\mathbf{D}^{q-j}_{t} f \right)(a) \frac{(t-a)^{m-p-j}}{\Gamma(1+m-p-j)} \right) \\ &= {}^{RL}_{a}\mathbf{D}^{p+q}_{t} f(t) + \sum_{j=1}^{n} \left({}^{RL}_{a}\mathbf{D}^{q-j}_{t} f \right)(a) \frac{(t-a)^{-p-j}}{\Gamma(-p-j+1)}. \end{aligned} $$

□

In conclusion, combining Lemmas 1.2.13, 1.2.16, and 1.2.17, we have the following Theorem.

Theorem 1.2.18. *For $p, q > 0$ and $n-1 \le q < n$ with $n \in \mathbb{Z}$ we have the following properties:*

$$ {}^{RL}_{a}\mathbf{D}^{p}_{t}\, {}^{RL}_{a}\mathbf{D}^{q}_{t} f(t) = {}^{RL}_{a}\mathbf{D}^{p+q}_{t} f(t) + \sum_{j=1}^{n} \left({}^{RL}_{a}\mathbf{D}^{q-j}_{t} f \right)(a) \frac{(t-a)^{-p-j}}{\Gamma(-p-j+1)} \tag{1.9} $$

$$ {}^{RL}_{a}\mathbf{D}^{-p}_{t}\, {}^{RL}_{a}\mathbf{D}^{q}_{t} f(t) = {}^{RL}_{a}\mathbf{D}^{q-p}_{t} f(t) - \sum_{j=1}^{n} \left({}^{RL}_{a}\mathbf{D}^{q-j}_{t} f \right)(a) \frac{(t-a)^{p-j}}{\Gamma(p-j+1)} \tag{1.10} $$

$$ {}^{RL}_{a}\mathbf{D}^{p}_{t}\, {}^{RL}_{a}\mathbf{D}^{-q}_{t} f(t) = {}^{RL}_{a}\mathbf{D}^{p-q}_{t} f(t) \tag{1.11} $$

$$ {}^{RL}_{a}\mathbf{D}^{-p}_{t}\, {}^{RL}_{a}\mathbf{D}^{-q}_{t} f(t) = {}^{RL}_{a}\mathbf{D}^{-p-q}_{t} f(t). \tag{1.12} $$

Lemma 1.2.19. *The Laplace transform of the Riemann-Liouville derivative with $a=0$, $p>0$, and $n-1 \le p < n$, is given by:*

$$ \mathcal{L}\left({}^{RL}_{0}\mathbf{D}^{-p}_{t} f(t); s \right) = s^{-p} F(s); $$

$$ \mathcal{L}\left({}^{RL}_{0}\mathbf{D}^{p}_{t} f(t); s \right) = s^{p} F(s) - \sum_{k=0}^{n-1} s^{k} \left({}^{RL}_{0}\mathbf{D}^{p-k-1}_{t} f \right)(0). $$

Proof. Let $p>0$ and $n \in \mathbb{N}$, with $n-1 \le p < n$, then

$$ {}^{RL}_{0}\mathbf{D}^{-p}_{t} f(t) = \frac{1}{\Gamma(p)} \int_0^t (t-\tau)^{p-1} f(\tau)\, d\tau = \frac{t^{p-1} * f(t)}{\Gamma(p)}. $$

Therefore, the Laplace transform is given by

$$\begin{aligned}\mathcal{L}\left({}_0^{RL}\mathbf{D}_t^{-p} f(t); s\right) &= \mathcal{L}\left(\frac{t^{p-1} * f(t)}{\Gamma(p)}; s\right)\\ &= \frac{1}{\Gamma(p)}\mathcal{L}\left(t^{p-1}; s\right)\mathcal{L}\left(f(t); s\right)\\ &= s^{-p}F(s).\end{aligned}$$

Now, consider ${}_0^{RL}\mathbf{D}_t^{p} f(t) = \frac{d^n}{dt^n}\,{}_0^{RL}\mathbf{D}_t^{p-n} f(t)$, then the Laplace transform is given by

$$\begin{aligned}\mathcal{L}\left({}_0^{RL}\mathbf{D}_t^{p} f(t); s\right) &= \mathcal{L}\left(\frac{d^n}{dt^n}\,{}_0^{RL}\mathbf{D}_t^{p-n} f(t); s\right)\\ &= s^n\mathcal{L}\left({}_0^{RL}\mathbf{D}_t^{p-n} f(t); s\right) - \sum_{k=0}^{n-1} s^{n-1-k}\left(\frac{d^k}{dt^k}\,{}_0^{RL}\mathbf{D}_t^{p-n} f(t)\right)_{t=0}\\ &= s^p F(s) - \sum_{k=0}^{n-1} s^{n-1-k}\left({}_0^{RL}\mathbf{D}_t^{p+k-n} f\right)(0)\\ [\text{set } j = n-1-k] \quad &= s^p F(s) - \sum_{j=0}^{n-1} s^{j}\left({}_0^{RL}\mathbf{D}_t^{p-j-1} f\right)(0)\end{aligned}$$

□

Remark 1.2.20. It should be mentioned that, in the above Lemma, we get an extra term compared to ordinary derivatives if we set $p \in \mathbb{N}$. However, this term is equal to $s^p f^{(-1)}(0)$, which means that as long as $f(t)$ is continuous at 0, which it has to be anyway if we want to talk about derivatives there, then $f^{(-1)}(0) = \lim_{t\to 0}\int_0^t f(\tau)\,d\tau = 0$.

1.3 Liouville fractional derivative

A specific case of the Riemann-Liouville definition is the Liouville definition, in which we take $a = -\infty$ as our lower bound and denote ${}^{L}\mathbf{D}_t^{\alpha} f(t) = {}_{-\infty}^{RL}\mathbf{D}_t$. However, it is not just as simple as putting $a = -\infty$, since some of the properties of the Riemann-Liouville definition have terms like $(t-a)^{\alpha}$. This is not a problem if $\alpha \le 0$, but $\alpha > 0$ is where the problem lies. There is, however, a relatively easy solution by imposing conditions on the functions that we use. Specifically, if we impose that

$$\lim_{x\to-\infty} x^{\alpha} f^{(k)}(x) = 0, \tag{1.13}$$

for all $k \in \mathbb{N}$ with $k < K$ for sufficiently large K and α[4], then we can deduce from Lemma 1.2.7 that for $0 \le m \le p < m+1$, we obtain

$${}^{L}\mathbf{D}_t^{p} f(t) = {}^{L}\mathbf{D}_t^{p-m-1} f^{(m+1)}.$$

Furthermore, for $0 \le m \le p < m+1$ and $k \in \mathbb{N}$, we have

$$\frac{d^k}{dt^k}\,{}^{L}\mathbf{D}_t^{p} f(t) = \frac{d^{k+m+1}}{dt^{k+m+1}}\,{}^{L}\mathbf{D}_t^{p-m-1} f(t) = {}^{L}\mathbf{D}_t^{k+p} f(t).$$

[4] K and α should be bigger than the orders of the derivatives that will be applied to $f(x)$.

Because of Equation (1.13), we can also see that, for any p, we obtain

$$ {}^{L}\mathbf{D}_t^p f^{(k)}(t) = {}^{L}\mathbf{D}_t^{p+k} f(t) $$

by Theorem 1.2.18. Hence, for any p and $0 \le n-1 \le q < n$, we have

$$ {}^{L}\mathbf{D}_t^p \, {}^{L}\mathbf{D}_t^q f(t) = {}^{L}\mathbf{D}_t^p \, {}^{L}\mathbf{D}_t^{q-n} f^{(n)}(t) = {}^{L}\mathbf{D}_t^{p+q-n} f^{(n)}(t) = {}^{L}\mathbf{D}_t^{p+q} f(t), $$

whenever $f(t)$ satisfies Equation (1.13). Since the above result was already true for $q < 0$, we can thus conclude that, for any $p, q \in \mathbb{R}$:

$$ \boxed{{}^{L}\mathbf{D}_t^p \, {}^{L}\mathbf{D}_t^q f(t) = {}^{L}\mathbf{D}_t^{p+q} f(t),} \tag{1.14} $$

whenever $f(t)$ satisfies Equation (1.13).

Example 1.3.1. Suppose $f(t) = e^{\omega t}$ with $0 < \omega \in \mathbb{R}$ and $\alpha > 0$, then

$$ \begin{aligned} {}^{L}\mathbf{D}_t^{-\alpha} e^{\omega t} &= \frac{1}{\Gamma(\alpha)} \int_{-\infty}^{t} (t-\tau)^{\alpha-1} e^{\omega\tau} \, d\tau \\ \left[\text{set } \tau = t - \frac{z}{\omega}\right] \quad &= \frac{1}{\Gamma(\alpha)} \int_0^{\infty} (z/\omega)^{\alpha-1} e^{-z+\omega t} \frac{1}{\omega} \, dz \\ &= e^{\omega t} \frac{\omega^{-\alpha}}{\Gamma(\alpha)} \int_0^{\infty} z^{\alpha-1} e^{-z} \, dz \\ &= \omega^{-\alpha} e^{\omega t}. \end{aligned} $$

△

In order to apply this to Fourier transforms, we would like such a statement with $i\omega$ rather than ω. By Dirichlet's convergence theorem, we can see that for $0 < \alpha < 1$ the integral is still convergent when $\omega \in \mathbb{R}$. Therefore, we find, for a Fourier transform and $0 < \alpha < 1$:

$$ \begin{aligned} {}^{L}\mathbf{D}_t^{-\alpha} f(t) &= {}^{L}\mathbf{D}_t^{-\alpha} \int_{-\infty}^{\infty} f(\omega) e^{i\omega t} \, d\omega \\ &= \frac{1}{\Gamma(\alpha)} \int_{-\infty}^{t} (t-\tau)^{\alpha-1} \int_{-\infty}^{\infty} f(\omega) e^{i\omega\tau} \, d\omega \, d\tau \\ &= \frac{1}{\Gamma(\alpha)} \int_{-\infty}^{\infty} f(\omega) \int_{-\infty}^{t} (t-\tau)^{\alpha-1} e^{i\omega\tau} \, d\tau \, d\omega \\ &= \int_{-\infty}^{\infty} f(\omega) (i\omega)^{-\alpha} e^{i\omega t} \, d\omega. \end{aligned} $$

Accordingly, we see that, for $0 < \alpha < 1$, we have

$$ \mathcal{F}\left({}^{L}\mathbf{D}_t^{-\alpha} f(t); \omega\right) = (i\omega)^{-\alpha} \mathcal{F}\left(f(t); \omega\right). $$

We can then combine the additivity of differential orders with the fact that the Fourier transform combines with integer derivatives, to get

$$ \boxed{\mathcal{F}\left({}^{L}\mathbf{D}_t^{\alpha} f(t); \omega\right) = (i\omega)^{\alpha} \mathcal{F}\left(f(t); \omega\right) \quad \text{for all } \alpha \in \mathbb{R}.} \tag{1.15} $$

1.4 Grünwald-Letnikov fractional derivative

The idea of this approach, on the other hand, is to start from the basic limit definition for derivatives, and trying to generalise from there: We do not introduce non-integer numbers until we have an integral formulation, which will turn out to be equivalent to the Riemann-Liouville definition.

Lemma 1.4.1. *A general formula for the n^{th} integer derivative is given by*

$$f^{(n)}(t) = \lim_{h\to 0} \frac{\sum_{r=0}^{n}(-1)^r\binom{n}{r}f(t-rh)}{h^n}.$$

Proof. For $n = 0$ the statement is trivially true. By the induction hypothesis, we now suppose it is true for n, then the following holds:

$$\begin{aligned}
f^{(n+1)}(t) &= \lim_{h\to 0} \frac{f^{(n)}(t) - f^{(n)}(t-h)}{h} \\
&= \lim_{h\to 0} \frac{\sum_{r=0}^{n}(-1)^r\binom{n}{r}f(t-rh) - \sum_{l=0}^{n}(-1)^l\binom{n}{l}f(t-(l+1)h)}{h^{n+1}} \\
&= \lim_{h\to 0} \frac{\sum_{r=0}^{n}(-1)^r\binom{n}{r}f(t-rh) + \sum_{l=0}^{n}(-1)^{l+1}\binom{n}{l}f(t-(l+1)h)}{h^{n+1}} \\
&= \lim_{h\to 0} \frac{\sum_{r=0}^{n}(-1)^r\binom{n}{r}f(t-rh) + \sum_{l=1}^{n+1}(-1)^l\binom{n}{l-1}f(t-lh)}{h^{n+1}} \\
&= \lim_{h\to 0} \frac{f(t) + (-1)^{n+1}f(t-(n+1)h) + \sum_{r=1}^{n}(-1)^r(\binom{n}{r}+\binom{n}{r-1})f(t-rh)}{h^{n+1}} \\
&= \lim_{h\to 0} \frac{f(t) + (-1)^{n+1}f(t-(n+1)h) + \sum_{r=1}^{n}(-1)^r\binom{n+1}{r}f(t-rh)}{h^{n+1}} \\
&= \lim_{h\to 0} \frac{\sum_{r=0}^{n+1}(-1)^r\binom{n+1}{r}f(t-rh)}{h^{n+1}},
\end{aligned}$$

which proves the statement. □

Here, the n in $\binom{n}{r} = \frac{n(n-1)\ldots(n-r+1)}{r!}$ can be trivially changed to $p \in \mathbb{N}$ to get

$$f_h^{(p)}(t) = \frac{1}{h^p}\sum_{r=0}^{n}(-1)^r\binom{p}{r}f(t-rh). \tag{1.16}$$

If we assume that $p \leq n$, then

$$\lim_{h\to 0} f_h^{(p)}(t) = \lim_{h\to 0}\frac{1}{h^p}\sum_{r=0}^{p}(-1)^r\binom{p}{r}f(t-rh) = f^{(p)}(t)$$

because $\binom{p}{r} = 0$ if $r > p$.

Now, consider $p \in \mathbb{Z}$ and let us denote

$$\begin{bmatrix} p \\ r \end{bmatrix} = \frac{p(p+1)\ldots(p+r-1)}{r!},$$

then we have

$$(-1)^r\begin{bmatrix} p \\ r \end{bmatrix} = \frac{-p(-p-1)\ldots(-p-r+1)}{r!} = \binom{-p}{r}.$$

This allows us to replace $p > 0$ in Equation (1.16) by $-p$, and we find

$$f_h^{(-p)}(t) = h^p \sum_{r=0}^{n} \begin{bmatrix} p \\ r \end{bmatrix} f(t - rh). \tag{1.17}$$

For fixed n, this is quite an uninteresting limit as $h \to 0$, but taking a limit along the lines of Riemann integration, and writing $nh = t - a$, with a some real constant, we can define the following:

Definition 1.4.2. The *Grünwald-Letnikov fractional integral* for $p \in \mathbb{N}$ is defined as

$${}^{GL}_{a}\mathbf{D}_t^{(-p)} f(t) = \lim_{\substack{h\to 0 \\ nh=t-a}} f_h^{-p}(t) = \lim_{\substack{h\to 0 \\ nh=t-a}} h^p \sum_{r=0}^{n} \begin{bmatrix} p \\ r \end{bmatrix} f(t - rh).$$

The *Grünwald-Letnikov fractional derivative* for $p \in \mathbb{N}$ is defined as

$${}^{GL}_{a}\mathbf{D}_t^{p} f(t) = \lim_{\substack{h\to 0 \\ nh=t-a}} f_h^{(p)}(t) = \lim_{\substack{h\to 0 \\ nh=t-a}} \frac{1}{h^p} \sum_{r=0}^{n} (-1)^r \binom{p}{r} f(t - rh).$$

Let us evaluate these limits.

Lemma 1.4.3. *For $p \in \mathbb{N}$, we have*

$${}^{GL}_{a}\mathbf{D}_t^{-p} f(t) = \frac{1}{(p-1)!} \int_a^t (t - \tau)^{p-1} f(\tau)\, d\tau.$$

Proof. For $p = 1$, then, by classical Riemann integration, we have

$$\begin{aligned}
{}^{GL}_{a}\mathbf{D}_t^{-1} f(t) &= \lim_{\substack{h\to 0 \\ nh=t-a}} \frac{1}{h} \sum_{r=0}^{n} \begin{bmatrix} 1 \\ r \end{bmatrix} f(t - rh) = \lim_{\substack{h\to 0 \\ nh=t-a}} \frac{1}{h} \sum_{r=0}^{n} f(t - rh) \\
&= \int_0^{t-a} f(t - z)\, dz = \int_a^t f(\tau)\, d\tau.
\end{aligned}$$

Now, by induction, assume it is true for some p. If we set $f_1(t) = \int_a^t f(\tau)\, d\tau$, then

$$\begin{aligned}
{}^{GL}_{a}\mathbf{D}_t^{-(p+1)} f(t) &= \lim_{\substack{h\to 0 \\ nh=t-a}} \frac{1}{h^{p+1}} \sum_{r=0}^{n} \begin{bmatrix} p+1 \\ r \end{bmatrix} f(t - rh) \\
&= \lim_{\substack{h\to 0 \\ nh=t-a}} \frac{1}{h^p} \sum_{r=0}^{n} \begin{bmatrix} p+1 \\ r \end{bmatrix} \left(f_1(t - rh) - f_1(t - (r+1)h)\right) \\
&= \lim_{\substack{h\to 0 \\ nh=t-a}} \left(\frac{1}{h^p} \sum_{r=0}^{n} \left(\begin{bmatrix} p \\ r \end{bmatrix} + \begin{bmatrix} p+1 \\ r-1 \end{bmatrix} \right) f_1(t - rh) - \frac{1}{h^p} \sum_{r=1}^{n+1} \begin{bmatrix} p+1 \\ r-1 \end{bmatrix} f_1(t - rh) \right) \\
&= {}^{GL}_{a}\mathbf{D}_t^{-p} f_1(t) + \lim_{\substack{h\to 0 \\ nh=t-a}} \frac{1}{h^p} \left(\begin{bmatrix} p+1 \\ -1 \end{bmatrix} f_1(t) - \begin{bmatrix} p+1 \\ n \end{bmatrix} f_1(t - (n+1)h) \right) \\
&= {}^{GL}_{a}\mathbf{D}_t^{-p} f_1(t) - (t-a)^p \lim_{n\to\infty} \frac{1}{n^p} \begin{bmatrix} p+1 \\ n \end{bmatrix} f_1\left(a - \frac{t-a}{n}\right),
\end{aligned}$$

where we used[5] that $\begin{bmatrix} p+1 \\ -1 \end{bmatrix} = 0$. Now, observe that

$$\lim_{n\to\infty} f_1\left(a - \frac{t-a}{n}\right) = \lim_{n\to\infty} \int_a^{a-\frac{t-a}{n}} f(\tau)\, d\tau = 0$$

and

$$\lim_{n\to\infty} \begin{bmatrix} p+1 \\ n \end{bmatrix} \frac{1}{n^p} = \lim_{n\to\infty} \frac{(p+1)(p+2)\dots(p+n)}{n^p n!} = \frac{1}{\Gamma(p+1)}, \tag{1.18}$$

where the latter identity can be found in [25, p. 4]. Combining the results of these limits, we now find that

$$\begin{aligned} {}^{GL}_{a}\mathbf{D}_t^{-(p+1)} f(t) &= {}^{GL}_{a}\mathbf{D}_t^{-p} f_1(t) - 0 \\ &= \frac{1}{(p-1)!} \int_a^t (t-\tau)^{p-1} f_1(\tau)\, d\tau \end{aligned}$$

and, using integration by parts, we get

$$\begin{aligned} {}^{GL}_{a}\mathbf{D}_t^{-(p+1)} f(t) &= \left[-\frac{(t-\tau)^p f_1(\tau)}{p!} \right]_{\tau=a}^{t} + \frac{1}{p!} \int_a^t (t-\tau)^p f(\tau)\, d\tau \\ &= \frac{1}{p!} \int_a^t (t-\tau)^p f(\tau)\, d\tau. \end{aligned}$$

□

Remark 1.4.4. A consequence of the above proof is that

$${}^{GL}_{a}\mathbf{D}_t^{-p} f(t) = {}^{GL}_{a}\mathbf{D}_t^{-(p-1)} \int_a^t f(\tau)\, d\tau = \dots = \underbrace{\int_a^t \cdots \int_a^t}_{\text{p times}} f(\tau)\, d\tau.$$

In order to get a more generalisable integral form out of the limit, we need the following Theorem.

Theorem 1.4.5. *(Letnikov, [25, p. 49]) Let $\alpha_{n,k}$ and β_k be sequences such that*

$$\lim_{k\to\infty} \beta_k = 1, \qquad \lim_{n\to\infty} \alpha_{n,k} = 0 \quad \text{for all } k,$$

$$\lim_{n\to\infty} \sum_{k=1}^{n} \alpha_{n,k} = A \quad \text{for all } k, \qquad \sum_{k=1}^{n} |\alpha_{n,k}| < K \quad \text{for all } n,$$

with K and A real numbers. Then

$$\lim_{n\to\infty} \sum_{k=1}^{n} \alpha_{n,k}\beta_k = A.$$

If we want to apply this theorem to

$${}^{GL}_{a}\mathbf{D}_t^{-p} f(t) = \lim_{\substack{h\to 0 \\ nh=t-a}} h^p \sum_{r=0}^{n} \begin{bmatrix} p \\ r \end{bmatrix} f(t-rh),$$

[5]We only defined $\begin{bmatrix} p \\ r \end{bmatrix}$ for positive r, but it is a reasonable extension to put $r < 0$ values to 0.

we first have to rewrite ${}^{GL}_{a}\mathbf{D}_t^{-p}f(t)$ as

$$\begin{aligned}
{}^{GL}_{a}\mathbf{D}_t^{-p}f(t) &= \lim_{\substack{h\to 0\\ nh=t-a}} h^p \sum_{r=0}^{n} \begin{bmatrix} p\\ r\end{bmatrix} f(t-rh)\\
&= \frac{1}{\Gamma(p)} \lim_{\substack{h\to 0\\ nh=t-a}} \sum_{r=0}^{n} \frac{\Gamma(p)}{r^{p-1}} \begin{bmatrix} p\\ r\end{bmatrix} h(rh)^{p-1} f(t-rh)\\
&= \frac{1}{\Gamma(p)} \lim_{n\to\infty} \sum_{r=0}^{n} \frac{\Gamma(p)}{r^{p-1}} \begin{bmatrix} p\\ r\end{bmatrix} \frac{t-a}{n}\left(r\frac{t-a}{n}\right)^{p-1} f\left(t-r\frac{t-a}{n}\right),
\end{aligned}$$

and take

$$\beta_r = \frac{\Gamma(p)}{r^{p-1}}\begin{bmatrix} p\\ r\end{bmatrix} \quad \text{and} \quad \alpha_{n,r} = \frac{t-a}{n}\left(r\frac{t-a}{n}\right)^{p-1} f\left(t-r\frac{t-a}{n}\right).$$

Again, using Equation (1.18), we see that

$$\begin{aligned}
\lim_{r\to\infty}\beta_r &= \lim_{r\to\infty} \frac{r^{p-1}\, r!}{p(p+1)\dots(p+r-1)r^{p-1}} \begin{bmatrix} p\\ r\end{bmatrix}\\
&= \lim_{r\to\infty} \frac{r^{p-1}\, r!}{p(p+1)\dots(p+r-1)r^{p-1}} \frac{p(p+1)\dots(p+r-1)}{r!}\\
&= 1.
\end{aligned}$$

Combining this with

$$\begin{aligned}
\lim_{n\to\infty}\sum_{r=0}^{n}\alpha_{n,r} &= \lim_{n\to\infty}\sum_{r=0}^{n} \frac{t-a}{n}\left(r\frac{t-a}{n}\right)^{p-1} f\left(t-r\frac{t-a}{n}\right)\\
&= \lim_{\substack{h\to 0\\ nh=t-a}} \sum_{r=0}^{n} h(rh)^{p-1} f(t-rh)\\
&= \int_a^t (t-\tau)^{p-1} f(\tau)\, d\tau,
\end{aligned}$$

we conclude that

$$\boxed{{}^{GL}_{a}\mathbf{D}_t^{-p}f(t) = \frac{1}{\Gamma(p)}\int_a^t (t-\tau)^{p-1} f(\tau)\, d\tau = {}^{RL}_{a}\mathbf{D}_t^{-p}f(t)}$$

is the generalised form of the Grünwald-Letnikov integral and that it is equal to the Riemann-Liouville integral.

Let us now consider and generalise the derivatives

$${}^{GL}_{a}\mathbf{D}_t^{p}f(t) = \lim_{\substack{h\to 0\\ nh=t-a}} f_h^{(p)}(t) = \lim_{\substack{h\to 0\\ nh=t-a}} \frac{1}{h^p}\sum_{r=0}^{n}(-1)^r \binom{p}{r} f(t-rh).$$

Using the binomial property $\binom{p}{r} = \binom{p-1}{r} + \binom{p-1}{r-1}$, we can write

$$
\begin{aligned}
f_h^{(p)}(t) &= \frac{1}{h^p}\sum_{r=0}^{n}(-1)^r\binom{p}{r}f(t-rh) \\
&= \frac{1}{h^p}\sum_{r=0}^{n}(-1)^r\binom{p-1}{r}f(t-rh) + \frac{1}{h^p}\sum_{r=1}^{n}(-1)^r\binom{p-1}{r-1}f(t-rh) \\
&= \frac{1}{h^p}\sum_{r=0}^{n}(-1)^r\binom{p-1}{r}f(t-rh) + \frac{1}{h^p}\sum_{r=0}^{n-1}(-1)^{r+1}\binom{p-1}{r}f(t-(r+1)h) \\
&= (-1)^n\binom{p-1}{n}\frac{1}{h^p}f(a) + \frac{1}{h^p}\sum_{r=0}^{n-1}(-1)^r\binom{p-1}{r}\Delta f(t-rh),
\end{aligned}
$$

where $\Delta f(t-rh) = f(t-rh) - f(t-(r+1)h)$. Repeating the above steps m times, we end up with

$$
f_h^{(p)}(t) = \sum_{k=0}^{m}(-1)^{n-k}\binom{p-k-1}{n-k}\frac{1}{h^p}\Delta^k f(a+kh) + \frac{1}{h^p}\sum_{r=0}^{n-m-1}(-1)^r\binom{p-m-1}{r}\Delta^{m+1}f(t-rh), \tag{1.19}
$$

where Δ^k is Δ applied k times. With this, we want to evaluate the limits, but let us do it for each term separately:

$$
\begin{aligned}
&\lim_{\substack{h\to 0\\ nh=t-a}}(-1)^{n-k}\binom{p-k-1}{n-k}\frac{1}{h^p}\Delta^k f(a+kh) \\
&= \lim_{\substack{h\to 0\\ nh=t-a}}(-1)^{n-k}\binom{p-k-1}{n-k}(n-k)^{p-k}\left(\frac{n}{n-k}\right)^{p-k}(nh)^{k-p}\frac{\Delta^k f(a+kh)}{h^k} \\
&= (t-a)^{k-p}\left(\lim_{n\to\infty}(-1)^{n-k}\binom{p-k-1}{n-k}(n-k)^{p-k}\right)\left(\lim_{n\to\infty}\left(\frac{n}{n-k}\right)^{p-k}\right)\lim_{h\to 0}\frac{\Delta^k f(a+kh)}{h^k} \\
&= \frac{f^{(k)}(a)(t-a)^{k-p}}{\Gamma(k-p+1)}.
\end{aligned}
$$

This last equality is true since the separate limits give

$$
\lim_{n\to\infty}(-1)^{n-k}\binom{p-k-1}{n-k}(n-k)^{p-k} = \lim_{n\to\infty}\frac{(k-p+1)(k-p+2)\ldots(-p+n)}{(n-k)^{k-p}(n-k)!} = \frac{1}{\Gamma(k-p+1)},
$$

$$
\lim_{n\to\infty}\left(\frac{n}{n-k}\right)^{p-k} = 1
$$

and

$$
\lim_{h\to 0}\frac{\Delta^k f(a+kh)}{h^k} = f^{(k)}(a).
$$

The other terms in Equation (1.19) are given by

$$\begin{aligned}
&\lim_{\substack{h\to 0\\ nh=t-a}} \frac{1}{h^p}\sum_{r=0}^{n-m-1}(-1)^r\binom{p-m-1}{r}\Delta^{m+1}f(t-rh)\\
&=\lim_{\substack{h\to 0\\ nh=t-a}} \frac{1}{\Gamma(m-p+1)}\sum_{r=0}^{n-m-1}(-1)^r\Gamma(m-p+1)\binom{p-m-1}{r}r^{p-m}h(rh)^{m-p}\frac{\Delta^{m+1}f(t-rh)}{h^{m+1}}.
\end{aligned}$$

Applying Theorem 1.4.5 with $\beta_r = (-1)^r\ \Gamma(m-p+1)\binom{p-m-1}{r}r^{p-m}$ and $\alpha_{n,r} = h(rh)^{m-p}\frac{\Delta^{m+1}f(t-rh)}{h^{m+1}}$ (again using $h = (t-a)/n$), we check that, using Equation (1.18), we have $\lim_{r\to\infty}\beta_r = 1$. We can also see that if $m-p > -1$,

$$\begin{aligned}
\lim_{n\to\infty}\sum_{r=0}^{n-m-1}\alpha_{n,r} &= \lim_{\substack{h\to 0\\ nh=t-a}}\sum_{r=0}^{n-m-1}h(rh)^{m-p}\frac{\Delta^{m+1}f(t-rh)}{h^{m+1}}\\
&=\int_a^t (t-\tau)^{m-p}f^{(m+1)}(\tau)\,d\tau.
\end{aligned}$$

With this, we can finally conclude that

$$\begin{aligned}
{}^{GL}_{\ a}\mathbf{D}^p_t f(t) &= \lim_{\substack{h\to 0\\ nh=t-a}} f_h^{(p)}(t)\\
&=\sum_{k=0}^{m}\frac{f^{(k)}(a)(t-a)^{k-p}}{\Gamma(k-p+1)}+\frac{1}{\Gamma(m-p+1)}\int_a^t (t-\tau)^{m-p}f^{(m+1)}(\tau)\,d\tau,
\end{aligned}$$

with $m \le p < m+1$. Now, by Lemma 1.2.7 we conclude that

$${}^{GL}_{\ a}\mathbf{D}^p_t f(t) = \sum_{k=0}^{m}\frac{f^{(k)}(a)(t-a)^{k-p}}{\Gamma(k-p+1)}+\frac{1}{\Gamma(m-p+1)}\int_a^t (t-\tau)^{m-p}f^{(m+1)}(\tau)\,d\tau = {}^{RL}_{\ a}\mathbf{D}^p_t f(t)$$

and, therefore, that

$$\boxed{{}^{GL}_{\ a}\mathbf{D}^p_t f(t) = {}^{RL}_{\ a}\mathbf{D}^p_t f(t) \quad \text{for all } p\in\mathbb{R}.} \tag{1.20}$$

1.5 Caputo fractional derivative

The Caputo derivative is similar in flavour to the Riemann-Liouville definition, but it interchanges the integral and differential order when we look at fractional derivatives.

Definition 1.5.1. The *Caputo fractional derivative* for non-integer $\alpha\in\mathbb{R}$ is given by

$${}^{C}_{a}\mathbf{D}^\alpha_t f(t) = \frac{1}{\Gamma(n-\alpha)}\int_a^t \frac{f^{(n)}(\tau)}{(t-\tau)^{\alpha-n+1}}\,d\tau \quad \text{with} \quad n-1<\alpha<n.$$

The first question is what happens if we take a limit of α going to an integer and if it will coincide with the regular derivative on integers. For $\alpha\to n-1$, we have

$$\begin{aligned}
\lim_{\alpha\to n-1}{}^{C}_{a}\mathbf{D}^\alpha_t f(t) &= \lim_{\alpha\to n-1}\frac{1}{\Gamma(n-\alpha)}\int_a^t \frac{f^{(n)}(\tau)}{(t-\tau)^{\alpha-n+1}}\,d\tau\\
&=\frac{1}{\Gamma(1)}\int_a^t f^{(n)}(\tau)\,d\tau\\
&=f^{(n-1)}(t)-f^{(n-1)}(a).
\end{aligned}$$

For $\alpha \to n$, we first integrate by parts to get

$$\begin{aligned}
{}_a^C\mathbf{D}_t^\alpha f(t) &= \frac{1}{\Gamma(n-\alpha)} \int_a^t \frac{f^{(n)}(\tau)}{(t-\tau)^{\alpha-n+1}}\, d\tau \\
&= \frac{f^{(n)}(a)(t-a)^{n-\alpha}}{\Gamma(n-\alpha+1)} + \frac{1}{\Gamma(n-\alpha+1)} \int_a^t \frac{f^{(n+1)}(\tau)}{(t-\tau)^{\alpha-n}}\, d\tau.
\end{aligned}$$

Now, simply taking the limit, we obtain

$$\begin{aligned}
\lim_{\alpha\to n} {}_a^C\mathbf{D}_t^\alpha f(t) &= \lim_{\alpha\to n} \frac{f^{(n)}(a)(t-a)^{n-\alpha}}{\Gamma(n-\alpha+1)} + \frac{1}{\Gamma(n-\alpha+1)} \int_a^t \frac{f^{(n+1)}(\tau)}{(t-\tau)^{\alpha-n}}\, d\tau \\
&= f^{(n)}(a) + \int_a^t f^{(n+1)}(\tau)\, d\tau \\
&= f^{(n)}(t).
\end{aligned}$$

We, therefore, find that the Caputo derivative is discontinuous at the integer derivatives, namely,

$$\boxed{\lim_{\alpha\uparrow n} {}_a^C\mathbf{D}_t^\alpha f(t) = \lim_{\alpha\downarrow n} {}_a^C\mathbf{D}_t^\alpha f(t) + f^{(n)}(a) = f^{(n)}(t).} \tag{1.21}$$

Let us consider some examples.

Example 1.5.2. The Caputo derivative of the power function $f(t) = (t-a)^\nu$ is given by

$${}_a^C\mathbf{D}_t^\alpha (t-a)^\nu = \frac{1}{\Gamma(n-\alpha)} \int_a^t \frac{\frac{d^n}{d\tau^n}(\tau-a)^\nu}{(t-\tau)^{\alpha-n+1}}\, d\tau.$$

We can now see that if ν is an integer smaller than n, then we have ${}_a^C\mathbf{D}_t^\alpha f(t) = 0$. If this is not the case, then we have

$$\begin{aligned}
{}_a^C\mathbf{D}_t^\alpha (t-a)^\nu &= \frac{1}{\Gamma(n-\alpha)} \int_a^t \frac{\Gamma(\nu+1)}{\Gamma(\nu-n+1)} (\tau-a)^{\nu-n} (t-\tau)^{-\alpha+n-1}\, d\tau \\
[\text{ set } \tau = a + z(t-a) \text{]} \quad &= \frac{\Gamma(\nu+1)}{\Gamma(n-\alpha)\Gamma(\nu-n+1)} \int_0^1 (z(t-a))^{\nu-n}((1-z)(t-a))^{-\alpha+n-1}(t-a)d\tau \\
&= \frac{\Gamma(\nu+1)}{\Gamma(n-\alpha)\Gamma(\nu-n+1)} (t-a)^{\nu-\alpha} \int_0^1 z^{\nu-n}(1-z)^{-\alpha+n-1}\, d\tau \\
&= \frac{\Gamma(\nu+1)}{\Gamma(n-\alpha)\Gamma(\nu-n+1)} (t-a)^{\nu-\alpha} B(\nu-n+1, n-\alpha) \\
&= \frac{\Gamma(\nu+1)}{\Gamma(\nu-\alpha+1)} (t-a)^{\nu-\alpha},
\end{aligned}$$

which is the same as for the Riemann-Liouville definition. △

By Lemma 1.2.7, we can see a relation between the Caputo and Riemann-Liouville definitions. In case that $0 \le n-1 < p < n$, namely,

$$\boxed{\begin{aligned}
{}_a^{RL}\mathbf{D}_t^p f(t) &= \sum_{k=0}^{n-1} \frac{f^{(k)}(a)(t-a)^{k-p}}{\Gamma(k-p+1)} + \frac{1}{\Gamma(n-p)} \int_a^t (t-\tau)^{n-p-1} f^{(n)}(\tau)\, d\tau \\
&= \sum_{k=0}^{n-1} \frac{f^{(k)}(a)(t-a)^{k-p}}{\Gamma(k-p+1)} + {}_a^C\mathbf{D}_t^p f(t),
\end{aligned}}$$

which means that for $0 \leq n-1 < p < n$,

$$\boxed{{}_a^C\mathbf{D}_t^p f(t) = {}_a^{RL}\mathbf{D}_t^p f(t) \quad \Longleftrightarrow \quad f^{(k)}(a) = 0 \quad \text{for all} \quad k = 0, 1, \dots, n-1.} \tag{1.22}$$

We can also see from the definition that

$${}_a^{RL}\mathbf{D}_t^{p-n} \frac{d^n}{dt^n} f(t) = \frac{1}{\Gamma(n-p)} \int_a^t (t-\tau)^{n-p-1} f^{(n)}(\tau)\, d\tau = {}_a^C\mathbf{D}_t^p f(t). \tag{1.23}$$

If we try to combine integer order derivatives with the Caputo derivatives, we can quickly find the following result. For $n-1 < \alpha < n$ and $0 \leq n, m \in \mathbb{Z}$, then $n+m-1 < \alpha+m < n+m$. Thus,

$$\begin{aligned}
{}_a^C\mathbf{D}_t^{\alpha+m} f(t) &= \frac{1}{\Gamma[(n+m)-(\alpha+m)]} \int_a^t \frac{f^{(n+m)}(\tau)}{(t-\tau)^{(\alpha+m)-(n+m)+1}}\, d\tau \\
&= \frac{1}{\Gamma(n-\alpha)} \int_a^t \frac{f^{(n+m)}(\tau)}{(t-\tau)^{\alpha-n+1}}\, d\tau \\
&= {}_a^C\mathbf{D}_t^\alpha f^{(m)}(t).
\end{aligned}$$

To put this result in contrast, with Riemann-Liouville we find

$${}_a^{RL}\mathbf{D}_t^{\alpha+m} f(t) = {}_a^{RL}\mathbf{D}_t^\alpha f^{(m)}(t) - \sum_{j=1}^{m+1} f^{(m-j)}(a) \frac{(t-a)^{-\alpha-j}}{\Gamma(-\alpha-j+1)}$$

by Theorem 1.2.18.

If we now interchange the orders, then, for the Caputo derivative, we have

$$\begin{aligned}
\frac{d^m}{dt^m} {}_a^C\mathbf{D}_t^\alpha f(t) &= \frac{d^m}{dt^m} \frac{1}{\Gamma(n-\alpha)} \int_a^t (t-\tau)^{n-\alpha-1} f^{(n)}(\tau)\, d\tau \\
&= \frac{1}{\Gamma(n-\alpha)} \int_a^t \frac{\Gamma(n-\alpha)}{\Gamma(n-\alpha-m)} (t-\tau)^{n-\alpha-m-1} f^{(n)}(\tau)\, d\tau \\
&= \frac{1}{\Gamma(n-\alpha-m)} \left(\left[\frac{(t-\tau)^{n-\alpha-m}}{n-\alpha-m} f^{(n)}(\tau) \right]_{\tau=a}^{t} + \int_a^t \frac{(t-\tau)^{n-\alpha-m}}{n-\alpha-m} f^{(n+1)}(\tau)\, d\tau \right) \\
&= \frac{1}{\Gamma(n-\alpha-m+1)} \left(-(t-a)^{n-\alpha-m} f^{(n)}(a) + \int_a^t (t-\tau)^{n-\alpha-m} f^{(n+1)}(\tau)\, d\tau \right) \\
&= -\frac{(t-a)^{n-\alpha-m} f^{(n)}(a)}{\Gamma(n-\alpha-m+1)} - \frac{(t-a)^{n-\alpha-m+1} f^{(n+1)}(a)}{\Gamma(n-\alpha-m+2)} \\
&\quad + \frac{1}{\Gamma(n-\alpha-m+2)} \int_a^t (t-\tau)^{n-\alpha-m+1} f^{(n+2)}(\tau)\, d\tau \\
&= \dots \\
&= -\sum_{k=0}^{m-1} \frac{(t-a)^{n-\alpha-m+k} f^{(n+k)}(a)}{\Gamma(n-\alpha-m+k+1)} + \frac{1}{\Gamma(n-\alpha)} \int_a^t (t-\tau)^{n-\alpha-1} f^{(n+m)}(\tau)\, d\tau \\
&= -\sum_{k=0}^{m-1} \frac{(t-a)^{n-\alpha-m+k} f^{(n+k)}(a)}{\Gamma(n-\alpha-m+k+1)} + {}_a^C\mathbf{D}_t^\alpha f^{(m)}(t).
\end{aligned}$$

Accordingly, if $f^{(k)}(a) = 0$ for $k = n, n+1, \ldots, n+m-1$, then we obtain

$$\boxed{\frac{d^m}{dt^m}\, {}_a^C\mathbf{D}_t^\alpha f(t) = {}_a^C\mathbf{D}_t^\alpha f^{(m)}(t) = {}_a^C\mathbf{D}_t^{\alpha+m} f(t).} \tag{1.24}$$

In contrast, with Riemann-Liouville, we do have $\frac{d^m}{dt^m}\, {}_a^{RL}\mathbf{D}_t^p f(t) = {}_a^{RL}\mathbf{D}_t^{p+m} f(t)$, but

$${}_a^{RL}\mathbf{D}_t^p f^{(m)}(t) = {}_a^{RL}\mathbf{D}_t^{p+m} f(t) + \sum_{k=0}^{m-1} f^{(k)}(a)\frac{(t-a)^{k-p-m}}{\Gamma(k-p-m+1)}.$$

Therefore, if $f^{(k)}(a) = 0$ for $k = 0, 1, \ldots, m-1$, we arrive at

$$\boxed{\frac{d^m}{dt^m}\, {}_a^{RL}\mathbf{D}_t^\alpha f(t) = {}_a^{RL}\mathbf{D}_t^\alpha \frac{d^m}{dt^m} f(t) = {}_a^{RL}\mathbf{D}_t^{\alpha+m} f(t).} \tag{1.25}$$

Remark 1.5.3. It is important to note that these last two results are in disagreement with Podlubny [25, p. 81].

Lemma 1.5.4. *The Laplace transform of the Caputo derivative of order $\alpha > 0$ and initial time $a = 0$, is given by*

$$\boxed{\mathcal{L}\left({}_0^C\mathbf{D}_t^\alpha f(t); s\right) = s^\alpha F(s) - \sum_{k=0}^{n-1} s^{\alpha-1-k} f^{(k)}(0)} \tag{1.26}$$

Proof. Suppose $n - 1 \leq \alpha < n$ for $n \in \mathbb{N}$, then ${}_0^C\mathbf{D}_t^\alpha f(t) = {}_0^{RL}\mathbf{D}_t^{\alpha-n} f^{(n)}(t)$. Therefore, by Lemma 1.2.19 and Example 1.1.11, we find

$$\begin{aligned}
\mathcal{L}\left({}_0^C\mathbf{D}_t^\alpha f(t); s\right) &= \mathcal{L}\left({}_0^{RL}\mathbf{D}_t^{\alpha-n} f^{(n)}(t); s\right) \\
&= s^{\alpha-n}\mathcal{L}\left(f^{(n)}(t); s\right) \\
&= s^{\alpha-n}\left(s^n F(s) - \sum_{k=0}^{n-1} s^{n-1-k} f^{(k)}(0)\right) \\
&= s^\alpha F(s) - \sum_{k=0}^{n-1} s^{\alpha-1-k} f^{(k)}(0).
\end{aligned}$$

□

1.6 Weyl fractional derivative

The Weyl fractional integral is based on the idea of Fourier transforms. To start with ordinary derivatives, as seen in Section 1.1.1, the derivative of order $n \in \mathbb{Z}$ can be given in Fourier space by

$$\mathcal{F}\left(\mathbf{D}^n f(t); \omega\right) = (i\omega)^n \mathcal{F}\left(f(t); \omega\right).$$

Clearly, this only works for functions which are Fourier transformable, i.e. $f(t) \in L^2(\mathbb{R}) := \left\{ f(x) \mid \left(\int_{-\infty}^{\infty} |f(x)|^2\, dx\right)^{1/2} < \infty \right\}$, and periodic functions. For these functions, the derivative can be easily generalised to non-integer n.

Definition 1.6.1. For $f(t) \in L^2(\mathbb{R}) = \left\{ g(t) \mid \left(\int_{-\infty}^{\infty} |g(t)|^2 \, dt \right)^{1/2} < \infty \right\}$, the *Weyl fractional integral* of order $\alpha \in \mathbb{R}$ is given by

$$ {}^{W}\mathbf{D}_t^{\alpha} f(t) = \mathcal{F}^{-1}\left((i\omega)^{\alpha} \mathcal{F}\left(f(t); \omega \right); t \right) = \frac{1}{2\pi} \int_{-\infty}^{\infty} \int_{-\infty}^{\infty} (i\omega)^{\alpha} f(\tau) e^{i\omega(t-\tau)} \, d\tau \, d\omega. $$

Lemma 1.6.2. *The Weyl definition is equivalent to the Liouville definition (from Section 1.3), if $f(t)$ satisfies Equation (1.13).*

Proof. We have already seen that $\mathcal{F}\left({}^{L}\mathbf{D}_t^{\alpha} f(t); \omega \right) = (i\omega)^{\alpha} \mathcal{F}\left(f(t); \omega \right)$. Therefore, we find that

$$ \begin{aligned} {}^{L}\mathbf{D}_t^{\alpha} f(t) &= \mathcal{F}^{-1}\left(\mathcal{F}\left({}^{L}\mathbf{D}_t^{\alpha}; \omega \right); t \right) \\ &= \mathcal{F}^{-1}\left((i\omega)^{\alpha} \mathcal{F}\left(f(t); \omega \right); t \right) \\ &= {}^{W}\mathbf{D}_t^{\alpha} f(t). \end{aligned} $$

□

In particular, we can see that any definition that is compatible with Fourier transforms under particular conditions is in fact equivalent to the Weyl definition, under those same conditions. It also means that, any definition that is compatible with Fourier transforms has to "know" about the entire past of a function.

Lemma 1.6.3. *Let $\alpha, \beta \in \mathbb{R}$. Then*

$$ \boxed{ {}^{W}\mathbf{D}_t^{\beta} \, {}^{W}\mathbf{D}_t^{\alpha} f(t) = {}^{W}\mathbf{D}_t^{\alpha+\beta} f(t). } $$

Proof. Using the fact that the Fourier transform is invertible, we find

$$ \begin{aligned} {}^{W}\mathbf{D}_t^{\beta} \, {}^{W}\mathbf{D}_t^{\alpha} f(t) &= {}^{W}\mathbf{D}_t^{\beta} \mathcal{F}^{-1}\left((i\omega)^{\alpha} f(\omega); t \right) \\ &= \mathcal{F}^{-1}\left((i\omega)^{\beta} \mathcal{F}\left(\mathcal{F}^{-1}\left((i\omega)^{\alpha} f(\omega); t \right); \omega \right); t \right) \\ &= \mathcal{F}^{-1}\left((i\omega)^{\beta} (i\omega)^{\alpha} f(\omega); t \right) \\ &= \mathcal{F}^{-1}\left((i\omega)^{\alpha+\beta} f(\omega); t \right) \\ &= {}^{W}\mathbf{D}_t^{\alpha+\beta} f(t). \end{aligned} $$

□

Remark 1.6.4. This is actually quite a remarkable Lemma, as this is not true for ordinary derivatives. The main reason this Lemma works is due to the restriction that $f(t) \in L^2(\mathbb{R})$. This prohibits one from adding any polynomial, like we have seen before with Riemann-Liouville and Caputo derivatives, since polynomials do not tend to 0 at infinity.

1.7 A summary of fractional derivatives

We use the notation ${}^{X}_{a}\mathbf{D}_t f(t)$ for the fractional derivative named after Riemann-Liouville, Liouvile, Grünwald-Letnikov, Caputo, and Weyl, with notation $X \in \{RL, L, GL, C, W\}$; for Liouville and Weyl, we omit the $a = -\infty$ from the notation to stress the need for the extra restrictions these definitions have. Here, we show various properties of fractional derivatives, the details of which can all be found in Sections 1.2-1.6.

- The following list is an overview of which formulas have been proven, in such order that, any one formula can be proven using only the formulas that came before it. Let $p, q > 0$, $\nu \in \mathbb{R}$, $n-1 \leq p < n$, and $m-1 \leq q < m$, with $n, m \in \mathbb{N}$. Then, for the Riemann-Liouville derivative, we have

$$ {}^{RL}_{a}\mathbf{D}_t^{-p} f(t) = \frac{1}{\Gamma(p)} \int_a^t (t-\tau)^{p-1} f(\tau)\, d\tau, \tag{1.27}$$

$$ {}^{RL}_{a}\mathbf{D}_t^{p} f(t) = \frac{d^n}{dt^n}\, {}^{RL}_{a}\mathbf{D}_t^{p-n} f(t), \tag{1.28}$$

$$ {}^{RL}_{a}\mathbf{D}_t^{p} (t-a)^{\nu} = \frac{\Gamma(\nu+1)}{\Gamma(\nu-p+1)} (t-a)^{\nu-p}, \tag{1.29}$$

$$ \frac{d^n}{dt^n}\, {}^{RL}_{a}\mathbf{D}_t^{\pm q} f(t) = {}^{RL}_{a}\mathbf{D}_t^{n\pm q} f(t), \tag{1.30}$$

$$ {}^{RL}_{a}\mathbf{D}_t^{p} f(t) = \sum_{k=0}^{n-1} f^{(k)}(a) \frac{(t-a)^{k-p}}{\Gamma(k-p+1)} + {}^{RL}_{a}\mathbf{D}_t^{p-n} f^{(n)}(t), \tag{1.31}$$

$$ {}^{RL}_{a}\mathbf{D}_t^{\pm q}\, {}^{RL}_{a}\mathbf{D}_t^{-p} f(t) = {}^{RL}_{a}\mathbf{D}_t^{\pm q-p} f(t), \tag{1.32}$$

$$ {}^{RL}_{a}\mathbf{D}_t^{q} f^{(n)}(t) = {}^{RL}_{a}\mathbf{D}_t^{n+q} f(t) + \sum_{k=0}^{n-1} \frac{f^{(k)}(a)(t-a)^{k-q-n}}{\Gamma(k-q-n+1)}, \tag{1.33}$$

$$ {}^{RL}_{a}\mathbf{D}_t^{-p}\, {}^{RL}_{a}\mathbf{D}_t^{p} f(t) = f(t) - \sum_{j=1}^{n} \left({}^{RL}_{a}\mathbf{D}_t^{p-j} f \right)(a) \frac{(t-a)^{p-j}}{\Gamma(p-j+1)}, \tag{1.34}$$

$$ {}^{RL}_{a}\mathbf{D}_t^{-p}\, {}^{RL}_{a}\mathbf{D}_t^{q} f(t) = {}^{RL}_{a}\mathbf{D}_t^{q-p} f(t) - \sum_{j=1}^{m} \left({}^{RL}_{a}\mathbf{D}_t^{q-j} f \right)(a) \frac{(t-a)^{p-j}}{\Gamma(p-j+1)}, \tag{1.35}$$

$$ {}^{RL}_{a}\mathbf{D}_t^{p}\, {}^{RL}_{a}\mathbf{D}_t^{q} f(t) = {}^{RL}_{a}\mathbf{D}_t^{p+q} f(t) + \sum_{j=1}^{m} \left({}^{RL}_{a}\mathbf{D}_t^{q-j} f \right)(a) \frac{(t-a)^{-p-j}}{\Gamma(-p-j+1)}, \tag{1.36}$$

$$ \mathcal{L}\left({}^{RL}_{0}\mathbf{D}_t^{-p} f(t); s \right) = s^{-p} F(s), \tag{1.37}$$

$$ \mathcal{L}\left({}^{RL}_{0}\mathbf{D}_t^{p} f(t); s \right) = s^{p} F(s) - \sum_{k=0}^{n-1} s^k \left({}^{RL}_{0}\mathbf{D}_t^{p-k-1} f \right)(0). \tag{1.38}$$

- A particular case of the Riemann-Liouville definition is when $a = -\infty$, called the Liouville fractional derivative. As one can see from the formulas above, one has to be careful with a possible divergence of the integrals when $a \to -\infty$. For this, it is necessary to assume that $\lim\limits_{t\to-\infty} f^{(n)}(t) t^{\alpha} = 0$, for all $n = 0, 1, \ldots, K$ and all $\alpha < K$ with K larger than the orders of the derivatives. Whenever a function satisfies this condition and is Fourier transformable[6], the Liouville derivative is compatible with Fourier transformations[7], in the sense that

$$\mathcal{F}\left({}^{L}\mathbf{D}_t^\alpha f(t);\omega\right) = (i\omega)^\alpha \mathcal{F}\left(f(t);\omega\right) \quad \text{for all } \alpha \in \mathbb{R}. \tag{1.39}$$

- The Grünwald-Letnikov derivative is equal to the Riemann-Liouville derivative as long as the functions are smooth enough[8]. It can be a particularly useful definition for numerical purposes, both by itself and for numerical calculations with Riemann-Liouville derivatives as they can be calculated faster with Grünwald-Letnikov derivatives as shown in MacDonald et al. [33] and Weilbeer [34].

- The Caputo definition is only valid for derivatives, while its integral form can be seen as the regular Riemann-Liouville integral. Another important property that one has to be careful with is when changing the order of Caputo derivatives, as it is discontinuous at the integers:

$$\lim_{\alpha\uparrow n} {}_a^C\mathbf{D}_t^\alpha f(t) = \lim_{\alpha\downarrow n} {}_a^C\mathbf{D}_t^\alpha f(t) + f^{(n)}(a) = f^{(n)}(t). \tag{1.40}$$

- A relation between the Riemann-Liouville and Caputo derivatives exists, and is given by

$${}_a^{RL}\mathbf{D}_t^p f(t) = \sum_{k=0}^{n-1} \frac{f^{(k)}(a)(t-a)^{k-p}}{\Gamma(k-p+1)} + {}_a^C\mathbf{D}_t^p f(t). \tag{1.41}$$

  This implies that the two definitions are equal if $f^{(k)}(a) = 0$ for all positive integers $k < p$, with p the order of the derivative. The Laplace transform of the Caputo derivative of order $n-1 \leq p < n$ with $n \in \mathbb{N}$, is given by

$$\mathcal{L}\left({}_0^C\mathbf{D}_t^p f(t);s\right) = s^p F(s) - \sum_{k=0}^{n-1} s^{p-k-1} f^{(k)}(0). \tag{1.42}$$

  Remark the difference with Riemann-Liouville, we essentially moved the fractional term from the order of the derivative to the power of s.

- The Weyl definition is directly based on Fourier transforms, which also implies one needs the entire history of a function in order to use it. As long as a function satisfies both the requirements of the derivative definition and is Fourier transformable, any definition that is compatible with Fourier transforms can be shown to be equivalent to the Weyl definition for those functions.

[6] Neither condition implies the other.
[7] Note, that this is not generally the case for Riemann-Liouville derivatives.
[8] They should be continuously differentiable up to an order higher than the order of the derivative

2 Fractional differential equations

One of the main applications of fractional derivatives can be found in fractional differential equations (FDE's). Before we discuss these, let us first give a reminder about ordinary differential equations (ODE's) and how some can be solved. We will then look at which initial conditions are needed for FDE's and solve some examples with different definitions and techniques. Finally, we will see which impacts the choice of definition has on the solution of an FDE.

2.1 Ordinary differential equations

Let us start by examining some properties of ODE's.

Example 2.1.1. Suppose $u'(t) = cu(t)$, for some constant $c \in \mathbb{R}$ and function $u(t)$. Let us denote the formal power-series expansion of $u(t)$ by

$$u(t) = \sum_{k=0}^{\infty} u_k \frac{t^k}{k!}.$$

If we substitute this expansion in the ODE, we find

$$\sum_{k=0}^{\infty} u_{k+1} \frac{t^k}{k!} = \sum_{k=0}^{\infty} c u_k \frac{t^k}{k!}$$

and we can see the recursive relation $u_{k+1} = cu_k$ for $k > 0$. This solves to $u_k = c^k u_0$, which gives

$$u(t) = \sum_{k=0}^{\infty} u_0 \frac{(ct)^k}{k!} = u_0 e^{ct},$$

where $u_0 = u(0)$ is the initial condition. △

Example 2.1.2. Suppose $u''(t) = cu(t)$ for some constant $c < 0$ and function $u(t)$. Taking the Fourier transform of both sides, we find $-\omega^2 u(\omega) = cu(\omega)$, or $(c + \omega^2)u(\omega) = 0$. Hence, either $\omega = \pm i\sqrt{c}$ or $u(\omega) = 0$. This admits a solution of the form $u(\omega) = A\,\delta(\omega - i\sqrt{c}) + B\,\delta(\omega + i\sqrt{c})$, for some constants A and B. We, therefore, find that

$$\begin{aligned} u(t) &= \int_{-\infty}^{\infty} u(\omega) e^{i\omega t}\, d\omega \\ &= \int_{-\infty}^{\infty} \left(A\,\delta(\omega - i\sqrt{c}) + B\,\delta(\omega + i\sqrt{c})\right) e^{i\omega t}\, d\omega \\ &= Ae^{\sqrt{c}t} + Be^{-\sqrt{c}t}. \end{aligned}$$

If we want to solve for A and B, using initial conditions, we need to set $u(0) = u_0$ and $u'(0) = u_0'$. These conditions give $A + B = u_0$ and $\sqrt{c}(A - B) = u_0'$, which has the solution $A = \frac{\sqrt{c}u_0 + u_0'}{2\sqrt{c}}$ and $B = \frac{\sqrt{c}u_0 - u_0'}{2\sqrt{c}}$. Hence,

$$u(t) = \frac{\sqrt{c}u_0 + u_0'}{2\sqrt{c}} e^{\sqrt{c}t} + \frac{\sqrt{c}u_0 - u_0'}{2\sqrt{c}} e^{-\sqrt{c}t} = u_0 \left(\frac{e^{\sqrt{c}t} + e^{-\sqrt{c}t}}{2}\right) + u_0' \left(\frac{e^{\sqrt{c}t} - e^{-\sqrt{c}t}}{2\sqrt{c}}\right).$$

Remark that this solution actually also works for $c > 0$, but our solving method does not work then, as $\omega = \pm i\sqrt{c}$ is not a solution, since both ω and $\sqrt{c}$ are real-valued. This is due to the restriction of Fourier transformable functions that they have to be integrable over $\mathbb{R}$, which is not the case for real exponents.

Now, suppose $c = -k^2$, then $\sqrt{c} = ik$ and we obtain

$$u(t) = u_0 \cos(kt) + u_0' \sin(kt).$$

$\triangle$

Example 2.1.3. Let us consider a similar equation as the previous example: $u''(t) = cu(t)$, but now with $c > 0$. Let us use the formal power series in order to solve it. We write $u(t) = \sum_{k=0}^{\infty} u_k \frac{t^k}{k!}$ and plugging this into the ODE we find

$$\sum_{k=0}^{\infty} u_{k+2} \frac{t^k}{k!} = \sum_{k=0}^{\infty} cu_k \frac{t^k}{k!},$$

which gives the recursive relation $u_{k+2} = cu_k$. Separating even and uneven indices, we find that $u_{2k} = c^k u_0$ and $u_{2k+1} = c^k u_1$. This gives us the solution

$$u(t) = \sum_{k=0}^{\infty} u_0 \frac{(t\sqrt{c})^{2k}}{(2k)!} + \frac{u_1}{\sqrt{c}} \frac{(t\sqrt{c})^{2k+1}}{(2k+1)!} = u_0 \left(\frac{e^{\sqrt{c}t} + e^{-\sqrt{c}t}}{2} \right) + u_1 \left(\frac{e^{\sqrt{c}t} - e^{-\sqrt{c}t}}{2\sqrt{c}} \right).$$

Note, that this is equal to the solution of the previous example. $\triangle$

Notice how the number of initial conditions is equal to the order of the derivative taken. Indeed, this is a property which holds for all ODE's. This property can be seen more generally in the following Example:

Example 2.1.4. (Initial conditions) Suppose we want to obtain $f(t) = g(t)$ from $\frac{d^n}{dt^n} f(t) = \frac{d^n}{dt^n} g(t)$ for a given $g(t)$. We can take the n^{th} integral, with initial time $t = 0$, to obtain

$$f(t) = g(t) + \sum_{k=0}^{n-1} \frac{f_k t^k}{k!}, \tag{2.1}$$

with f_k some arbitrary constants. Since we want f to be equal to g, we have to demand that $f^{(k)}(0) = g^{(k)}(0)$, for all $k = 0, 1, \ldots, n-1$, to remove the extra polynomial. $\triangle$

2.2 Initial conditions for FDE's

Let us use the setup of Example 2.1.4, but for fractional order. Suppose $\alpha > 0$, $n - 1 \leq \alpha < n$, for some $n \in \mathbb{Z}$, and we want to obtain $f(t) = g(t)$ by solving ${}^{RL}_{0}\mathbf{D}^{\alpha}_{t} f(t) = {}^{RL}_{0}\mathbf{D}^{\alpha}_{t} g(t)$. We can integrate this equation, using Theorem 1.2.18, to get

$$f(t) = g(t) + \sum_{j=1}^{n} f_j \frac{t^{\alpha-j}}{\Gamma(\alpha - j + 1)}. \tag{2.2}$$

This means that, for non-integer α, we need the initial conditions $({}^{RL}_{0}\mathbf{D}^{\alpha-j}_{t} f)(0) = ({}^{RL}_{0}\mathbf{D}^{\alpha-j}_{t} g)(0)$ for $j = 1, 2, \ldots, n$ to get $f(t) = g(t)$.

Example 2.2.1. Suppose we want to solve $f(t) = g(t)$ from ${}^{RL}_{0}\mathbf{D}_t^{1/2} f(t) = {}^{RL}_{0}\mathbf{D}_t^{1/2} g(t)$, then we need the initial condition $({}^{RL}_{0}\mathbf{D}_t^{-1/2} f)(0) = ({}^{RL}_{0}\mathbf{D}_t^{-1/2} g)(0)$. Observe that this is a condition on a fractional integral rather than a derivative. △

Suppose we want to do the same as before, but now with Caputo derivatives rather than Riemann-Liouville derivatives. Recall the relation between the two derivatives of order $\alpha > 0$ with $n-1 \leq \alpha < n$:

$$ {}^{C}_{0}\mathbf{D}_t^{\alpha} f(t) = {}^{RL}_{0}\mathbf{D}_t^{\alpha-n} f^{(n)}(t). $$

This combined with Theorem 1.2.18 implies that

$$ {}^{RL}_{0}\mathbf{D}_t^{-\alpha}\, {}^{C}_{0}\mathbf{D}_t^{\alpha} f(t) = {}^{RL}_{0}\mathbf{D}_t^{-\alpha}\, {}^{RL}_{0}\mathbf{D}_t^{\alpha-n} f^{(n)}(t) = \mathbf{D}^{-n} f^{(n)}(t) = f(t) - \sum_{k=0}^{n-1} \frac{f^{(k)}(0) t^k}{k!}. \tag{2.3} $$

This means that solving ${}^{C}_{0}\mathbf{D}_t^{\alpha} f(t) = {}^{C}_{0}\mathbf{D}_t^{\alpha} g(t)$, will give

$$ f(t) = g(t) + \sum_{k=0}^{n-1} \frac{f_k t^k}{k!}, $$

and we need the initial conditions $f^{(k)}(0) = g^{(k)}(0)$, for $k = 0, 1, \ldots, n-1$.

Example 2.2.2. Suppose we want to solve $f(t) = g(t)$ from ${}^{C}_{0}\mathbf{D}_t^{1/2} f(t) = {}^{C}_{0}\mathbf{D}_t^{1/2} g(t)$, then, by the above argument, we only need $f(0) = g(0)$ as the initial condition. △

Suppose we want to solve $f(t) = g(t)$ from ${}^{W}\mathbf{D}_t^{\alpha} f(t) = {}^{W}\mathbf{D}_t^{\alpha} g(t)$, then, since any orders directly add up, we directly get $f(t) = g(t)$ by integration. Interestingly, there is no need for any boundary conditions due to the restrictions needed for Fourier transforms to be used. The functions $f(t)$ and $g(t)$ need to go to 0 quickly enough for $t \to \pm\infty$, restricting us from adding any polynomial, since these do not go to 0 when $t \to \pm\infty$.

2.3 Some example fractional differential equations

As seen in Section 2.1, there are many ways to solve ODE's. Which method works best is highly dependant on the type of equation one is dealing with. In particular for FDE's, some methods do not even work with some definitions of fractional derivatives. As shown in Chapter 1, Fourier transforms are only compatible with Weyl and Liouville transformations, while Laplace transformations only work with Riemann-Liouville and Caputo derivatives with initial time $a = 0$. In this Section, we will try some different methods with all nonequivalent compatible derivatives that we discussed in Chapter 1.

2.3.1 Solutions obtained by Fourier transformations

Let us start with $t_0 = -\infty$ as the initial time of a system and use Weyl fractional differential operators. Let $\alpha, \beta, \gamma, a, b, c \in \mathbb{R}$ and $g(t)$ some Fourier transformable function, then we can use Fourier transforms to solve the following examples:

Example 2.3.1. Suppose that

$$a\,{}^W\mathbf{D}_t^\alpha f(t) = g(t),$$

then the Fourier transform of both sides gives
$f(\omega) = \frac{(i\omega)^{-\alpha}}{a} g(\omega)$, or $f(t) = \frac{1}{a}\,{}^W\mathbf{D}_t^{-\alpha} g(t)$. △

Example 2.3.2. Suppose that

$$a\,{}^W\mathbf{D}_t^\alpha f(t) + b\,{}^W\mathbf{D}_t^\beta f(t) = g(t),$$

then the Fourier transform of both sides gives $a(i\omega)^\alpha f(\omega) + b(i\omega)^\beta f(\omega) = g(\omega)$, or

$$f(\omega) = \frac{g(\omega)}{a(i\omega)^\alpha + b(i\omega)^\beta}.$$

Fourier transforming back, we find

$$f(t) = \int_{-\infty}^{\infty} \frac{g(\omega)e^{i\omega t}}{a(i\omega)^\alpha + b(i\omega)^\beta}\, d\omega = \frac{1}{2\pi}\int_{-\infty}^{\infty}\int_{-\infty}^{\infty} \frac{g(\tau)e^{i\omega(t-\tau)}}{a(i\omega)^\alpha + b(i\omega)^\beta}\, d\tau\, d\omega.$$

△

Example 2.3.3. Suppose that

$${}^W\mathbf{D}_t^2 f(t) + {}^W\mathbf{D}_t^{1/2} f(t) = \sin(t).$$

The Fourier transform of the sine is given by

$$\begin{aligned}\sin(\omega) &= \frac{1}{2\pi}\int_{-\infty}^{\infty} \sin(t)e^{-i\omega t}\, dt = \frac{1}{4i\pi}\int_{-\infty}^{\infty} \left(e^{it} - e^{-it}\right) e^{-i\omega t}\, dt \\ &= \frac{1}{4i\pi}\int_{-\infty}^{\infty} \left(e^{i(1-\omega)t} - e^{-i(1+\omega)t}\right)\, dt = \frac{\delta(1-\omega) - \delta(1+\omega)}{2i}.\end{aligned}$$

By Example 2.3.2, we thus find that

$$\begin{aligned}f(t) &= \int_{-\infty}^{\infty} \frac{(\delta(1-\omega) - \delta(1+\omega))e^{i\omega t}}{2i(-\omega^2 + (i\omega)^{1/2})}\, d\omega \\ &= \frac{1}{2i}\left(\frac{e^{it}}{-1+\sqrt{i}} - \frac{e^{-it}}{-1+\sqrt{-i}}\right) \\ &= \frac{1}{2i}\left(\frac{i\sin(t)+\cos(t)}{-1+\sqrt{i}} + \frac{i\sin(t)-\cos(t)}{-1+\sqrt{-i}}\right) \\ &= \frac{1}{2}\left(\frac{1}{-1+\sqrt{i}} + \frac{1}{-1+\sqrt{-i}}\right)\sin(t) \\ &\quad + \frac{1}{2i}\left(\frac{1}{-1+\sqrt{i}} - \frac{1}{-1+\sqrt{-i}}\right)\cos(t) \\ &= \frac{-1}{2}\sin(t) + \frac{-(1+\sqrt{2})}{2}\cos(t).\end{aligned}$$

Remark that, even though many complex numbers appear in the calculation, the final answer is a real-valued function. A plot of this solution can be seen in Figure 5, and one can see it behaves like a shifted sine. △

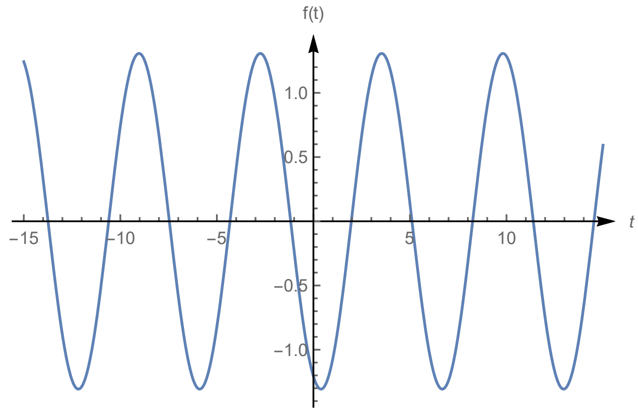

Figure 5: A plot of the solution of Example 2.3.3.

Example 2.3.4. Suppose that

$$ {}^{W}\mathbf{D}_t^{1/2} f(t) - f(t) = \sin(t), $$

then, by the last two examples, we find

$$
\begin{aligned}
f(t) &= \int_{-\infty}^{\infty} \frac{(\delta(1-\omega) - \delta(1+\omega))e^{i\omega t}}{2i((i\omega)^{1/2} - 1)}\, d\omega \\
&= \frac{e^{it}}{2i(\sqrt{i} - 1)} - \frac{e^{-it}}{2i(\sqrt{-i} - 1)} \\
&= \frac{1}{4}(-(\sqrt{2}+1) + i)e^{it} - \frac{1}{4}(\sqrt{2} + 1 + i)e^{-it} \\
&= \frac{1}{4}\left(-2\sin(t) - 2(\sqrt{2}+1)\cos(t)\right) \\
&= \frac{-1}{2}\sin(t) - \frac{1}{2(\sqrt{2}+1)}\cos t.
\end{aligned}
$$

△

Example 2.3.5. Suppose that

$$ a\, {}^{W}\mathbf{D}_t^{\alpha} f(t) + b\, {}^{W}\mathbf{D}_t^{\beta} f(t) + c = g(t). $$

The Fourier transform of a constant c can be found as $c(\omega) = \frac{1}{2\pi}\int_{-\infty}^{\infty} ce^{-i\omega t} dt = c\,\delta(\omega)$. Hence, the Fourier transform of the equation gives $a(i\omega)^{\alpha} f(\omega) + b(i\omega)^{\beta} f(\omega) + c\,\delta(\omega) = g(\omega)$, or

$$ f(\omega) = \frac{g(\omega)}{a(i\omega)^{\alpha} + b(i\omega)^{\beta} + c\,\delta(\omega)} = \begin{cases} \frac{g(\omega)}{a(i\omega)^{\alpha} + b(i\omega)^{\beta}}, & \text{for } \omega \neq 0 \\ 0, & \text{for } \omega = 0 \end{cases} $$

and one can take the inverse Fourier transform of $f(\omega)$ to get the final solution

$$ f(t) = \int_{-\infty}^{\infty} \frac{g(\omega)e^{i\omega t}}{a(i\omega)^{\alpha} + b(i\omega)^{\beta} + c\,\delta(\omega)}\, d\omega. $$

△

2.3.2 Solutions obtained by power series expansions

Formal power series can be a useful method for constructing solutions of ODE's [35, 36]. On the other hand, they only work in a few particular cases for FDE's. The main problem using them in FDE's comes from the property of Example 1.2.5, namely that ${}^{RL}_{0}\mathbf{D}^{\alpha}_{t} t^n = \frac{n!}{\Gamma(n-\alpha+1)} t^{n-\alpha}$, which means that we can no longer match up coefficients of t^n with $n \in \mathbb{N}$. The specific cases where we can use them are those where all derivative orders in the FDE are an integer multiple of some real number $p \neq 0$. In that case, we can make a formal power series

$$f(t) = \sum_{k=0}^{\infty} a_k \frac{t^{pk}}{\Gamma(pk+1)}$$

so that we can still match up all coefficients.

Example 2.3.6. Suppose we want to solve

$$a\, {}^{RL}_{0}\mathbf{D}^{np}_{t} f(t) + b\, {}^{RL}_{0}\mathbf{D}^{mp}_{t} f(t) = g(t)$$

for $n, m \in \mathbb{N}$, $n > m$, $0 \neq a, b, p \in \mathbb{R}$, and $g(t)$ some function which can be represented by a formal power series $g(t) = \sum_{k=0}^{\infty} g_k \frac{t^{pk}}{\Gamma(pk+1)}$. We can introduce the formal power series $f(t) = \sum_{k=0}^{\infty} f_k \frac{t^{pk}}{\Gamma(pk+1)}$ and substitute this into the FDE to find

$$\sum_{k=0}^{\infty} f_k \left(a \frac{t^{p(k-n)}}{\Gamma(p(k-n)+1)} + b \frac{t^{p(k-m)}}{\Gamma(p(k-m)+1)} \right) = \sum_{k=0}^{\infty} g_k \frac{t^{pk}}{\Gamma(pk+1)}.$$

We can then match up the powers to get

$$\sum_{k=-n}^{\infty} a f_{k+n} \frac{t^{pk}}{\Gamma(pk+1)} + \sum_{j=-m}^{\infty} b f_{j+m} \frac{t^{pj}}{\Gamma(pj+1)} = \sum_{k=0}^{\infty} g_k \frac{t^{pk}}{\Gamma(pk+1)}.$$

This gives three separate cases:

- For $-n \leq k < -m$, then $a f_{k+n} = 0$. In other words: $f_k = 0$ for $k = 0, 1, \ldots, n-m-1$.
- For $-m \leq k < 0$, then $a f_{k+n} + b f_{k+m} = 0$, or $f_k = -\frac{b}{a} f_{k-n+m}$ for $k = n-m, \ldots, n-1$.
- For $k \geq 0$, then $a f_{k+n} + b f_{k+m} = g_k$, or $f_k = \frac{g_{k-n} - b f_{k+m-n}}{a}$ for $k \geq n$.

Note that the first case has $n - m$ conditions while the second case has m conditions. That means that in total there are n explicit conditions while the rest is recursively generated by the last case.

If we take a specific case, like ${}^{RL}_{0}\mathbf{D}^{2}_{t} f(t) + {}^{RL}_{0}\mathbf{D}^{1/2}_{t} f(t) = g(t)$, then we have $p = \frac{1}{2}$, $n = 4$, and $m = 1$. We thus get $f_k = 0$ for $k = 0, 1, 2$, $f_3 = -f_0 = 0$, and $f_k = g_{k-4} - f_{k-3}$ for $k \geq 4$. Evaluating the first few values, we see a pattern emerging in Table 1. Namely, that $f_k = g_{k-3} - g_{k-6} + g_{k-9} - \cdots + g_{(k \mod 3)}$, or if we suppose that $k = 3s + r$ for $s \in \mathbb{N}$ and $r \in \{0, 1, 2\}$, then

$$f_{3s+r} = \sum_{j=0}^{s-1} (-1)^j g_{3(s-j-1)+r}.$$

$f_0 = 0$	$f_1 = f_2 = 0$	$f_3 = -f_0 = 0$
$f_4 = g_0 - f_1 = g_0$	$f_5 = g_1 - f_2 = g_1$	$f_6 = g_2 - f_3 = g_2$
$f_7 = g_3 - f_4 = g_3 - g_0$	$f_8 = g_4 - f_5 = g_4 - g_1$	$f_9 = g_5 - f_6 = g_5 - g_2$
$f_{10} = g_6 - f_7 = g_6 - g_3 + g_0$	$f_{11} = g_7 - f_8 = g_7 - g_4 + g_1$	$f_{12} = g_8 - f_9 = g_8 - g_5 + g_2$

Table 1: The first few f_k in the formal power series in Example 2.3.6.

Therefore, we find that

$$\begin{aligned} f(t) &= \sum_{k=0}^{\infty} \frac{f_k t^{k/2}}{\Gamma(k/2+1)} = \sum_{s=0}^{\infty} \frac{f_{3s} t^{3s/2}}{\Gamma(3s/2+1)} + \frac{f_{3s+1} t^{(3s+1)/2}}{\Gamma((3s+1)/2+1)} + \frac{f_{3s+2} t^{(3s+2)/2}}{\Gamma((3s+2)/2+1)} \\ &= \sum_{s=0}^{\infty} \sum_{j=0}^{s-1} (-1)^j \left(\frac{g_{3(s-j-1)} t^{3s/2}}{\Gamma(3s/2+1)} + \frac{g_{3(s-j-1)+1} t^{(3s+1)/2}}{\Gamma((3s+1)/2+1)} + \frac{g_{3(s-j-1)+2} t^{(3s+2)/2}}{\Gamma((3s+2)/2+1)} \right). \end{aligned}$$

Although this is a correct answer, it might not be the most insightful one.

△

Remark 2.3.7. We should ask which functions can be expressed as the power series that we used in this example. To see this, let us consider a function $f(t)$ that is smooth on $(0, \infty)$. In this case, we know that we can write it as a Taylor series $f(t) = \sum_{k \geq 0} f^{(k)}(1) \frac{(t-1)^k}{k!}$. Now, for $p \neq 0$, we can write $f(t) = f\left((t^p)^{1/p}\right) = f_p(t^p)$ where we define $f_p(t) = f(t^{1/p})$. Since f_p is again a smooth function on $(0, \infty)$, we can write f_p as a Taylor series $f_p(t) = \sum_{k \geq 0} f_p^{(k)}(1) \frac{(t-1)^k}{k!}$, where we choose $1 \in (0, \infty)$ as the expansion point. This now allows us to find

$$f(t) = f_p(t^p) = \sum_{k \geq 0} f_p^{(k)}(1) \frac{(t^p - 1)^k}{k!} =: \sum_{k \geq 0} a_k \frac{t^{pk}}{\Gamma(pk+1)}, \tag{2.4}$$

where the a_k can be found by expanding all powers and collecting all corresponding terms by their order of t. More precisely, we can use the binomial theorem to see that

$$f(t) = \sum_{k \geq 0} \sum_{j=0}^{k} \binom{k}{j} (-1)^{k-j} f_p^{(k)}(1) \frac{t^{pj}}{k!} = \sum_{k \geq 0} \sum_{j=0}^{k} \frac{(-1)^{k-j} f_p^{(k)}(1)}{j!(k-j)!} t^{pj}.$$

Thus, collecting all equal order terms, we see that

$$a_n = \frac{\Gamma(pn+1)}{n!} \sum_{k \geq n} \frac{(-1)^{k-n} f_p^{(k)}(1)}{(k-n)!}$$

and we can see that we need an infinite amount of terms to know a single a_n. One might wonder why we do not just use a fractional derivative Taylor series at 1 then, as this only requires a single derivative of f. However, if we use the fractional derivative ${}_0^{RL}\mathbf{D}_t$, then we have

$${}_0^{RL}\mathbf{D}_t^{\alpha} (t-1)^{\nu} \neq \frac{\Gamma(\nu+1)}{\Gamma(\nu-\alpha+1)} (t-1)^{\nu-\alpha}.$$

The reason this is no longer equal is mostly due to the integral no longer giving the Beta function for the prefactor: not using $(t-0)$ but $(t-1)$ will change the lower integration boundary in the

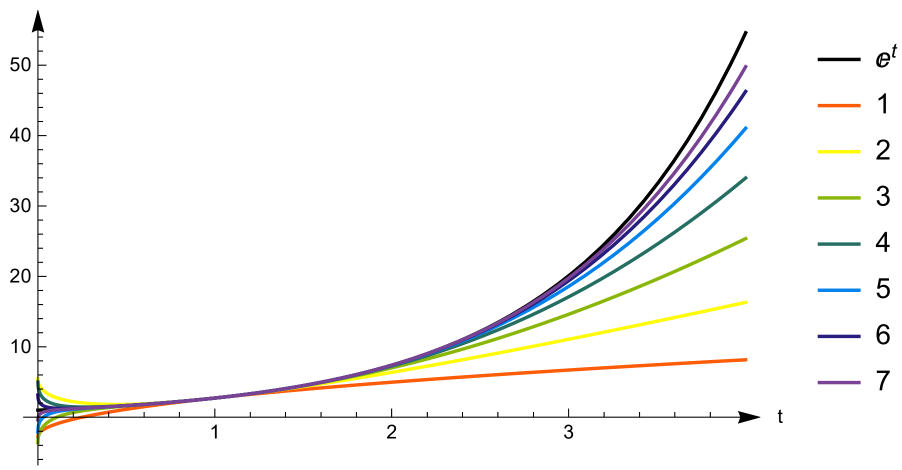

(a) The first 7 orders of the exponential.

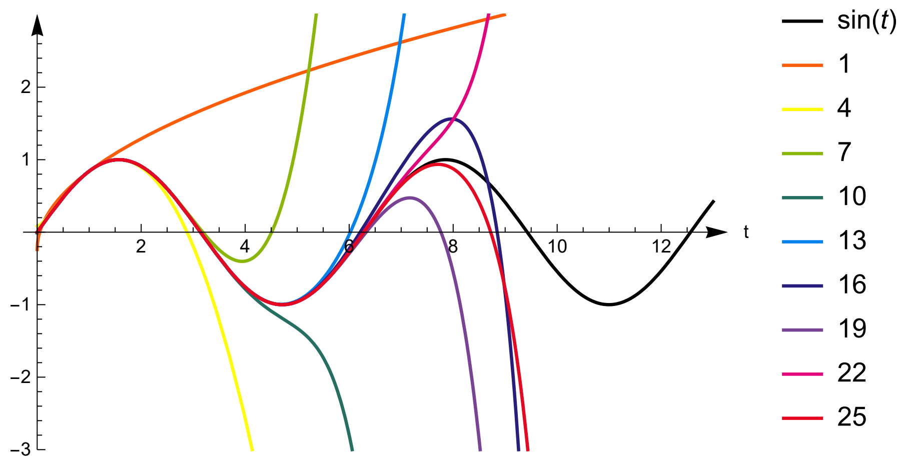

(b) Some of the first orders from 1 to 25 of the sine, skipping 3 at a time.

Figure 6: Some fractional power series expansions of e^t (Fig. **(a)**) and $\sin(t)$ (Fig. **(b)**) around $t = 1$, with $p = 0.5$. These are expansions of the form $f_{1/2}(1) + f_{1/2}^{(1)}(1)(\sqrt{t} - 1) + f_{1/2}^{(2)}(1)(\sqrt{t} - 1)^2 + f_{1/2}^{(3)}(1)(\sqrt{t} - 1)^3 + \cdots + f_{1/2}^{(n)}(1)(\sqrt{t} - 1)^n$ with n as indicated in the legends.

integral from 0 to $1/(1 - t)$. This property makes it impossible to make nice relations between the coefficients in the power series and the derivatives of f.

We can, however, properly examine the fractional expansion at 1 using f_p. The first few orders of these expansions have been plotted in Figure 6 for the exponential and sine functions for $p = 0.5$. These seem to indicate that the fractional power series can be cut off quite nicely around the expansion point $t = 1$.

One might wonder if, similarly to a Taylor series, it is possible to write the fractional expansion in terms of fractional derivatives (i.e. write $f(t) = \sum_{k=0}^{\infty} (\mathbf{D}_t^{pk} f)(1)(t - 1)^{pk}/\Gamma(pk + 1)$ for some fractional derivative). El-Ajou et al. [37] have proven Theorem 2.3.8 which is close to this idea.

Theorem 2.3.8. *[37, Theorem 3.5] Suppose that f has a fractional power series expansion at t_0 of the form:*

$$f(t) = \sum_{n=0}^{\infty} c_n (t-t_0)^{n\alpha}, \quad 0 \leq m-1 < \alpha \leq m, \quad t_0 \leq t < t_0 + R, \tag{2.5}$$

with $m \in \mathbb{N}$ and $R > 0$. If $f(t)$ is continuous on $[t_0, t_0+R)$ and $\left({}^C_{t_0}\mathbf{D}^\alpha_t\right)^n f(t)$ are continuous on (t_0, t_0+R) for $n \in \mathbb{N}$, then the coefficients c_n have the form

$$c_n = \frac{\left({}^C_{t_0}\mathbf{D}^\alpha_t\right)^n f(t_0)}{\Gamma(n\alpha+1)}, \tag{2.6}$$

where $\left({}^C_{t_0}\mathbf{D}^\alpha_t\right)^n = {}^C_{t_0}\mathbf{D}^\alpha_t \cdot {}^C_{t_0}\mathbf{D}^\alpha_t \cdot \ldots \cdot {}^C_{t_0}\mathbf{D}^\alpha_t$ is the Caputo derivative at t_0 of order α repeated n-times.

Proof. By assumption we know that $f(t) = \sum_{n=0}^{\infty} c_n (t-t_0)^{n\alpha}$. Plugging in $t = t_0$, we find that $c_0 = f(t_0)$. Taking the derivative of the function we also see that

$${}^C_{t_0}\mathbf{D}^\alpha_t f(t) = c_1 \Gamma(\alpha+1) + c_2 \frac{\Gamma(2\alpha+1)}{\Gamma(\alpha+1)}(t-t_0)^\alpha + c_3 \frac{\Gamma(3\alpha+1)}{\Gamma(2\alpha+1)}(t-t_0)^{2\alpha} + \ldots,$$

on the domain $[t_0, t_0+R)$. Plugging in $t = t_0$ again, we find that ${}^C_{t_0}\mathbf{D}^\alpha_t f(t_0) = c_1 \Gamma(\alpha+1)$ or $c_1 = \frac{{}^C_{t_0}\mathbf{D}^\alpha_t f(t_0)}{\Gamma(\alpha+1)}$. Taking another derivative we find that

$$\left({}^C_{t_0}\mathbf{D}^\alpha_t\right)^2 f(t) = c_2 \Gamma(2\alpha+1) + c_3 \frac{\Gamma(3\alpha+1)}{\Gamma(\alpha+1)}(t-t_0)^\alpha + c_4 \frac{\Gamma(4\alpha+1)}{\Gamma(2\alpha+1)}(t-t_0)^{2\alpha} + \ldots.$$

At $t = t_0$ this gives $c_2 = \frac{\left({}^C_{t_0}\mathbf{D}^\alpha_t\right)^2 f(t_0)}{\Gamma(2\alpha+1)}$. Repeating the above steps n times gives us the formula $c_n = \frac{\left({}^C_{t_0}\mathbf{D}^\alpha_t\right)^n f(t_0)}{\Gamma(n\alpha+1)}$, which completes the proof of the generalised Taylor series formula

$$f(t) = \sum_{n=0}^{\infty} \frac{\left({}^C_{t_0}\mathbf{D}^\alpha_t\right)^n f(t_0)}{\Gamma(n\alpha+1)}(t-t_0)^{n\alpha}. \tag{2.7}$$

□

Remark 2.3.9. The generalised Taylor formula in Theorem 2.3.8 only works with the Caputo derivative. This is due to its property that the Caputo derivative of a constant is always zero. Using this property and repeated differentiation rather than higher order differentiation, recall that orders do not simply combine in fractional derivatives, allows us to get rid of lower order terms and keep only the term of the order that we have differentiated to. This is what makes the proof work here.

Corollary 2.3.10. *Combining the result of Remark 2.3.7 that all smooth functions have a power series expansion around $t_0 \in (0, \infty)$ with the result of Theorem 2.3.8 that all such functions have a generalised Taylor series, we can conclude that all smooth functions have a generalised Taylor series of the form*

$$f(t) = \sum_{n=0}^{\infty} \frac{\left({}^C_{t_0}\mathbf{D}^\alpha_t\right)^n f(t_0)}{\Gamma(n\alpha+1)}(t-t_0)^{n\alpha}. \tag{2.8}$$

2.3.3 Solutions obtained by Laplace transformations

Laplace transformations can be a powerful tool when analysing linear FDE's. The biggest drawback, though, is the need to transform back to $f(t)$ from $F(s)$. This can be, depending on the FDE, relatively easy or very hard to find a closed form. We present some examples where we make use of Example 1.1.14, which showed that $\mathcal{L}\left(t^{pm+q-1}E_{p,q}^{(m)}(at^p);s\right) = \frac{m!\,s^{p-q}}{(s^p-a)^{m+1}}$, or in particular

$$\mathcal{L}\left(t^{q-1}E_{p,q}(at^p);s\right) = \frac{s^{p-q}}{s^p-a}. \tag{2.9}$$

We have seen that both Riemann-Liouville and Caputo are the main (nonequivalent) derivatives compatible with Laplace transformations. Therefore, we will try some examples with both types of derivatives.

Example 2.3.11. Suppose that

$$a\,{}^{RL}_{0}\mathbf{D}^{\alpha}_{t}f(t) + b\,{}^{RL}_{0}\mathbf{D}^{\beta}_{t}f(t) = g(t)$$

for some function $g(t)$ and $\alpha, \beta > 0$ with $n-1 \leq \alpha < n$ and $m-1 \leq \beta < m$. Applying the Laplace transform and using Lemma 1.2.19, we obtain

$$as^{\alpha}F(s) + bs^{\beta}F(s) - a\sum_{k=0}^{n-1}s^k\left({}^{RL}_{0}\mathbf{D}^{\alpha-k-1}_{t}f\right)(0) - b\sum_{j=0}^{m-1}s^j\left({}^{RL}_{0}\mathbf{D}^{\beta-j-1}_{t}f\right)(0) = G(s).$$

Denoting $a_k = a\left({}^{RL}_{0}\mathbf{D}^{\alpha-k-1}_{t}f\right)(0)$ and $b_j = b\left({}^{RL}_{0}\mathbf{D}^{\beta-j-1}_{t}f\right)(0)$, this can be rewritten to

$$F(s) = \frac{G(s) + \sum_{k=0}^{n-1}s^k a_k + \sum_{j=0}^{m-1}s^j b_j}{as^{\alpha}+bs^{\beta}}. \tag{2.10}$$

Here, we can see the limitations of Laplace transforms, as calculating the inverse transform of this $F(s)$ is quite troublesome, specifically with the denominator being a sum of different powers of s. For some specific combinations of powers there are known inverses, such as $\mathcal{L}^{-1}\left(\frac{a}{a^2+s^2};t\right) = \sin(at)$, but there is no general formula for finding $\mathcal{L}^{-1}\left(\frac{1}{F(s)};t\right)$. To see this, we first remark that $\mathcal{L}(\delta(t);s) = \int_0^{\infty}\delta(t)e^{-st}\,dt = e^0 = 1$, and thus that $\mathcal{L}^{-1}(1;t) = \delta(t)$. Now, if $\mathcal{L}(\delta(t);s) = 1 = F(s)G(s) = \mathcal{L}(f(t)*g(t);s)$, then finding $\mathcal{L}^{-1}\left(\frac{1}{F(s)};t\right)$ is equivalent to finding a function $g(t)$ such that $f(t)*g(t) = \delta(t)$.

If we choose some specific values, say ${}^{RL}_{0}\mathbf{D}^{1/2}_{t}f(t) - bf(t) = g(t)$, then $F(s)$ becomes

$$F(s) = \frac{G(s)+a_0}{s^{1/2}-b}.$$

Using Equation (2.9) and plugging in a_0, we then find that

$$f(t) = g(t) * \left(\frac{1}{\sqrt{t}}E_{\frac{1}{2},\frac{1}{2}}(b\sqrt{t})\right) + a\left({}^{RL}_{0}\mathbf{D}^{-1/2}_{t}f\right)(0)\,\frac{1}{\sqrt{t}}E_{\frac{1}{2},\frac{1}{2}}(b\sqrt{t}). \tag{2.11}$$

Choosing another specific value, say ${}^{RL}_{0}\mathbf{D}^{2}_{t}f(t) - b\,{}^{RL}_{0}\mathbf{D}^{\beta}_{t}f(t) = g(t)$, with $0 < \beta < 1$, then

$$F(s) = \frac{(G(s)+a_0+a_1 s+b_0)\,s^{-\beta}}{s^{2-\beta}-b}.$$

Again, using Equation (2.9), we then find that

$$f(t) = (a_0 + b_0)tE_{2-\beta,2}(bt^{2-\beta}) + a_1 E_{2-\beta,1}(bt^{2-\beta}) + g(t) * \left(tE_{2-\beta,2}(bt^{2-\beta})\right). \tag{2.12}$$

In fact, Equation (2.9) is general enough to solve the general FDE that we started with: $a\,{}^{RL}_{0}\mathbf{D}^{\alpha}_{t} f(t) + b\,{}^{RL}_{0}\mathbf{D}^{\beta}_{t} f(t) = g(t)$ with the Laplace solution as in Equation (2.10), then we can rewrite it as

$$F(s) = \frac{G(s)}{a}\frac{s^{-\beta}}{s^{\alpha-\beta}+b/a} + \sum_{k=0}^{n-1}\frac{a_k}{a}\frac{s^{k-\beta}}{s^{\alpha-\beta}+b/a} + \sum_{j=0}^{m-1}\frac{b_j}{a}\frac{s^{j-\beta}}{s^{\alpha-\beta}+b/a}.$$

Now, we can simply fill in the transforms to find

$$\begin{aligned} f(t) = \frac{1}{a}\Bigg[& g(t) * \left(t^{\alpha-1}E_{\alpha-\beta,\alpha}\left(-\frac{b}{a}t^{\alpha-\beta}\right)\right) + \sum_{k=0}^{n-1} a_k t^{\alpha-k-1}E_{\alpha-\beta,\alpha-k}\left(-\frac{b}{a}t^{\alpha-\beta}\right) \\ & + \sum_{j=0}^{m-1} b_j t^{\alpha-j-1}E_{\alpha-\beta,\alpha-j}\left(-\frac{b}{a}t^{\alpha-\beta}\right)\Bigg], \end{aligned} \tag{2.13}$$

where we remind that $a_k = a\left({}^{RL}_{0}\mathbf{D}^{\alpha-k-1}_{t} f\right)(0)$ and $b_j = b\left({}^{RL}_{0}\mathbf{D}^{\beta-j-1}_{t} f\right)(0)$. △

Example 2.3.12. We will consider the same type of FDE as the previous Example, but now with Caputo derivatives:

$$a\,{}^{C}_{0}\mathbf{D}^{\alpha}_{t} f(t) + b\,{}^{C}_{0}\mathbf{D}^{\beta}_{t} f(t) = g(t)$$

for some function $g(t)$ and $\alpha, \beta > 0$ with $n-1 \le \alpha < n$ and $m-1 \le \beta < m$. The Laplace transform with the Caputo derivatives gives us $as^{\alpha}F(s) + bs^{\beta}F(s) - a\sum_{k=0}^{n-1} s^{\alpha-k-1}f^{(k)}(0) - b\sum_{j=0}^{m-1} s^{\beta-j-1}f^{(j)}(0) = G(s)$ which can be rewritten into

$$F(s) = \frac{G(s) + a\sum_{k=0}^{n-1} s^{\alpha-k-1}f^{(k)}(0) + b\sum_{j=0}^{m-1} s^{\beta-j-1}f^{(j)}(0)}{as^{\alpha}+bs^{\beta}}. \tag{2.14}$$

To use Equation (2.9), we can rewrite this into

$$\begin{aligned} F(s) &= \frac{G(s)}{as^{\alpha}+bs^{\beta}} + \sum_{k=0}^{n-1} af^{(k)}(0)\frac{s^{\alpha-k-1}}{as^{\alpha}+bs^{\beta}} + \sum_{j=0}^{m-1} bf^{(j)}(0)\frac{s^{\beta-j-1}}{as^{\alpha}+bs^{\beta}} \\ &= \frac{G(s)}{a}\frac{s^{-\beta}}{s^{\alpha-\beta}+b/a} + \sum_{k=0}^{n-1}\frac{af^{(k)}(0)}{a}\frac{s^{\alpha-\beta-k-1}}{s^{\alpha-\beta}+b/a} + \sum_{j=0}^{m-1}\frac{bf^{(j)}(0)}{a}\frac{s^{-j-1}}{s^{\alpha-\beta}+b/a}. \end{aligned}$$

Now, with Equation (2.9), we can see that the inverse transform is given by

$$\begin{aligned} f(t) = \frac{1}{a}\Bigg[& g(t) * \left(t^{\alpha-1}E_{\alpha-\beta,\alpha}\left(-\frac{b}{a}t^{\alpha-\beta}\right)\right) + \sum_{k=0}^{n-1} af^{(k)}(0)t^{k}E_{\alpha-\beta,k+1}\left(-\frac{b}{a}t^{\alpha-\beta}\right) \\ & + \sum_{j=0}^{m-1} bf^{(j)}(0)t^{\alpha-\beta+j}E_{\alpha-\beta,\alpha-\beta+j+1}\left(-\frac{b}{a}t^{\alpha-\beta}\right)\Bigg]. \end{aligned} \tag{2.15}$$

Taking a look at the same particular cases as the previous Example, we find that the FDE ${}_0^C\mathbf{D}_t^{1/2} f(t) - bf(t) = g(t)$ solves to

$$f(t) = g(t) * \left(\frac{1}{\sqrt{t}} E_{\frac{1}{2},\frac{1}{2}}\left(b\sqrt{t}\right)\right) + f(0) E_{\frac{1}{2},1}\left(b\sqrt{t}\right), \tag{2.16}$$

while ${}_0^C\mathbf{D}_t^2 f(t) - b\,{}_0^C\mathbf{D}_t^\beta f(t) = g(t)$, with $0 < \beta < 1$, solves to

$$\begin{aligned} f(t) &= g(t) * \left(t E_{2-\beta,2}\left(bt^{2-\beta}\right)\right) + f(0)E_{2-\beta,1}\left(bt^{2-\beta}\right) \\ &\quad + f^{(1)}(0) t E_{2-\beta,2}\left(bt^{2-\beta}\right) - bf(0)t^{2-\beta}E_{2-\beta,3-\beta}\left(bt^{2-\beta}\right) \end{aligned} \tag{2.17}$$

△

To the best of our knowledge, these general closed-form solutions shown here in Example 2.3.11 and 2.3.12 are the first time the solutions are shown in this shape with finitely many terms and a single convolution, although solutions with infinitely many terms have been found before. This *new* form has the big advantage that it allows for many calculations that use the solution to be done much more easily. This form with two variable derivative orders also allows for a very general application.

2.4 Differences between definitions

In Section 2.3, we have seen some solutions for particular FDE's with different definitions of fractional derivatives and now we aim to see what impact the choice of definition will have on the final solution. We already know that the definition will have an impact on which initial conditions are required, but in this section we investigate if we can still obtain equal solutions for different fractional derivatives, if they give fundamentally different solutions or closely related solutions.

Example 2.4.1. Let us begin with comparing solutions of the FDE

$$\mathbf{D}_t^{1/2} f(t) - bf(t) = g(t). \tag{2.18}$$

We have seen some solutions for this equation using different definitions:

- For the Caputo derivative

$$f_C(t) = g(t) * \left(\frac{1}{\sqrt{t}} E_{\frac{1}{2},\frac{1}{2}}\left(b\sqrt{t}\right)\right) + f(0) E_{\frac{1}{2},1}\left(b\sqrt{t}\right).$$

- For the Riemann-Liouville derivative:

$$f_{RL}(t) = g(t) * \left(\frac{1}{\sqrt{t}} E_{\frac{1}{2},\frac{1}{2}}\left(b\sqrt{t}\right)\right) + \left({}_0^{RL}\mathbf{D}_t^{-1/2} f\right)(0)\, \frac{1}{\sqrt{t}} E_{\frac{1}{2},\frac{1}{2}}\left(b\sqrt{t}\right).$$

- For the Weyl derivative:

$$f_W(t) = \frac{1}{2\pi} \int_{-\infty}^{\infty} \int_{-\infty}^{\infty} \frac{g(\tau) e^{i\omega(t-\tau)}}{\sqrt{i\omega} - b}\, d\tau\, d\omega.$$

Clearly, the first terms of f_C and f_{RL} are equal. Indeed, we expect them to be equal, as this part is independent of initial conditions and the two definitions are equivalent when the initial conditions are zero. Their second terms, although similarly structured, are not equal:

$$\begin{aligned}
\frac{1}{\sqrt{t}} E_{\frac{1}{2},\frac{1}{2}}\left(b\sqrt{t}\right) &= \sum_{k=0}^{\infty} \frac{b^k t^{(k-1)/2}}{\Gamma(k/2+1/2)} \\
[\text{shift } k \to k+1] \quad &= \sum_{k=-1}^{\infty} \frac{b^{k+1} t^{k/2}}{\Gamma(k/2+1)} \\
&= \sum_{k=0}^{\infty} \frac{b^{k+1} t^{k/2}}{\Gamma(k/2+1)} + \frac{b^0 t^{-1/2}}{\Gamma(1/2)} \\
&= bE_{\frac{1}{2},1}\left(b\sqrt{t}\right) + \frac{1}{\sqrt{\pi t}}.
\end{aligned}$$

Notice how the extra term will vanish for large t which means that, for large t, the two solutions f_C and f_{RL} will tend to the same value if $bf(0) = \left({}^{RL}_{0}\mathbf{D}_t^{-1/2} f\right)(0)$. It is also clear that they will differ significantly for small t, as the difference scales with $t^{-1/2}$.

We also solved a specific case for the Weyl derivative with $b = 1$ and $g(t) = \sin(t)$, which gave

$$f_W(t) = \frac{-1}{2}\sin(t) - \frac{1}{2(\sqrt{2}+1)}\cos t.$$

All three solutions for this case have been plotted in Figure 7a with some initial conditions such that we can compare f_C with f_{RL}. Since f_W has no initial conditions, another logical comparison is with the initial conditions for f_C and f_{RL} to be the value of f_W. This has been done in Figure 7b where we can see that f_W still behaves quite differently from the other solutions. This might be a consequence of the sign of the second term in the FDE. Classically this sign would change the solution from a periodic function to an exponential one. Therefore, we should see what happens if we choose b to be negative.

In the case $b = -1$, for example, we find

$$\begin{aligned}
f_W(t) &= \int_{-\infty}^{\infty} \frac{(\delta(1-\omega) - \delta(1+\omega))e^{i\omega t}}{2i((i\omega)^{1/2}+1)}\, d\omega \\
&= \frac{e^{it}}{2i(\sqrt{i}+1)} - \frac{e^{-it}}{2i(\sqrt{-i}+1)} \\
&= \frac{1-\sqrt{2}-i}{4}(i\sin(t)+\cos(t)) + \frac{1-\sqrt{2}+i}{4}(-i\sin(t)+\cos(t)) \\
&= \frac{1}{2}\sin(t) + \frac{1-\sqrt{2}}{4}\cos(t),
\end{aligned}$$

$$f_C(t) = g(t) * \left(\frac{1}{\sqrt{t}} E_{\frac{1}{2},\frac{1}{2}}\left(-\sqrt{t}\right)\right) + f(0)E_{\frac{1}{2},1}\left(-\sqrt{t}\right),$$

and

$$f_{RL}(t) = g(t) * \left(\frac{1}{\sqrt{t}} E_{\frac{1}{2},\frac{1}{2}}\left(-\sqrt{t}\right)\right) + \left({}^{RL}_{0}\mathbf{D}_t^{-1/2} f\right)(0)\, \frac{1}{\sqrt{t}} E_{\frac{1}{2},\frac{1}{2}}\left(-\sqrt{t}\right).$$

As one can see Figure 8a and 8b, this time all the solutions match up quite nicely for initial conditions equal to f_W. For initial conditions set to 1, we see in Figure 8c that they start a bit differently, but for large t they converge to the same solution again. The conclusion then, is that even the signs in an FDE can be the determining factor for the relation between the different definition solutions.

△

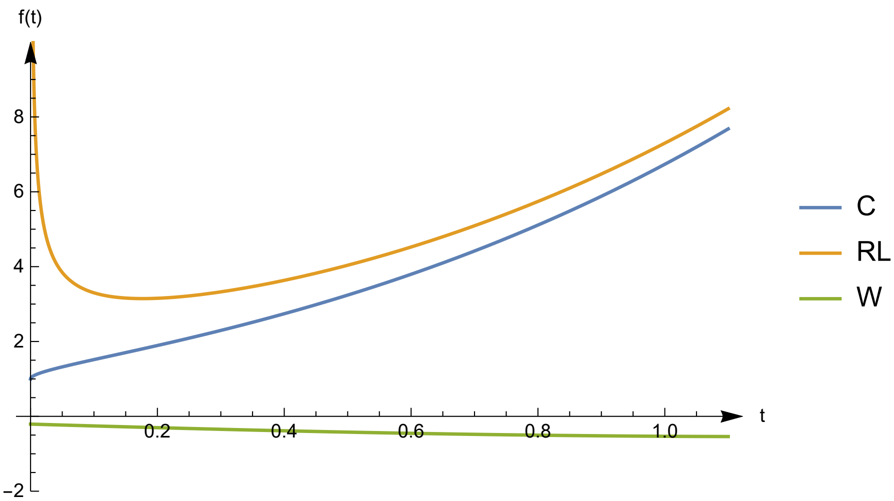

(a) $f(0) = 1$ and $\left({}^{RL}_{0}\mathbf{D}_t^{-1/2} f\right)(0) = 1$. f_C and f_{RL} go towards each other asymptotically.

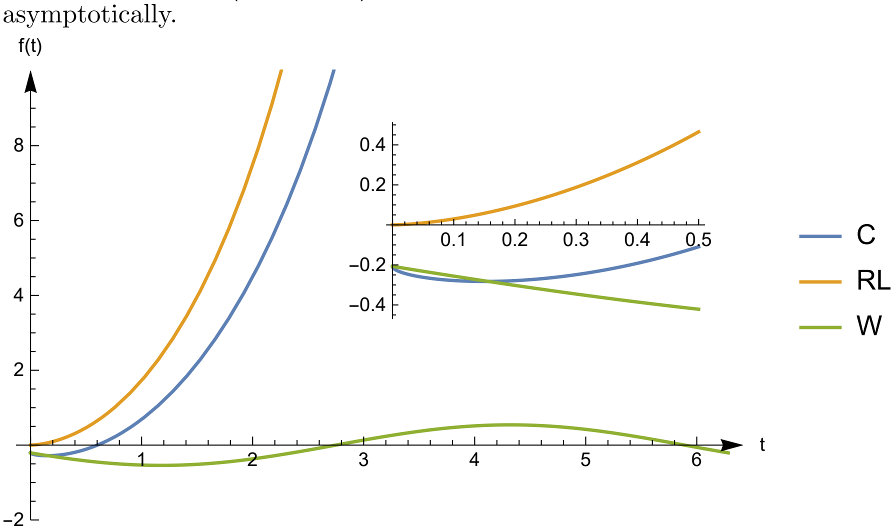

(b) $f(0) = f_W(0) = -\frac{1}{2(\sqrt{2}+1)}$ and $\left({}^{RL}_{0}\mathbf{D}_t^{-1/2} f\right)(0) = \left({}^{RL}_{0}\mathbf{D}_t^{-1/2} f_W\right)(0) = 0$. f_C and f_{RL} no longer go towards each other asymptotically. Remark that f_{RL} is in this case the null initial condition solution for both f_C and f_{RL}.

Figure 7: A comparison of the solutions f_C, f_{RL} and f_W of Equation (2.18) with $b = 1$ and $g(t) = \sin(t)$ and initial conditions as stated .

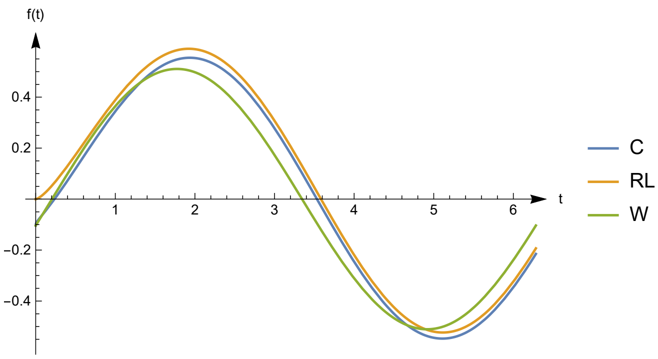

(a) Beginning of the solutions.

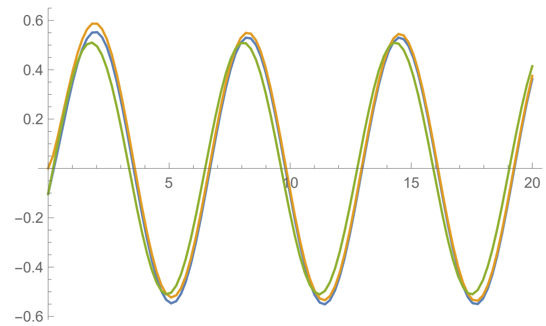

(b) Behaviour over a few periods.

Figure (a,b): $f(0) = f_W(0) = \frac{1-\sqrt{2}}{4}$, and $\left({}^{RL}_{0}\mathbf{D}_t^{-1/2} f\right)(0) = \left({}^{RL}_{0}\mathbf{D}_t^{-1/2} f_W\right)(0) = 0$.

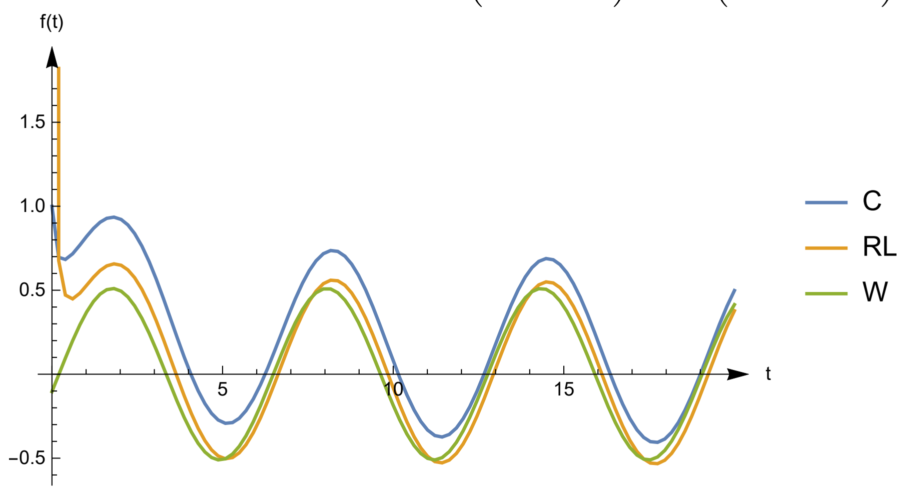

(c) $f(0) = 1$, and $\left({}^{RL}_{0}\mathbf{D}_t^{-1/2} f\right)(0) = 1$. Although slowly, they all seem co converge to the same solution for large t.

Figure 8: A comparison of the solutions f_C, f_{RL} and f_W of Equation (2.18) with $g(t) = \sin(t)$, $b = -1$, and initial conditions as stated.

Example 2.4.2. Now, we compare solutions of the FDE

$$\mathbf{D}_t^2 f(t) + \mathbf{D}_t^{1/2} f(t) = g(t). \tag{2.19}$$

Using the different definitions we have found the following solutions:

- For the Caputo derivative:

$$\begin{aligned} f_C(t) &= g(t) * \left(tE_{3/2,2}\left(-t^{3/2}\right)\right) + f(0)E_{3/2,1}\left(-t^{3/2}\right) \\ &\quad + f^{(1)}(0)tE_{3/2,2}\left(-t^{3/2}\right) + f(0)t^{3/2}E_{3/2,5/2}\left(-t^{3/2}\right). \end{aligned}$$

- For the Riemann-Liouville derivative:

$$\begin{aligned} f_{RL}(t) &= g(t) * \left(tE_{3/2,2}\left(-t^{3/2}\right)\right) + f(0)E_{3/2,1}\left(-t^{3/2}\right) \\ &\quad + f^{(1)}(0)tE_{3/2,2}\left(-t^{3/2}\right) + \left({}^{RL}_{0}\mathbf{D}_t^{-1/2} f\right)(0)tE_{3/2,2}\left(-t^{3/2}\right). \end{aligned}$$

- For the Weyl derivative:

$$f_W(t) = \frac{1}{2\pi}\int_{-\infty}^{\infty}\int_{-\infty}^{\infty}\frac{g(\tau)e^{i\omega(t-\tau)}}{-\omega^2 - \sqrt{i\omega}}\, d\tau\, d\omega.$$

Like mentioned in the previous example, the first terms of f_C and F_{RL} are equal. The next two terms are actually also identical, since these come from the initial conditions of the ordinary second order derivative, which makes the last term the only difference between them, whilst f_W is again completely different.

Since we have seen an exact solution for f_W with $g(t) = \sin(t)$, let us focus on that specific case in order to compare the solutions. As seen in Example 2.3.3, we then have

$$f_W(t) = -\frac{1}{2}\sin(t) - \frac{1+\sqrt{2}}{2}\cos(t).$$

Plotting this with f_C and f_{RL} with all initial conditions set to 1, we get Figure 9a and 9b. We could also compare with zero initial conditions, in which case Riemann-Liouville and Caputo derivatives are equal, this case can be seen in Figure 9c and 9d. If we try to set initial conditions to match up with f_W, then we use $f_W(0) = -\frac{1+\sqrt{t}}{2}$, $f_W^{(1)}(0) = -\frac{1}{2}$, and $\left({}^{RL}_{0}\mathbf{D}_t^{-1/2} f_W\right)(0) = 0$, which gives Figure 9e and 9f.

In all non-zero initial condition cases (Figure 9a, 9b, 9e, and 9f), we see that f_C seems to keep its distance from the other solutions while f_{RL} tends to f_W in all cases. This difference is due to the fractional initial condition of f_C : $f(0)t^{3/2}E_{3/2,5/2}\left(-t^{3/2}\right)$, which tends to $f(0)$ as $t \to \infty$. As the other initial conditions match with f_{RL}, while the fractional initial condition of f_{RL}, although slowly, does tend to 0 at infinity. This makes for an interesting situation where the attempt to match up $f_W(0) = f_C(0)$ specifically causes them to differ by the constant $f_W(0)$ at large t. In fact, the fractional initial condition $f(0)t^{3/2}E_{3/2,5/2}\left(-t^{3/2}\right)$ does not even contribute to $f_C(0)$ as it vanishes there. This term really is the result of the non-local properties of fractional derivatives.

△

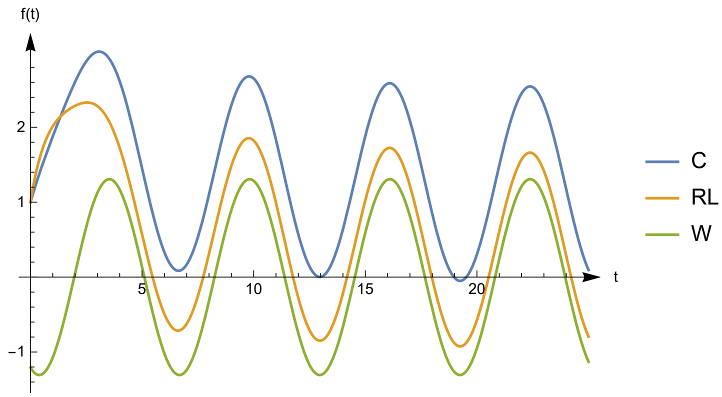

(a) Beginning of the solutions.

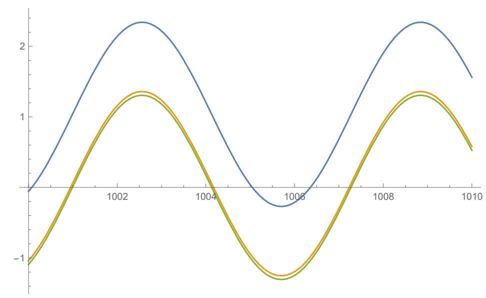

(b) Behaviour at $t \approx 1000$.

Figure (a,b): All initial conditions set to 1. At large t, we see that $f_{RL}(t) \approx f_W(t)$ while $f_C(t)$ stays above the other two solutions, even though it behaves similarly.

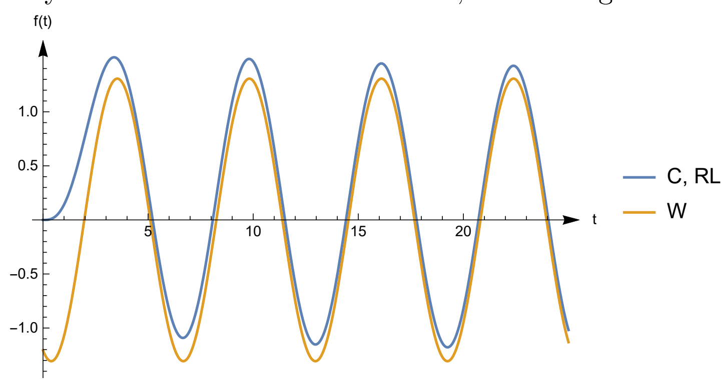

(c) Beginning of the solutions.

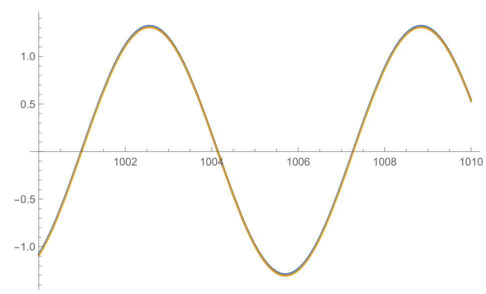

(d) Behaviour at $t \approx 1000$.

Figure (c,d): All initial conditions set to 0. At large t, we see that $f_{RL}(t) = f_C(t) \approx f_W(t)$.

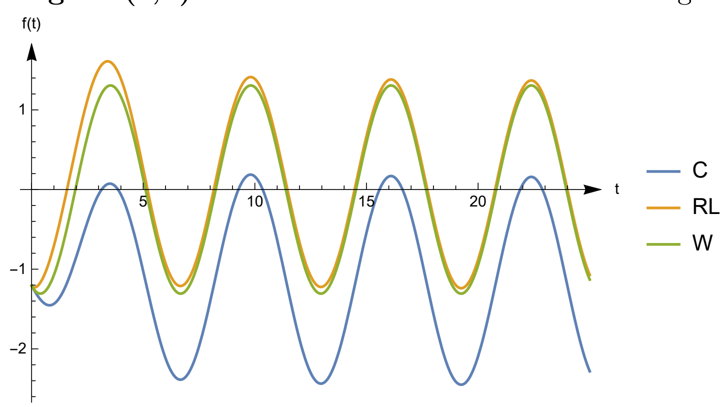

(e) Beginning of the solutions.

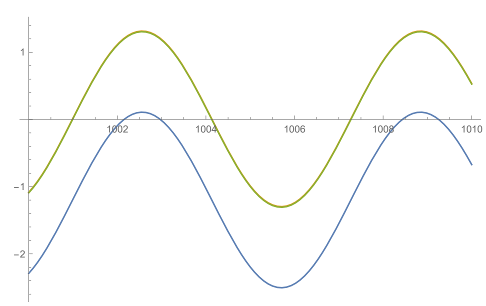

(f) Behaviour at $t \approx 1000$.

Figure (e,f): All initial conditions set to be equal to those of f_W. At large t, we see that $f_{RL}(t) \approx f_W(t)$ while $f_C(t)$ stays below the other two solutions, although it behaves similarly.

Figure 9: A comparison of the solutions f_C, f_{RL} and f_W of Equation (2.19) with $g(t) = \sin(t)$ and initial conditions as stated below each Figure.

Example 2.4.3. We can actually show a bit more general case that includes all the previous examples. Namely, the equation

$$a\mathbf{D}_t^{\alpha} f(t) + b\mathbf{D}_t^{\beta} f(t) = g(t), \tag{2.20}$$

for $g(t) = \sin(t)$, $a, b \in \mathbb{R}$, $1 < \alpha \leq 2$, and $0 < \beta \leq 1$. This allows us to solve the integral for f_W:

$$\begin{aligned} f_W(t) &= \int_{-\infty}^{\infty} \frac{(\delta(1-\omega) - \delta(1+\omega))e^{i\omega t}}{2i(a(i\omega)^{\alpha} + b(i\omega)^{\beta})}\, d\omega \\ &= \frac{e^{it}}{2i(ai^{\alpha} + bi^{\beta})} - \frac{e^{-it}}{2i(a(-i)^{\alpha} + b(-i)^{\beta})} \\ &= \frac{e^{it}}{2i(ae^{i\pi\alpha/2} + be^{i\pi\beta/2})} - \frac{e^{-it}}{2i(ae^{3i\pi\alpha/2} + be^{3i\pi\beta/2})}. \end{aligned}$$

This leads to the three solutions

$$\begin{aligned} f_W(t) &= \frac{e^{it}}{2i(ae^{i\pi\alpha/2} + be^{i\pi\beta/2})} - \frac{e^{-it}}{2i(ae^{3i\pi\alpha/2} + be^{3i\pi\beta/2})}, \\ f_C(t) &= \frac{1}{a}\left[g(t) * \left(t^{\alpha-1} E_{\alpha-\beta,\alpha}\left(-\frac{b}{a} t^{\alpha-\beta} \right) \right) + af(0) E_{\alpha-\beta,1}\left(-\frac{b}{a} t^{\alpha-\beta} \right) \right. \\ &\quad \left. + af^{(1)}(0) t E_{\alpha-\beta,2}\left(-\frac{b}{a} t^{\alpha-\beta} \right) + bf(0) t^{\alpha-\beta} E_{\alpha-\beta,\alpha-\beta+1}\left(-\frac{b}{a} t^{\alpha-\beta} \right) \right], \\ f_{RL}(t) &= \frac{1}{a}\left[g(t) * \left(t^{\alpha-1} E_{\alpha-\beta,\alpha}\left(-\frac{b}{a} t^{\alpha-\beta} \right) \right) + a\left({}^{RL}_{0}\mathbf{D}_t^{\alpha-1} f \right)(0) t^{\alpha-1} E_{\alpha-\beta,\alpha}\left(-\frac{b}{a} t^{\alpha-\beta} \right) \right. \\ &\quad \left. + a\left({}^{RL}_{0}\mathbf{D}_t^{\alpha-2} f \right)(0) t^{\alpha-2} E_{\alpha-\beta,\alpha-1}\left(-\frac{b}{a} t^{\alpha-\beta} \right) + b\left({}^{RL}_{0}\mathbf{D}_t^{\beta-1} f \right)(0) t^{\alpha-1} E_{\alpha-\beta,\alpha}\left(-\frac{b}{a} t^{\alpha-\beta} \right) \right]. \end{aligned}$$

Notice that the attempt of comparing these solutions is a 9 dimensional problem when we include initial conditions. For some specific values for the constants and with one parameter left as a variable, we have made Figure 10. Both plots show one side with very similar solutions, and one side where they all seem to behave differently. △

Remark 2.4.4. Figure 10 includes some solutions that we have seen in earlier examples. We can see the solutions of Example 2.4.1 for both $b = 1$ and $b = -1$ in Figure 10a, which also shows the sign of b is very important for similarity of solutions. We can also see solutions of Example 2.4.2 in Figure 10b and see how this FDE solution changes for different values of $0 < \beta < 1$. Note that the endpoints $\beta \in \{0, 1\}$ in Figure 10b represent solutions of the equations $f''(t) + f(t) = \sin(t)$ and $f''(t) + f'(t) = \sin(t)$, which respectively can be seen as equations representing respectively a particle in a square potential and a free particle in a viscous fluid, both with a sine force being applied.

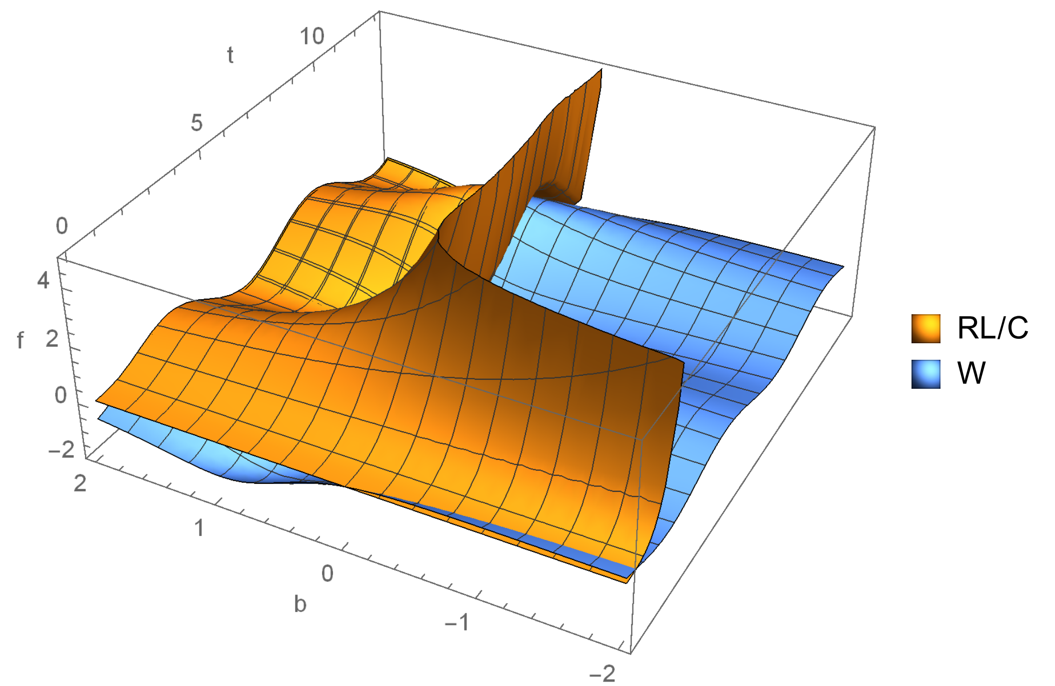

(a) $\beta = 1/2$ and $-2 < b < 2$, with all initial conditions set to zero.

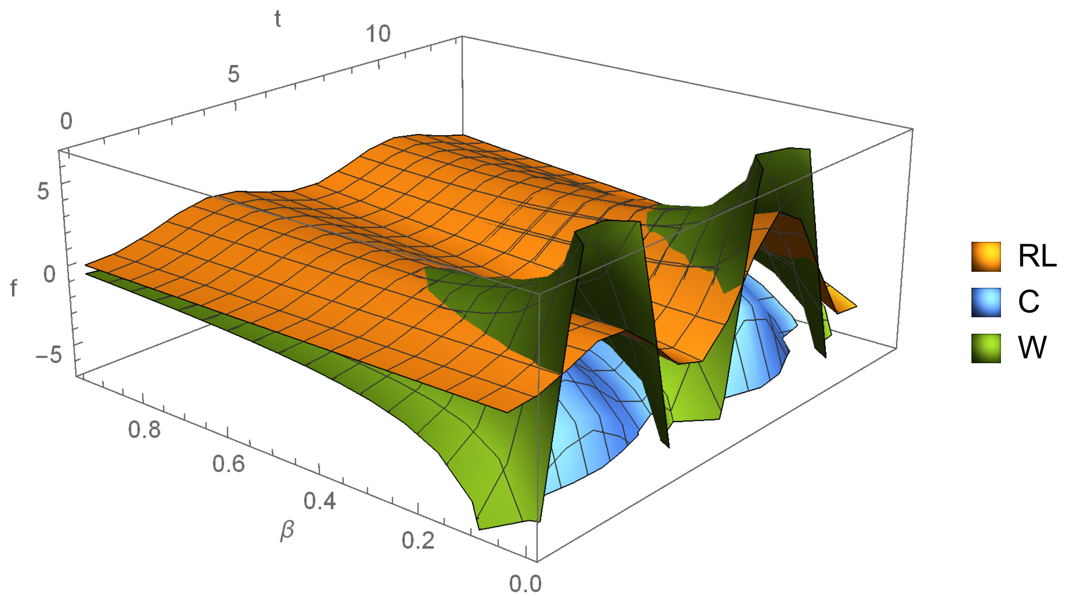

(b) $b = 1$ and $0 < \beta < 1$, with all initial conditions set to those of f_W.

Figure 10: A flow of the solutions f_{RL}, f_C and f_W of Equation (2.20) for different values of b and β, with $a = 1$, $\alpha = 2$, and initial conditions as specified. Small parts of the boundaries have been left out because this gave clear numerical errors.

3 Quantum many-body systems

In this chapter, we lay the foundations upon which we will be building a fractional theory of time glasses. We will discuss Brownian motion, the Caldeira-Leggett model, a TLS bath, RFOT theory, the Gardner phase, and time Crystals. Brownian motion is a classical example of many-body interactions, where a mean field approach allows it to be described in a single particle formulation with a stochastic external force. Its quantized form is described by the Caldeira-Leggett model [38–43] where a particle is coupled to a bath of harmonic oscillators. Truncating these oscillators gives a bath of two-level systems [44] which will give an effective description in the form of the fractional Langevin equation in the ultra-cold limit. An important theory in the description of glasses is the RFOT theory [17], which effectively describes a glass as a collection of hard spheres, where the packing density plays a critical role. Although the Gardner phase was first discovered in spin-glasses [18], it was much more recently found to occur in normal hard-sphere glass, where a more collective behaviour starts to occur at very high density [19]. Time crystals, first described by F. Wilczek [21, 45], are crystalline structures not in space but in time, thus breaking time-translation symmetry. All these structures show collective effects which will be important in our study of time glass.

3.1 Classical Brownian motion

Brownian motion was already observed by the Romans[9] [46], but it is mostly credited to Robert Brown, who observed it in 1827 while he was studying pollen. The pollen were suspended in water and released their spreads, which executed a jittery motion. Classically, we can imagine a microscopic ball in a bath of some fluid, with a mass $M \geq 0$ of roughly an order of magnitude larger than the mass $m \geq 0$ of the molecules composing the fluid ($M \gg m$). The particles in the bath move around due to their thermal energy, accordingly, every so often a particle will collide with the ball and bounce off exerting a force on the ball in the direction of movement. Since this thermal movement is randomly distributed as a Gaussian, this force is on average zero, but it will change the velocity of the ball between collisions due to the relatively similar masses. If we look at timescales larger than the timescale between collisions, then we can model this "random force" as $f(t)$ described by a Gaussian probability density[10]

$$P[f(t)] = \frac{1}{\sqrt{2\sigma\pi}} e^{f(t)^2/2\sigma^2}, \tag{3.1}$$

with the standard deviation σ to be determined by physical quantities such as temperature and mass. We can summarise these variables in the properties

$$\langle f(t) \rangle = \int_{-\infty}^{\infty} f(t) P[f(t)] \, df(t) = 0 \tag{3.2}$$

and

$$\langle f(t) f(t') \rangle = \int_{-\infty}^{\infty} \int_{-\infty}^{\infty} f(t) P[f(t)] f(t') P[f(t')] \, df(t) \, df(t') = K\delta(t - t'), \tag{3.3}$$

where the latter describes that collisions happen instantaneously and are completely uncorrelated. We can then describe this movement by $M \frac{d^2}{dt^2} q(t) = f(t)$, where $q(t)$ is the position of the ball at

[9] In the philosophical poem *De rerum natura* by Titus Lucretius Carus (c. 60 BC) about the motion of dust particles in the air.

[10] We see $f(t)$ as a stochastic variable f with an index t.

time t. We can also include a friction term $\eta \frac{d}{dt} q(t)$, with $\eta > 0$, to model the friction of the ball moving through the fluid, and a potential term $V'[q(t)]$ to model energetically favourable positions in space. All these combined give the so called *Langevin equation*:

$$M \frac{d^2}{dt^2} q(t) + \eta \frac{d}{dt} q(t) + V'(q(t)) = f(t), \quad \text{where } \begin{cases} \langle f(t) \rangle = 0, \\ \langle f(t) f(t') \rangle = K\delta(t - t'). \end{cases} \tag{3.4}$$

For at most quadratic potentials $V(q)$, this equation is a well-understood second-order linear ordinary differential equation, with a stochastic term $f(t)$. It can even be solved to an integral form, which allows for a straightforward calculation of statistical properties of $q(t)$. For higher-order potentials, the Langevin equation becomes non-linear and thereby much more complicated to solve.

Example 3.1.1. Suppose that $V(q) = a + bq + \frac{c}{2} q^2$, then the Langevin equation becomes

$$M \frac{d^2}{dt^2} q(t) + \eta \frac{d}{dt} q(t) + b + cq(t) = f(t).$$

Taking the Laplace transform, we find

$$Ms^2 Q(s) - Msq(0) - Mq'(0) + \eta s Q(s) - \eta q(0) + \frac{b}{s} + cQ(s) = F(s)$$

and rearranging the expression gives

$$Q(s) = \frac{F(s) - \frac{b}{s} + (Ms + \eta) q(0) + Mq'(0)}{Ms^2 + \eta s + c}.$$

To simplify the fraction, we factorise and decompose it as

$$\begin{aligned} \frac{1}{Ms^2 + \eta s + c} &= \frac{1}{M\left(s - \frac{-\eta + \sqrt{\eta^2 - 4Mc}}{2M}\right)\left(s - \frac{-\eta + \sqrt{\eta^2 - 4Mc}}{2M}\right)} \\ &= \frac{A}{\left(s - \frac{-\eta + \sqrt{\eta^2 - 4Mc}}{2M}\right)} + \frac{B}{\left(s - \frac{-\eta - \sqrt{\eta^2 - 4Mc}}{2M}\right)} \\ &= M \frac{A\left(s - \frac{-\eta - \sqrt{\eta^2 - 4Mc}}{2M}\right) + B\left(s - \frac{-\eta + \sqrt{\eta^2 - 4Mc}}{2M}\right)}{Ms^2 + \eta s + c} \\ &= \frac{M(A + B)s + (A + B)\frac{\eta}{2} + (A - B)\frac{\sqrt{\eta^2 - 4Mc}}{2}}{Ms^2 + \eta s + c}. \end{aligned}$$

This implies that $A + B = 0$ and $A - B = \frac{2}{\sqrt{\eta^2 - 4Mc}}$. Therefore, we find that $A = \frac{1}{\sqrt{\eta^2 - 4Mc}}$ and $B = \frac{-1}{\sqrt{\eta^2 - 4Mc}}$. Hence, we get

$$Q(s) = \frac{F(s) - \frac{b}{s} + (Ms + \eta) q(0) + Mq'(0)}{\sqrt{\eta^2 - 4Mc}} \left[\frac{1}{\left(s - \frac{-\eta + \sqrt{\eta^2 - 4Mc}}{2M}\right)} - \frac{1}{\left(s - \frac{-\eta - \sqrt{\eta^2 - 4Mc}}{2M}\right)} \right].$$

Recall from Example 1.1.14 that we have

$$\mathcal{L}^{-1}\left(\frac{1}{s-a};t\right) = E_{1,1}(at) = e^{at}, \tag{3.5}$$

$$\mathcal{L}^{-1}\left(\frac{s}{s-a};t\right) = t^{-1}E_{1,0}(at) = ae^{at}, \tag{3.6}$$

$$\mathcal{L}^{-1}\left(\frac{s^{-1}}{s-a};t\right) = tE_{1,2}(at) = \frac{e^{at}-1}{a}. \tag{3.7}$$

We thus find that

$$\begin{aligned} q(t) = \Bigg[& f(t) * \left(e^{\frac{-\eta+\sqrt{\eta^2-4Mc}}{2M}t} - e^{\frac{-\eta-\sqrt{\eta^2-4Mc}}{2M}t}\right) - b\left(\frac{e^{\frac{-\eta+\sqrt{\eta^2-4Mc}}{2M}t}-1}{\frac{-\eta+\sqrt{\eta^2-4Mc}}{2M}} - \frac{e^{\frac{-\eta-\sqrt{\eta^2-4Mc}}{2M}t}-1}{\frac{-\eta-\sqrt{\eta^2-4Mc}}{2M}}\right) \\ & + Mq(0)\left(\frac{-\eta+\sqrt{\eta^2-4Mc}}{2M}e^{\frac{-\eta+\sqrt{\eta^2-4Mc}}{2M}t} - \frac{-\eta-\sqrt{\eta^2-4Mc}}{2M}e^{\frac{-\eta-\sqrt{\eta^2-4Mc}}{2M}t}\right) \\ & + \left(\eta q(0) + Mq'(0)\right)\left(e^{\frac{-\eta+\sqrt{\eta^2-4Mc}}{2M}t} - e^{\frac{-\eta-\sqrt{\eta^2-4Mc}}{2M}t}\right)\Bigg] \frac{1}{\sqrt{\eta^2-4Mc}}. \end{aligned} \tag{3.8}$$

Some physical observations about this solution:

- The choice of zero energy level a does not change the solution;
- The increase of η will damp movement faster;
- The linear potential term b induces a drift in the opposite direction;
- The convolution with f consists of two parts: An integral over f, which is the direct result of classical mechanics, and a damping term.

△

If we set $V = 0$ in the above example, we find the free particle solution

$$q(t) = \frac{1}{\eta}f(t) * \left(1 - e^{\frac{-\eta t}{M}}\right) + q(0) + \frac{M}{\eta}q'(0)\left(1 - e^{\frac{-\eta t}{M}}\right). \tag{3.9}$$

From this, we can determine the expected position

$$\langle q(t)\rangle = q(0) + \frac{M}{\eta}q'(0)\left(1 - e^{\frac{-\eta t}{M}}\right), \tag{3.10}$$

the velocity

$$q'(t) = \frac{1}{M}f(t) * e^{-\frac{\eta t}{M}} + q'(0)e^{-\frac{\eta t}{M}}, \tag{3.11}$$

and thus the mean square velocity (MSV)

$$\begin{aligned}
\langle q'(t)^2\rangle &= \left\langle \left(\frac{1}{M}f(t) * e^{-\frac{\eta t}{M}} + q'(0)e^{-\frac{\eta t}{M}}\right)^2 \right\rangle \\
&= \frac{e^{-\frac{2\eta t}{M}}}{M^2}\int_0^t\int_0^t \langle f(\tau)f(\tau')\rangle e^{\frac{\eta(\tau+\tau')}{M}}\, d\tau\, d\tau' + \frac{2q'(0)e^{-\frac{\eta t}{M}}}{M}\langle f(t)\rangle * e^{-\frac{\eta t}{M}} + q'(0)^2 e^{-2\frac{\eta t}{M}} \\
&= \frac{e^{-\frac{2\eta t}{M}}}{M^2}\int_0^t\int_0^t K\delta(\tau-\tau')e^{\frac{\eta(\tau+\tau')}{M}}\, d\tau\, d\tau' + q'(0)^2 e^{-\frac{2\eta t}{M}} \\
&= \frac{Ke^{-\frac{2\eta t}{M}}}{M^2}\int_0^t e^{\frac{2\eta\tau}{M}}\, d\tau + q'(0)^2 e^{-\frac{2\eta t}{M}} \\
&= \frac{K}{2\eta M} + e^{-\frac{2\eta t}{M}}\left(q'(0)^2 - \frac{K}{2\eta M}\right),
\end{aligned}$$

which gives insight into the typical velocity of a particle. At large t, where we expect thermal equilibrium, we find that the mean square velocity becomes constant:

$$\langle q'(t)^2\rangle_{eq} = \frac{K}{2\eta M}. \tag{3.12}$$

In the thermal kinetics picture, we know that the kinetic energy $\frac{1}{2}mv^2$ is related to the temperature. Indeed, from the equipartition theorem [47], we know that a thermal system in equilibrium must have

$$\langle q'(t)^2\rangle_{eq} = \frac{k_B T}{M}. \tag{3.13}$$

This means that we need to set $K = 2\eta k_B T$ if we want the MSV to describe a physical system. Particularly, if we want the system to be in equilibrium from the start, then this also demands that $\langle q'(0)^2\rangle = \frac{K}{2\eta M}$.

We can also look at the mean square displacement (MSD), which provides an indication of the most likely displacement that one can expect a particle to have in a certain time. In the free particle case, the MSD is given by

$$\begin{aligned}
\langle [q(t)-q(0)]^2\rangle &= \left\langle \left[\frac{1}{\eta}f(t) * \left(1 - e^{\frac{-\eta t}{M}}\right)\frac{q'(0)M}{\eta}\left(1 - e^{\frac{-\eta t}{M}}\right)\right]^2 \right\rangle \\
&= \frac{1}{\eta^2}\int_0^t\int_0^t \langle f(\tau)f(\tau')\rangle \left(1 - e^{-\frac{\eta\tau}{M}}\right)\left(1 - e^{-\frac{\eta\tau'}{M}}\right) d\tau\, d\tau' \\
&\quad + \frac{\langle q'(0)^2\rangle M^2}{\eta^2}\left(1 - 2e^{\frac{-\eta t}{M}} + e^{2\frac{-\eta t}{M}}\right) \\
&= \frac{K}{\eta^2}\int_0^t \left(1 - e^{-\frac{\eta\tau}{M}}\right)^2 d\tau + \frac{MK}{2\eta^3}\left(1 - 2e^{\frac{-\eta t}{M}} + e^{2\frac{-\eta t}{M}}\right).
\end{aligned}$$

Evaluating the integral then gives

$$\begin{aligned}
\langle [q(t)-q(0)]^2\rangle &= \frac{K}{\eta^2}t + \frac{2MK}{\eta^3}e^{-\frac{\eta t}{M}} - \frac{MK}{2\eta^3}e^{-\frac{2\eta t}{M}} - \frac{3MK}{2\eta^3} + \frac{MK}{2\eta^3}\left(1 - 2e^{\frac{-\eta t}{M}} + e^{2\frac{-\eta t}{M}}\right) \\
&= \frac{K}{\eta^2}t + \frac{MK}{\eta^3}e^{-\frac{\eta t}{M}} - \frac{MK}{\eta^3}.
\end{aligned}$$

The small-t behaviour of the MSD is given by

$$\langle [q(t \ll M/\eta) - q(0)]^2 \rangle \approx \frac{K}{\eta^2} t + \frac{MK}{\eta^3}\left(1 - \frac{\eta t}{M} + \frac{\eta^2 t^2}{2M^2}\right) - \frac{MK}{\eta^3} = \frac{Kt^2}{2\eta M} = \frac{k_B T}{M} t^2, \tag{3.14}$$

while the large-t behaviour is given by

$$\langle [q(t \gg M/\eta) - q(0)]^2 \rangle \approx \frac{K}{\eta^2} t - \frac{MK}{\eta^3}. \tag{3.15}$$

3.2 The Caldeira-Leggettt model

We will closely follow Ref. [38] in this Section to characterise the Caldeira-Leggett model, used to describe quantum dissipation. Since Lagrangian dynamics obey conservation of energy and dissipation removes energy from a particle, we have to look at both the system of interest and the bath, which is exerting friction onto the system. We, therefore, take a Lagrangian of the form

$$L = L_S + L_B + L_I + L_{CT}, \tag{3.16}$$

where

$$L_S = \frac{1}{2} M \dot{q}^2 - V(q), \tag{3.17}$$

$$L_B = \sum_j \frac{1}{2} m_j \dot{q}_j^2 - \frac{1}{2} m_j \omega_j^2 q_j^2, \tag{3.18}$$

$$L_I = \sum_j C_j q_j q, \tag{3.19}$$

$$L_{CT} = -\sum_j \frac{1}{2} \frac{C_j^2}{m_j \omega_j^2} q^2, \tag{3.20}$$

are respectively the Lagrangian of the system of interest L_S with position q, the bath L_B, the interaction L_I, and a counter-term L_{CT}. The bath L_B is composed of many non-interacting harmonic oscillators with coordinates q_j, masses m_j and natural frequencies ω_j; all oscillators are interacting with the system through L_I by a coupling constant C_j. The classical equations of motion are given by the Euler-Lagrange equation in the form

$$M\ddot{q} = -V'(q) + \sum_j C_j q_j - \sum_j \frac{C_j^2}{m_j \omega_j^2} q, \tag{3.21}$$

$$m_j \ddot{q}_j = -m_j \omega_j^2 q_j + C_j q. \tag{3.22}$$

The Laplace transform of Eq. (3.22) can be rewritten into

$$\begin{aligned} q_j(s) &= \frac{\dot{q}_j(0)}{s^2 + \omega_j^2} + \frac{s q_j(0)}{s^2 + \omega_j^2} + \frac{C_j q(s)}{m_j (s^2 + \omega_j^2)} \\ &= \frac{\dot{q}_j(0)}{s^2 + \omega_j^2} + \frac{s q_j(0)}{s^2 + \omega_j^2} + \frac{C_j q(s)}{m_j}\left(\frac{1}{\omega_j^2} - \frac{1}{\omega_j^2}\frac{s^2}{s^2 + \omega_j^2}\right), \end{aligned} \tag{3.23}$$

where we have extracted a term which will cancel out with the counter term later. We can now see that the solution $q_j(t)$ is given by

$$\begin{aligned} q_j(t) &= \frac{\dot{q}_j(0)}{\omega_j}\sin(\omega_j t) + q_j(0)\cos(\omega_j t) + \frac{C_j q(t)}{m_j\omega_j^2} - \mathcal{L}^{-1}\left(\frac{C_j q(s)}{m_j\omega_j^2}\frac{s^2}{s^2+\omega_j^2}; t\right) \\ &= \frac{\dot{q}_j(0)}{\omega_j}\sin(\omega_j t) + q_j(0)\cos(\omega_j t) + \frac{C_j q(t)}{m_j\omega_j^2} - \frac{\mathrm{d}}{\mathrm{d}t}\mathcal{L}^{-1}\left(\frac{C_j q(s)}{m_j\omega_j^2}\frac{s}{s^2+\omega_j^2}; t\right) \\ &= \frac{\dot{q}_j(0)}{\omega_j}\sin(\omega_j t) + q_j(0)\cos(\omega_j t) + \frac{C_j q(t)}{m_j\omega_j^2} - \frac{\mathrm{d}}{\mathrm{d}t}\left\{\frac{C_j}{m_j\omega_j^2} q(t) * \cos(\omega_j t)\right\}. \end{aligned} \tag{3.24}$$

We can now insert this solution into Eq. (3.21) to find

$$M\ddot{q} + V'(q) + \sum_j \frac{\mathrm{d}}{\mathrm{d}t}\left\{\frac{C_j^2}{m_j\omega_j^2} q(t) * \cos(\omega_j t)\right\} = \sum_j C_j\left[\frac{\dot{q}_j(0)}{\omega_j}\sin(\omega_j t) + q_j(0)\cos(\omega_j t)\right], \tag{3.25}$$

where we see that the counter term has cancelled with the extracted term from the harmonic oscillators. Next, we consider the spectral function given by the retarded dynamical susceptibility of the bath

$$J(\omega) = \mathrm{Im}\,\mathcal{F}\left[-i\theta(t-t')\left\langle\left[\sum_j C_j q_j(t), \sum_{j'} C_{j'} q_{j'}(t')\right]\right\rangle\right]. \tag{3.26}$$

Taking the Fourier transform of Eq. (3.22), we see that

$$q_j(\omega) = -\frac{C_j}{m_j(\omega^2-\omega_j^2)} q(\omega), \tag{3.27}$$

which means that the dynamical susceptibility of the interaction strength $\sum_j C_j q_j(t)$ to the system is given by

$$\chi_B(\omega) = -\sum_j \frac{C_j^2}{m_j(\omega^2-\omega_j^2)} = \sum_j\left(\frac{C_j^2}{2m_j\omega_j(\omega+\omega_j)} - \frac{C_j^2}{m_j\omega_j(\omega-\omega_j)}\right). \tag{3.28}$$

We now shift $\omega \pm \omega_j \to \omega \pm \omega_j + i\epsilon$ with $\epsilon \to 0$ which gives the identity

$$\mathrm{Im}\,\frac{1}{(\omega\pm\omega_j)+i\epsilon} = -\pi\delta(\omega\pm\omega_j). \tag{3.29}$$

Inserting this into the dynamical susceptibility, we find that the spectral function is given by

$$J(\omega) = \mathrm{Im}\,\chi_B(\omega) = \frac{\pi}{2}\sum_j \frac{C_j^2}{m_j\omega_j}\left(\delta(\omega-\omega_j) - \delta(\omega+\omega_j)\right) = \frac{\pi}{2}\sum_j \frac{C_j^2}{m_j\omega_j}\delta(\omega-\omega_j), \tag{3.30}$$

where the latter identity is because both ω and ω_j are positive. We will see that the summation in the LHS of Eq. (3.25) can be interpreted as a friction term F_{fr}. To show this, we rewrite

$$\begin{aligned} F_{fr} &:= \sum_j \frac{\mathrm{d}}{\mathrm{d}t}\left\{\frac{C_j^2}{m_j\omega_j^2} q(t) * \cos(\omega_j t)\right\} \\ &= \frac{\mathrm{d}}{\mathrm{d}t}\left\{\int_0^t d\tau \int_0^\infty d\omega \sum_j \frac{C_j^2}{m_j\omega_j^2}\delta(\omega-\omega_j)\cos[\omega(t-\tau)]q(\tau)\right\} \\ &= \frac{\mathrm{d}}{\mathrm{d}t}\left\{\frac{2}{\pi}\int_0^t d\tau \int_0^\infty d\omega \frac{J(\omega)}{\omega}\cos[\omega(t-\tau)]q(\tau)\right\}. \end{aligned} \tag{3.31}$$

For an Ohmic bath, the spectral function can be effectively described by

$$J(\omega) = \begin{cases} \eta\omega & \text{if } \omega < \Omega \\ 0 & \text{if } \omega > \Omega, \end{cases} \tag{3.32}$$

where Ω is a high-frequency cutoff. Inserting this spectral function into Eq. (3.31) and taking the limit $\Omega \to \infty$, we find that

$$\begin{aligned} F_{fr} &= \frac{2\eta}{\pi}\frac{\mathrm{d}}{\mathrm{d}t}\left\{\int_0^t d\tau \int_0^\infty d\omega \cos[\omega(t-\tau)]q(\tau)\right\} \\ &= 2\eta\frac{\mathrm{d}}{\mathrm{d}t}\left\{\int_0^t d\tau\delta(t-\tau)q(\tau)\right\} \\ &= \eta\dot{q}(t), \end{aligned} \tag{3.33}$$

which is indeed a classical friction term. Next, we focus on the RHS of Eq. (3.25), which can be interpreted as a force

$$f(t) := \sum_j C_j \left[\frac{\dot{q}_j(0)}{\omega_j}\sin(\omega_j t) + q_j(0)\cos(\omega_j t)\right] \tag{3.34}$$

that depends on all microscopic states of the bath. Assuming the bath is in thermodynamic equilibrium, we know that the oscillators follow the equipartition theorem. In the classical limit, we therefore know that we have

$$\langle q_j(0)\rangle = \langle \dot{q}_j(0)\rangle = \langle \dot{q}_j(0)q_j(0)\rangle = 0, \tag{3.35}$$

$$\langle \dot{q}_j(0)\dot{q}_{j'}(0)\rangle = \frac{k_B T}{m_j}\delta_{jj'}, \tag{3.36}$$

$$\langle q_j(0)q_{j'}(0)\rangle = \frac{k_B T}{m_j\omega_j^2}\delta_{jj'}. \tag{3.37}$$

Using these relations we see immediately that $\langle f(t)\rangle = 0$ by linearity of the expectation. However, for the mean square force we find

$$\begin{aligned} \langle f(t)f(t')\rangle &= \left\langle \sum_{j\,j'} C_j C_{j'} \left[\frac{\dot{q}_j(0)}{\omega_j}\sin(\omega_j t) + q_j(0)\cos(\omega_j t)\right]\left[\frac{\dot{q}_{j'}(0)}{\omega_{j'}}\sin(\omega_{j'} t') + q_{j'}(0)\cos(\omega_{j'} t')\right]\right\rangle \\ &= \sum_{j\,j'} C_j C_{j'} \left[\frac{1}{\omega_j\omega_{j'}}\left\langle \dot{q}_j(0)\dot{q}_{j'}(0)\right\rangle \sin(\omega_j t)\sin(\omega_{j'}t') + \left\langle q_j(0)q_{j'}(0)\right\rangle \cos(\omega_j t)\cos(\omega_{j'}t')\right. \\ &\quad \left. + \frac{1}{\omega_j}\left\langle \dot{q}_j(0)q_{j'}(0)\right\rangle \sin(\omega_j t)\cos(\omega_{j'}t') + \frac{1}{\omega_{j'}}\left\langle q_j(0)\dot{q}_{j'}(0)\right\rangle \cos(\omega_j t)\sin(\omega_{j'}t')\right] \\ &= \sum_{j\,j'} C_j C_{j'} \left[\frac{1}{\omega_j\omega_{j'}}\frac{k_B T}{m_j}\delta_{jj'}\sin(\omega_j t)\sin(\omega_{j'}t') + \frac{k_B T}{m_j\omega_j^2}\delta_{jj'}\cos(\omega_j t)\cos(\omega_{j'}t')\right], \end{aligned} \tag{3.38}$$

where we have used the linearity in the expectation and plugged in the expectations for the oscillators. Using the delta functions we find

$$\begin{aligned}\langle f(t)f(t')\rangle &= k_BT\sum_j \frac{C_j^2}{m_j\omega_j^2}\left[\sin(\omega_j t)\sin(\omega_j t') + \cos(\omega_j t)\cos(\omega_j t')\right]\\ &= k_BT\sum_j \frac{C_j^2}{m_j\omega_j^2}\cos[\omega_j(t-t')]\\ &= k_BT\int_0^\infty d\omega\sum_j \frac{C_j^2}{m_j\omega_j^2}\delta(\omega-\omega_j)\cos[\omega(t-t')]\\ &= \frac{2k_BT}{\pi}\int_0^\infty d\omega\frac{J(\omega)}{\omega}\cos[\omega(t-t')],\end{aligned} \tag{3.39}$$

where we have identified the spectral function. Plugging in the macroscopic form $J(\omega) = \eta\omega$, where we remember the limit $\Omega \to \infty$, we then get

$$\langle f(t)f(t')\rangle = \frac{2\eta k_BT}{\pi}\int_0^\infty d\omega\cos[\omega(t-t')] = 2\eta k_BT\delta(t-t'), \tag{3.40}$$

which means that $f(t)$ is a white-noise force. Finally, plugging Eq. (3.33) and (3.40) into (3.25), we find the well-known Langevin equation

$$M\ddot{q} + V'(q) + \eta\dot{q} = f(t), \tag{3.41}$$

with $\langle f(t)\rangle = 0$ and $\langle f(t)f(t)\rangle = 2\eta k_BT\delta(t-t')$.

3.3 Two-level systems bath

The spectral function plays a crucial role in the Caldeira-Leggett model. An interesting question is therefore which other spectral functions are possible, and how this changes the physics. A two-level systems (TLS) bath is, among other properties, a bath which is known to have a temperature dependent spectral function, and has been previously discussed in Refs. [44, 48, 49]. Each particle in this bath consists of a sort of TLS — such as a spin-1/2 medium, a particle in a double well potential, or a truncated harmonic oscillator. Although any of these systems can be equally described, we will use the spin-1/2 formulation for this problem. In Ref. [44], they take a Hamiltonian

$$H = \frac{\hat{p}^2}{2M} + V(x) + \sum_j \frac{\hbar\omega_j}{2}\sigma_{zj} - x\sum_j C_j\sigma_{xj}, \tag{3.42}$$

where the first two terms are for a particle at position x in a potential $V(x)$, the third term characterises the TLS bath and the last term describes the interaction between the TLS bath and the particle. Furthermore, C_j is the interaction strength, ω_j is the natural frequency, and $\sigma_{zj/xj}$ are the Pauli matrices, all indexed for each TLS in the bath.

As we have seen in the previous section, the spectral function is crucial for determining the friction and stochastic terms in the Langevin equation. For this TLS bath, Ref. [48] shows that the spectral function is given in microscopic quantities as

$$J(\omega, T) = \sum_j \pi C_j^2\tanh\left(\frac{\hbar\omega_j}{2k_BT}\right)\delta(\omega_j-\omega). \tag{3.43}$$

Ref. [48] then continues with the assumption that the spectral function is effectively given by

$$J(\omega, T) = \begin{cases} \frac{\pi}{2}\eta\omega^s \tanh\left(\frac{\hbar\omega_j}{2k_B T}\right) & \text{if } \omega < \Omega \\ 0 & \text{if } \omega > \Omega, \end{cases} \tag{3.44}$$

where the microscopic variables are encapsulated into a single macroscopic quantity η, Ω is a cutoff frequency, and the tangent-hyperbolic term retains the temperature dependence.

In Chapter 4, we will take a low-temperature limit of this system. This will yield a simpler power relation $J(\omega) \sim \omega^s$, which will allow us to derive the fractional Langevin equation including a Caputo fractional derivative. In comparison, Ref. [44] analyses the system for finite temperatures and finds "dynamical localisation". We will show that the low-temperature limit will give a glassy behaviour in the form of a time glass described by fractional dynamics.

3.4 Glasses, Gardner phase & time crystals

In this Section, we show some systems with a very strong collective behaviour. We begin with a discussion of some of the theories in the research field of glasses, before showing how one of these theories can produce a fractal collective behaviour, and how periodic behaviour can occur in time instead of space. Glasses have an amorphous[11] structure, yet they behave as a solid. This makes for an interesting theory, as the particles seem to be best described as flowing, but the overall structure has to remain solid.

One attempt to describe this glass phase begins with a hard-sphere model, where each sphere can freely move around in a vacuum, but the spheres cannot pass through each other, which can cause a global jamming (or caging) in the right circumstances[12], for more theories and descriptions see Refs. [15, 16, 50–54]. Next, we will describe the Gardner phase, recently understood to occur in glasses [19, 55]. Its main feature is a fractal structure in the energy landscape [20], which can be related to a fractal hierarchy of cages inside cages [56]. We will then show how a similar, but finite, structure can emerge out of the fractional Langevin equation.

The key-feature of the glasses is a temporary and extreme slowdown of dynamics. There are several types of theories which achieve this in different ways. They can be roughly categorised into three types [57]:

- Low-temperature phase transition:

  These involve phases where there are liquid and solid like regions and the temperature governs the size of these regions. Below a transition temperature T_C the liquid regions become sparse enough that the overall structure becomes solid.

- High-temperature critical points:

  These involve a preferred local structure inside a liquid. Upon cooling this liquid, clusters start to grow locally. However, once it has grown large enough to meet other clusters, boundary layers form due to the misalignment of crystal structure, creating regions of frustration.

- Theories without dynamical or thermodynamic transitions:

  These theories show no singularities at any temperature and include many different ideas. An example is an amorphous phase with configurational excitations.

[11] Amorphous meaning that there is no long-range spacial order.
[12] Such as high pressure or density.

It should be mentioned that none of these theories has been completely successful in their description. All theories so far have their strengths and weaknesses and there are different conditions in which one theory might work better than another. We will, however, only highlight a theory with a low-temperature phase transition, namely, the RFOT theory, as this theory is most relevant for the dynamics that we will encounter when analysing the fractional Langevin equation in the sub-Ohmic regime.

Random first-order transition theory

In Random first-order transition (RFOT) theory, we view a glass as a liquid that is composed of hard spheres, *i.e.*, each particle has a fixed radius R and two particles are not allowed to get closer to each other than $2R$. The particles can be effectively modelled by a potential

$$V_{i,j}(|x_i - x_j|) = \begin{cases} \infty & \text{if } |x_i - x_j| < 2R \\ 0 & \text{if } |x_i - x_j| > 2R, \end{cases} \tag{3.45}$$

for each pair of particles i and j. The particles can thus be described by Newtonian dynamics, where every collision between two particles exchanges momentum according to Newton's laws of motion.

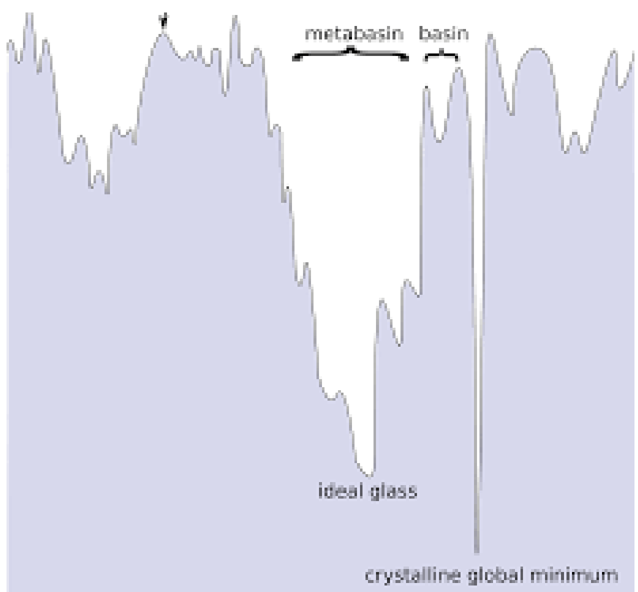

Figure 11: Extracted from Ref. [58, Fig. 4]. A schematic representation of the energy landscape of hard spheres. The glass phase occurs at the bottom of a meta-basin, where there is an enormous energy required to jump to the crystalline global minimum, where there is optimal sphere packing.

Examining the extreme cases, we can imagine that at very low densities a particle will flow for a while before hitting another particle; this low density limit describes a liquid state, as illustrated in the left column of Figure 12. On the other hand, increasing the density past a critical ϕ_d, we can imagine that the spheres become highly packed and they become trapped by their neighbours, as there is physically no space to pass between them. The highest density state is the crystal state in which the spheres form an exact hexagonal packing. What makes this transition from liquid to solid interesting, however, is that it is a very unlikely process to go from a less-efficient randomly-packed state to the crystal state. The randomly-packed states are therefore meta-stable, meaning that the state is in a local energy minimum, instead of the global energy minimum, as illustrated in Figure 11. Given enough time, however, will allow for random events to happen in the system and slowly shift the phase towards the crystalline phase [17].

In the meta-stable glass states, the spheres will have some wiggle room because the packing is not optimal. This means that the MSD, which encapsulates this type of movement, will have a typical shape where, at first, the particle can move freely, until it bumps into its neighbours. Hence, the MSD will start off as $\sim t^2$ and, after some time, it will saturate at the typical cage size, as illustrated in the middle column of Figure 12.

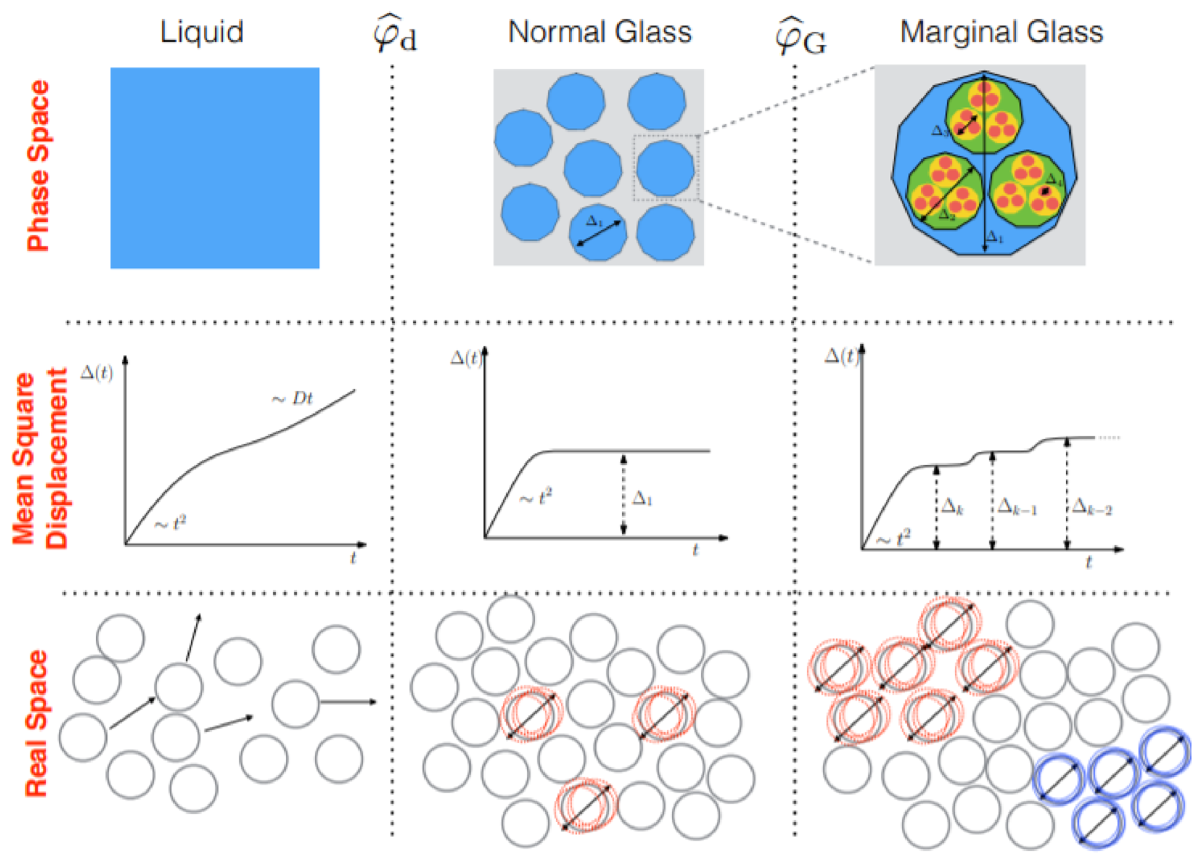

Figure 12: Extracted from Ref. [19, Fig. 3]. Three phases of hard spheres: The liquid or Brownian phase in which the hard spheres are free to move around. The MSD shows a ballistic start until the particles have time to hit other particles and the MSD becomes linear with diffusion constant D. Increasing the density ϕ past the critical density ϕ_d we enter the normal glass phase. In this phase, the hard spheres are dense enough that they can no longer freely move around. Instead, they jiggle inside a cage formed by their neighbours. This can also be seen in the MSD where the particle shows ballistic motion until it hits the cage size Δ_t where it saturates. Increasing the density over the critical density ϕ_G, we enter the marginal glass phase. In this phase, although particles are still trapped by their neighbours, there is collective movement of these neighbours (red spheres). This collective movement happens in a fractal manner with cages inside cages inside cages (with cage sizes Δ_k). In the MSD this will show as infinitely many meta-stable plateaus with ballistic motion between plateaus. These plateaus also occur periodic in time.

Gardner phase

The Gardner phase was first discovered by Elisabeth Gardner in spin-glasses making use of replica symmetry breaking [18]. Over 30 years later, it was understood that the Gardner phase occurs in many more materials. Here, we will focus on the Gardner phase in glasses, sometimes also called marginal glass. It occurs when a hard-sphere glass model, such as RFOT, is put under sufficiently high density or pressure. In Ref. [19], the authors show marginal glass in the hard-sphere RFOT model, and we encourage the interested reader to find more about it there.

In Figure 12, three important regimes of hard-sphere models have been shown: The liquid, glass, and marginal glass phases. They can be characterised by the density of spheres ϕ with critical densities ϕ_d (Figure 12 left transition) between a liquid and a glass and ϕ_G (Figure 12 right transition) between a glass and a marginal glass. In the low-density liquid-phase, the MSD shows a ballistic start until the particles have time to hit other particles and the MSD becomes linear with diffusion constant D. Increasing the density past the critical density ϕ_d, we enter the normal glass phase. In this phase, the hard spheres are dense enough that they can no longer freely move around. Instead, they jiggle inside a cage formed by their neighbours. This can also be seen in the MSD, where the particle shows ballistic motion until it hits the cage size Δ_t, and then saturates.

Increasing the density over the critical density ϕ_G, the system enters the marginal glass phase. In this phase, although particles are still trapped by their neighbours, there is collective movement with these neighbours. This collective motion happens in a fractal manner with cages inside cages. In the MSD this will show as infinitely many meta-stable plateaus, with ballistic motion between plateaus. These plateaus occur periodically in time (right column Figure 12). The most important feature of the Gardner phase is the fractal structure in the energy landscape [20]. This fractal structure makes for infinitely many meta-stable states. The existing theory is, however, only exactly solvable in infinite dimension, but critical properties of jamming have been shown to be independent of dimension [20] and these results are therefore still applicable to finite-dimensional systems. There have also been experiments claiming to have observed the Gardner phase [59, 60], with the data showing all expected features of the Gardner phase, even though they have only measured during a finite time.

Time crystals

Time crystals were first conjectured by Wilczek [21]. They are materials which in their ground state feature not periodicity in space, like a crystal, but periodicity in time. In other words, there is spontaneous time-translation symmetry breaking. After its proposal, there was much debate on the possibility of its existence, as people thought that it could cause for possible perpetual motion machines. It turns out, however, that this is not possible and a time crystal will always need an energy source. The physics involved show that such a time crystal would only be possible in two kinds of systems [61, 62].

The first system, most related to the perpetual motion question, is a driven system. As external energy is required to keep the system in periodic motion, this should not sound surprising. However, what is interesting is that these systems can show emergent frequencies that are different from (but perhaps related to) the driving frequency. The second possible case is in open systems, where there is a bath surrounding the system and energy exchange is allowed. This is a method to keep enough energy available for the system to stay in periodic motion without actively forcing energy in. Periodicity in these systems is completely emergent as the bath has no inherent periodicity.

The first experimental observation of a discrete time crystal was done in Ref. [22] in a spin chain of trapped atomic ions under the influence of a periodic Floquet many-body localisation Hamiltonian. Furthermore, discrete time crystals have also received much attention recently [63–65], as the discreteness makes them more feasible for experimental setups.

4 Time glass: A fractional calculus approach

In this chapter, we show a new contribution to the field of glasses and time materials, making use of fractional Caputo derivatives. We begin with analysing the solution of the fractional Langevin equation with static and thermal initial conditions. We show how exponents emerge, which depend on the order of the fractional derivative, and how the mean square displacement will saturate for a low enough order. In this range, we show how a periodicity emerges with several meta-stable plateaus before an overall freezing. Finally, we conclude how this phase is describing the recently conjectured time glass. This original contribution can also be found in Ref. [66].

4.1 Solution of the fractional Langevin equation

Although we have found more general solutions, we will first focus on the simpler cases before considering the more general case in the next chapter. If we look at the fractional Langevin equation with $\alpha = 2$ and potential $V(q) = 0$, then we have

$$M\frac{d^2q(t)}{dt^2} + \eta \mathbf{D}_t^\beta q(t) = f(t), \tag{4.1}$$

with $\langle f(t)\rangle = 0$ and $\langle f(t)f(t')\rangle = K\delta(t-t')$. If we use Riemann-Liouville derivatives, set $0 \leq \beta < 1$ and start the system at $t = 0$, then Example 2.3.11 gives us the solution

$$\begin{aligned} q(t) = \frac{1}{M}\Big[& f(t) * \left(tE_{2-\beta,2}\left(-\frac{\eta}{M}t^{2-\beta}\right)\right) + Mq(0)E_{2-\beta,1}\left(-\frac{\eta}{M}t^{2-\beta}\right) \\ & + \left(Mq'(0) + \eta\, {}^{RL}_{\ \,0}\mathbf{D}_t^{\beta-1} q(0)\right) tE_{2-\beta,2}\left(-\frac{\eta}{M}t^{2-\beta}\right)\Big]. \end{aligned} \tag{4.2}$$

If we use Caputo derivatives, set $0 \leq \beta < 1$ and start the system at $t = 0$, then Example 2.3.12 gives us the solution

$$\begin{aligned} q(t) = \frac{1}{M}\Big[& f(t) * \left(tE_{2-\beta,2}\left(-\frac{\eta}{M}t^{2-\beta}\right)\right) + Mq(0)E_{2-\beta,1}\left(-\frac{\eta}{M}t^{2-\beta}\right) \\ & + Mq'(0)tE_{2-\beta,2}\left(-\frac{\eta}{M}t^{2-\beta}\right) + \eta q(0)t^{2-\beta}E_{2-\beta,3-\beta}\left(-\frac{\eta}{M}t^{2-\beta}\right)\Big]. \end{aligned} \tag{4.3}$$

4.1.1 Static initial conditions

Since zero initial conditions live in the realm where Caputo and Riemann-Liouville derivatives are equal, it is interesting to analyse this regime. This would in practice mean that the bath is connected to the system at zero Kelvin. If we thus assume our particle to have been sitting completely still at the origin, *i.e.* $q(t \leq 0) = 0$, then the solutions obtained with Riemann-Liouville and Caputo derivatives are equal and given by

$$q(t) = \frac{1}{M}f(t) * \left(tE_{2-\beta,2}\left(-\frac{\eta}{M}t^{2-\beta}\right)\right). \tag{4.4}$$

We can do some quick simulations using this formula, modelling the random impacts as delta functions and generate some random numbers for the mean time between collisions and the strength of the force applied. In Figure 13, two of these simulations are shown for the values $\beta = 1$ (yellow) and $\beta = 0.5$ (blue). These are respectively classical diffusion and subdiffusion and the simulations

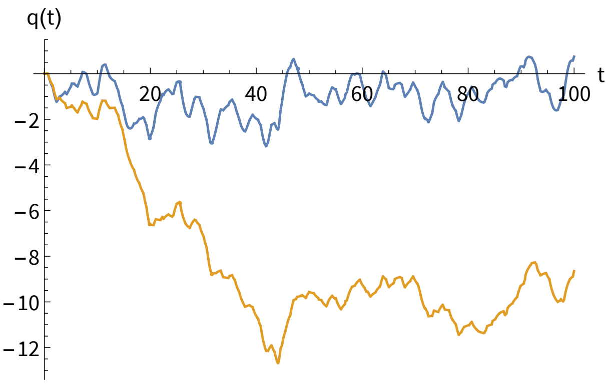

(a)

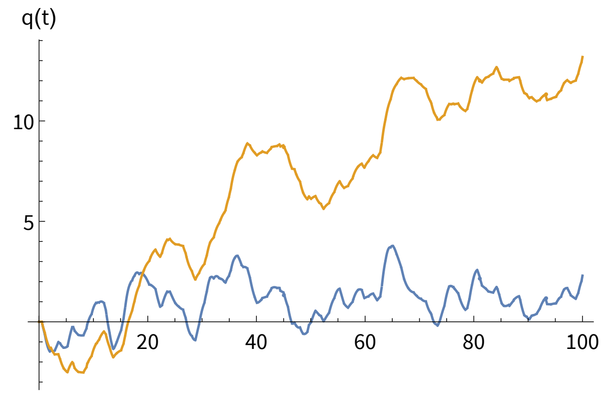

(b)

Figure 13: Two simulations of a random walk for $M = \eta = 1$, with $\beta = 1$ (yellow) and $\beta = 0.5$ (blue). The same randomly generated force is being applied to both particles. Particles in the sub-diffusive range ($\beta < 1$) typically stay more localised compared to ordinary Brownian motion.

indicate that this is indeed the case: the yellow particle is moving in one direction for a long time, while the blue particle remains closer to the starting position.

Analysing the statistics of this solution, we see that the average value of the position

$$\langle q(t)\rangle = \frac{1}{M}\langle f(t)\rangle * \left(tE_{2-\beta,2}\left(-\frac{\eta}{M}t^{2-\beta}\right)\right) = \frac{1}{M}0 * \left(tE_{2-\beta,2}\left(-\frac{\eta}{M}t^{2-\beta}\right)\right) = 0 \tag{4.5}$$

and, assuming $t \leq t'$, that the position-position correlation

$$\begin{aligned}
\langle q(t)q(t')\rangle &= \frac{1}{M^2}\left\langle \left[f(t) * \left(tE_{2-\beta,2}\left(-\frac{\eta}{M}t^{2-\beta}\right)\right)\right]\left[f(t') * \left(t'E_{2-\beta,2}\left(-\frac{\eta}{M}t'^{2-\beta}\right)\right)\right]\right\rangle \\
&= \frac{1}{M^2}\left\langle \int_0^t f(t-\tau)\tau E_{2-\beta,2}\left(-\frac{\eta}{M}\tau^{2-\beta}\right)\, d\tau \int_0^{t'} f(t'-\tau')\tau' E_{2-\beta,2}\left(-\frac{\eta}{M}\tau'^{2-\beta}\right)\, d\tau'\right\rangle \\
&= \frac{1}{M^2}\int_0^t\int_0^{t'} \langle f(t-\tau)f(t'-\tau')\rangle\, \tau E_{2-\beta,2}\left(-\frac{\eta}{M}\tau^{2-\beta}\right)\tau' E_{2-\beta,2}\left(-\frac{\eta}{M}\tau'^{2-\beta}\right)\, d\tau\, d\tau' \\
&= \frac{1}{M^2}\int_0^t\int_0^{t'} K\delta\left((t-\tau)-(t'-\tau')\right)\tau E_{2-\beta,2}\left(-\frac{\eta}{M}\tau^{2-\beta}\right)\tau' E_{2-\beta,2}\left(-\frac{\eta}{M}\tau'^{2-\beta}\right)\, d\tau\, d\tau' \\
&= \frac{K}{M^2}\int_0^t \tau E_{2-\beta,2}\left(-\frac{\eta}{M}\tau^{2-\beta}\right)\left(\tau-(t-t')\right)E_{2-\beta,2}\left(-\frac{\eta}{M}\left(\tau-(t-t')\right)^{2-\beta}\right)\, d\tau.
\end{aligned}$$

In particular, for $t = t'$, we get the *mean square displacement* (MSD)

$$\langle q(t)^2\rangle = \frac{K}{M^2}\int_0^t \left(\tau E_{2-\beta,2}\left(-\frac{\eta}{M}\tau^{2-\beta}\right)\right)^2\, d\tau. \tag{4.6}$$

We can calculate the behaviour at small t using the power series of the Mittag-Leffler function, which for $|t| \ll (M/\eta)^{1/(2-\beta)}$ gives

$$
\begin{aligned}
\langle q(t)^2 \rangle &= \frac{K}{M^2} \int_0^t \left(\tau \sum_{k=0}^{\infty} \frac{\left(-\frac{\eta}{M}\tau^{2-\beta}\right)^k}{\Gamma((2-\beta)k+2)} \right)^2 \, d\tau \\
&\approx \frac{K}{M^2} \int_0^t \left(\frac{\tau}{\Gamma(2)} \right)^2 \, d\tau \\
&= \frac{Kt^3}{3M^2}.
\end{aligned}
$$

Here, we have found a universal t^3 behaviour for diffusion, which is also found in Richardson's law for quantum turbulence [67].

Numerical evaluation of the MSD for some small values of beta are given in Figure 14a, while Figure 14b shows the behaviour for more general values between zero and one.

In Figure 14b and 15, one observes that for small β , the MSD seems to saturate at some point. Particularly, Figure 15 presents the transition from $\beta = 1$ to $\beta = 0$, which highlights a very non-linear interpolation with a lot of structure and seemingly saturating values. We would like to understand when this saturating behaviour occurs but for this we will need the following Theorem:

Theorem 4.1.1. *(Wang, Zhou and O'Regan [68, Lemma 1.1] or Gorenflo et al. [69, Theorem 4.3]) Let $\alpha \in (0, 2)$ and $0 < \beta \in \mathbb{R}$ be arbitrary. Then, for $p = \lfloor \beta/\alpha \rfloor$, the following asymptotic expansions hold:*

$$
E_{\alpha,\beta}(z) = \frac{1}{\alpha} z^{(1-\beta)/\alpha} \exp\left(z^{1/\alpha}\right) - \sum_{k=1}^{p} \frac{z^{-k}}{\Gamma(\beta - \alpha k)} + O\left(z^{-1-p}\right) \qquad \text{as } z \to \infty; \tag{4.7}
$$

$$
E_{\alpha,\beta}(z) = -\sum_{k=1}^{p} \frac{z^{-k}}{\Gamma(\beta - \alpha k)} + O\left(|z|^{-1-p}\right) \qquad \text{as } z \to -\infty. \tag{4.8}
$$

Applying this theorem to the results of the MSD, we can get a long term behaviour. Namely, for $0 < \beta < 2$, but $\beta \neq \frac{1}{2}$, $t > t_l \gg 1$ and $\eta/M > 0$, we have

$$
\begin{aligned}
\langle q(t)^2 \rangle &= \frac{K}{M^2} \int_0^t \left(\tau E_{2-\beta,2}\left(-\frac{\eta}{M}\tau^{2-\beta}\right) \right)^2 \, d\tau \\
&= \langle q(t_l)^2 \rangle + \frac{K}{M^2} \int_{t_l}^t \left(\tau E_{2-\beta,2}\left(-\frac{\eta}{M}\tau^{2-\beta}\right) \right)^2 \, d\tau \\
&\approx \langle q(t_l)^2 \rangle + \frac{K}{M^2} \int_{t_l}^t \left(\frac{\tau}{\frac{\eta}{M}\tau^{2-\beta}\Gamma(2-(2-\beta))} \right)^2 \, d\tau \\
&= \langle q(t_l)^2 \rangle + \frac{K}{\eta^2 \Gamma(\beta)^2} \int_{t_l}^t \tau^{2\beta-2} \, d\tau \\
&= \langle q(t_l)^2 \rangle + \frac{K}{(2\beta-1)\eta^2\Gamma(\beta)^2} \left(t^{2\beta-1} - t_l^{2\beta-1} \right) \\
&= \left(\langle q(t_l)^2 \rangle - \frac{Kt_l^{2\beta-1}}{(2\beta-1)\eta^2\Gamma(\beta)^2} \right) + \frac{Kt^{2\beta-1}}{(2\beta-1)\eta^2\Gamma(\beta)^2},
\end{aligned}
$$

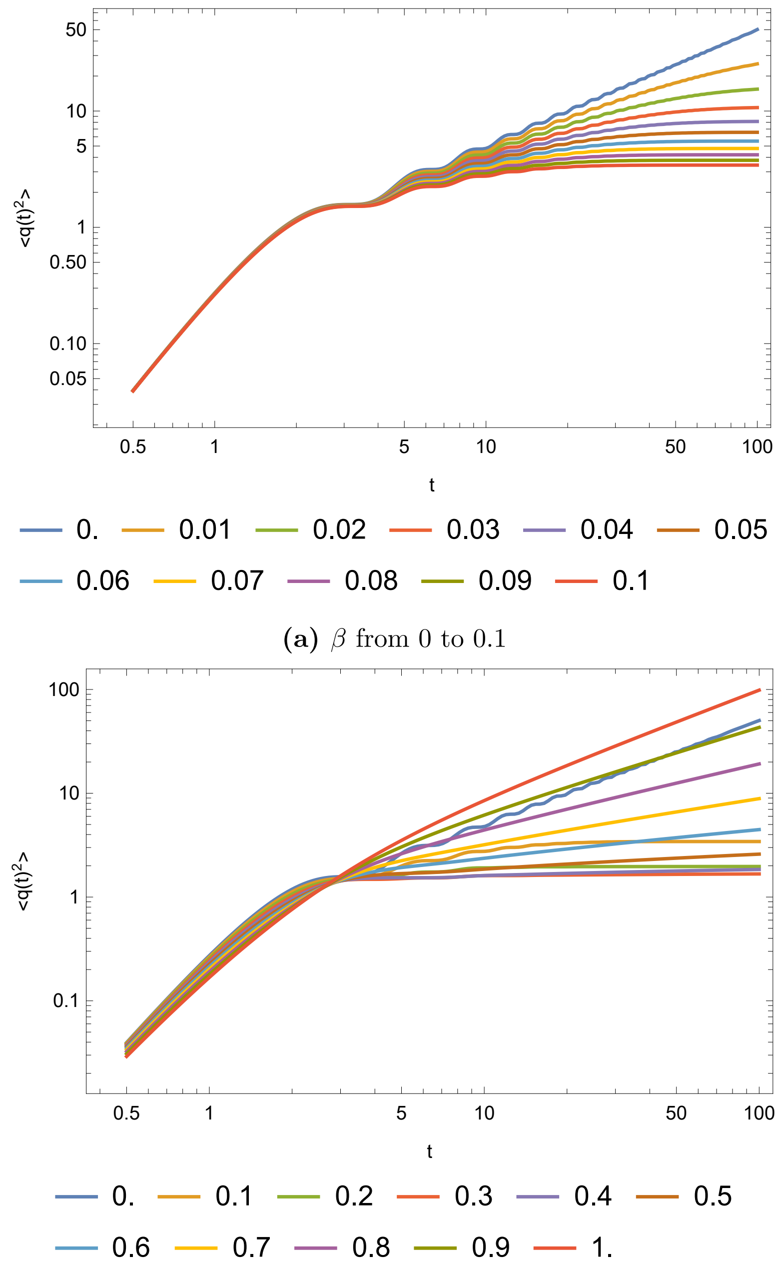

(a) β from 0 to 0.1

(b) β from 0 to 1

Figure 14: Numerical evaluation of the MSD for $K = M = \eta = 1$ and β as indicated in the legend.

while for $\beta = \frac{1}{2}$, we have

$$\begin{aligned}\langle q(t)^2\rangle &\approx \langle q(t_l)^2\rangle + \frac{K}{\eta^2\Gamma(1/2)^2}\int_{t_l}^{t}\tau^{-1}\,d\tau \\ &= \langle q(t_l)^2\rangle + \frac{K}{\eta^2\pi}\ln\left(\frac{t}{t_l}\right).\end{aligned}$$

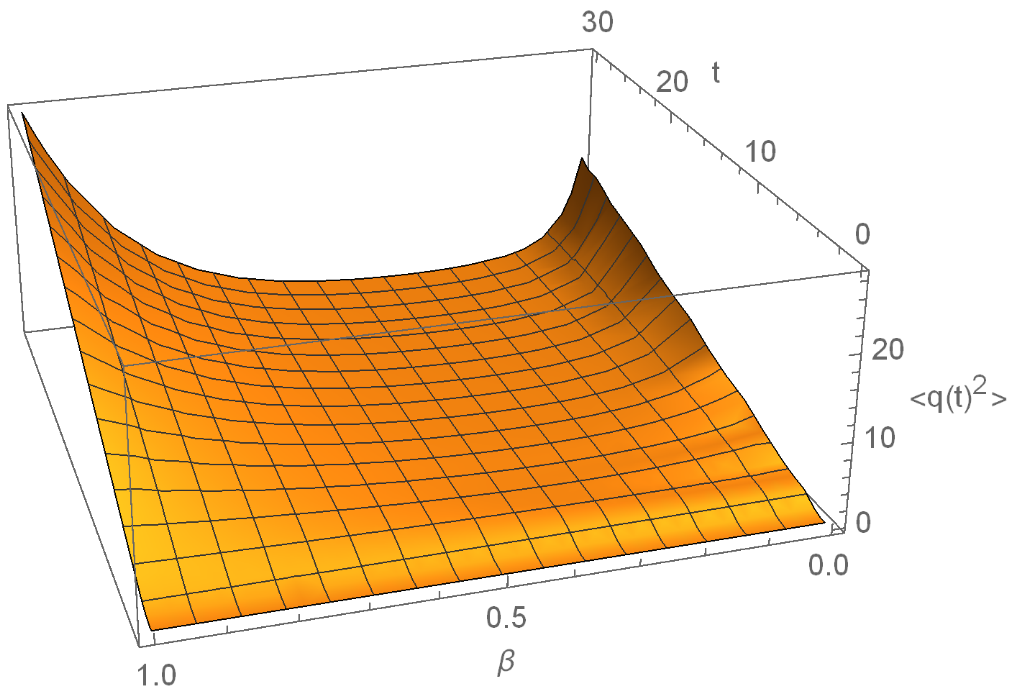

Figure 15: Numerical evaluation of the MSD for $K = M = \eta = 1$, as a function of β and time.

In particular, this means that the MSD will stop growing at large timescales only if $0 < \beta < 1/2$.

Some interesting cases are $\beta = 1$ and $\beta = 0$, as these correspond to known physical systems. For $\beta = 1$, we retrieve the classical Langevin equation and we have the static solution

$$q(t) = \frac{1}{M} f(t) * tE_{1,2}\left(-\frac{\eta}{M}t\right) = \frac{1}{\eta} f(t) * \left(1 - e^{-\frac{\eta}{M}t}\right), \tag{4.9}$$

which is indeed equal to the classical solution.
For $\beta = 0$, we get the equation

$$M\frac{d^2q(t)}{dt^2} + \eta q(t) = f(t),$$

which is a particle moving in a square potential $V(q(t)) = \eta q(t)^2/2$. This gives a harmonic oscillator type solution

$$\begin{aligned} q(t) &= \frac{1}{M} f(t) * tE_{2,2}\left(-\frac{\eta}{M}t^2\right) \\ &= \frac{1}{M} f(t) * t\frac{\sinh\left(\sqrt{-\frac{\eta}{M}t^2}\right)}{\sqrt{-\frac{\eta}{M}t^2}} \\ &= \frac{1}{\sqrt{M\eta}} f(t) * \sin\left(\sqrt{\frac{\eta}{M}}t\right). \end{aligned}$$

4.1.2 Thermal initial conditions

In the physical world, static initial conditions only arise at zero Kelvin, or by connecting the thermal bath instantaneously to the system of interest. Since this is difficult to achieve, it is more realistic to assume a non-zero initial velocity, although the initial position can still be chosen to be zero, based on the chosen axis positions. We will therefore assume the initial conditions $q(0) = 0$ and $\dot{q}(0) = v_0$. In equilibrium, the equipartition theorem would then imply that $\langle v_0 \rangle = 0$ and $\langle v_0^2 \rangle = kT/M$. In this section, however, we will replace the fractional derivative order β by s to avoid confusion with the use of $\beta = 1/kT$ in statistical physics.

Using these initial conditions, we will have to utilise a fractional derivative that allows for ordinary boundary conditions. Hence, here we will utilise the Caputo derivative. Substituting these initial conditions into Eq. (4.3), we find that

$$q(t) = \frac{1}{M} f(t) * \left[t E_{2-s,2} \left(-\frac{\eta}{M} t^{2-s} \right) \right] + v_0 t E_{2-s,2} \left(-\frac{\eta}{M} t^{2-s} \right). \tag{4.10}$$

Applying the usual statistical mechanics tools, we can find the MSD

$$\begin{aligned} \langle q(t)^2 \rangle &= \left\langle \left\{ \frac{1}{M} f(t) * \left[t E_{2-s,2} \left(-\frac{\eta}{M} t^{2-s} \right) \right] \right\}^2 \right\rangle + \left[v_0 t E_{2-s,2} \left(-\frac{\eta}{M} t^{2-s} \right) \right]^2 \\ &\quad + 2 v_0 t E_{2-s,2} \left(-\frac{\eta}{M} t^{2-s} \right) \times \frac{1}{M} \langle f(t) \rangle * \left[t E_{2-s,2} \left(-\frac{\eta}{M} t^{2-s} \right) \right] \\ &= \frac{K}{M^2} \int_0^t \left[\tau E_{2-s,2} \left(-\frac{\eta}{M} \tau^{2-s} \right) \right]^2 d\tau + \left[v_0 t E_{2-s,2} \left(-\frac{\eta}{M} t^{2-s} \right) \right]^2. \end{aligned} \tag{4.11}$$

If we now analyse the new v_0 term compared to the static initial conditions, we can see that its expansion for $t \ll (M/\eta)^{s-2}$ is given by

$$\left[v_0 t E_{2-s,2} \left(-\frac{\eta}{M} t^{2-s} \right) \right]^2 \approx v_0^2 t^2 \frac{1}{\Gamma(2)} = v_0^2 t^2. \tag{4.12}$$

Since this is bigger than the t^3 contribution from the static MSD, we find the new short-term expansion

$$\left\langle q \left(t \ll \left(\frac{M}{\eta} \right)^{s-2} \right)^2 \right\rangle = v_0^2 t^2, \tag{4.13}$$

or in other words, the short-time expansion yields a ballistic motion.

The long-term expansion remains unchanged, however. This can be easily seen because the expression is similar to the static MSD, but without being integrated in time. Hence, the expansion of the new term will be 1 order of t lower (hence t^{2s-2}) and thus negligible for any $s < 1$ and $t \gg (M/\eta)^{s-2}$. Therefore, we retain the logarithmic expansion for $s = 0.5$, and else the expansion is given by

$$\left\langle q \left(t \gg \left(\frac{M}{\eta} \right)^{s-2} \right)^2 \right\rangle \sim \frac{K t^{2s-1}}{(2s-1) \eta^2 \Gamma(s)^2}. \tag{4.14}$$

Remark that, for $s < 0.5$, this exponent is negative, which means that the system will stop growing and saturate at long times. This will be crucial for the following Section.

4.2 Time glass

We now come to the most important scientific contribution of this thesis, also available in Ref. [66]. Time glasses have been recently conjectured by Wilczek [23]. With a time glass, we mean a system which in equilibrium has an overall glassy structure, in the sense that the MSD is finite at infinite times, but which also shows a periodic glassy behaviour. To better understand this, we first recall that the MSD of a glass shows ballistic behaviour followed by saturation (recall Figure 12). The periodic glassy behaviour can then be encapsulated in a staircase-like MSD with plateaus followed by ballistic motion, similar to the Gardner phase in glass. An important difference, however, is that the Gardner phase shows an infinite staircase MSD. This is therefore not an overall glassy state, as this will blow up as time goes on.

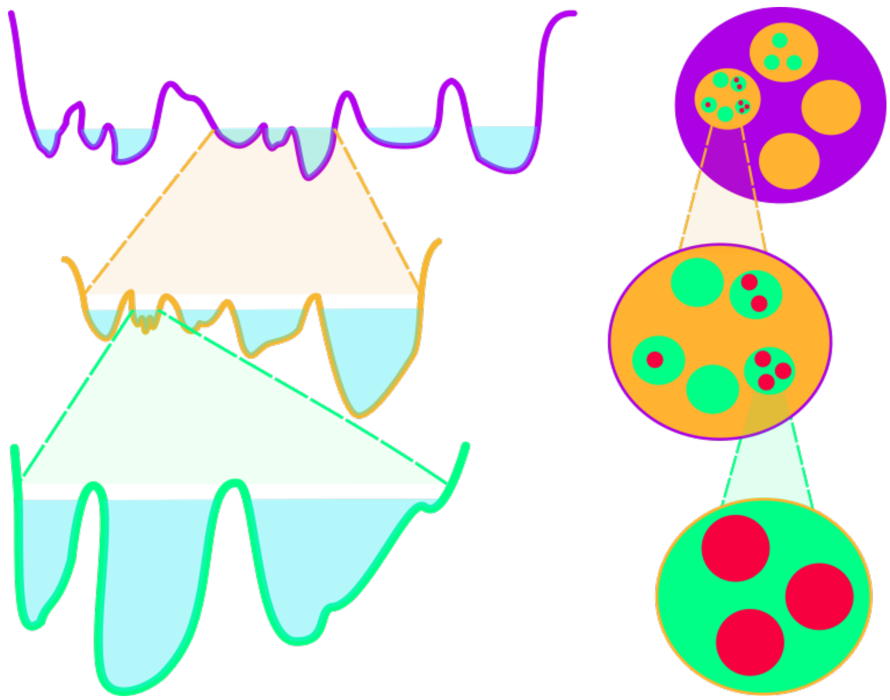

Figure 16: Left: A free energy landscape with fractal-like metastable minima. Right: A hierarchy of cages inside cages. Here, the total energy landscape (purple) has four local minima corresponding to the total number of large orange cages. Zooming in on one of these minima, we see five smaller local minima implying five smaller green cages inside this orange cage. Moreover, inside one green cage there are 3 red cages, and so forth.

The Energy landscape in Fig. 16 of this time-glass system is very closely related to the Gardner phase in glass. The most important difference is that the fractality in the landscape is only to finite depth, increasing in generation when $s \to 0$. The local minima in the energy landscape correspond to the cages on the right. A local minimum inside a larger local minimum will effectively act as a cage inside a cage. The particle will first only explore the larger cage before being trapped in the smaller cage.

In Fig. 17, the MSD of the fractional Langevin equation (see Eq. 4.11) has been plotted for several values of s from zero to one. It shows ballistic short-time behaviour in all cases. For $s = 1$, we retrieve the conventional Langevin equation, which describes Brownian motion. The MSD shows a crossover from a ballistic ($\sim t^2$) to a linear dependence in time, characteristic of a liquid [Fig. 17(a)]. For $s \lesssim 0.5$, instead, the MSD saturates at large times, thus describing a glass [Fig. 17(b)]. We find that a particularly interesting regime is provided by small values of s, in the interval $0 < s \lesssim 0.1$. In this case, a sequence of small metastable plateaus characterises a finite-depth fractal glass phase, before the conventional glass regime is reached at larger times [Fig. 17(c)]. For $s = 0$, the "marginal

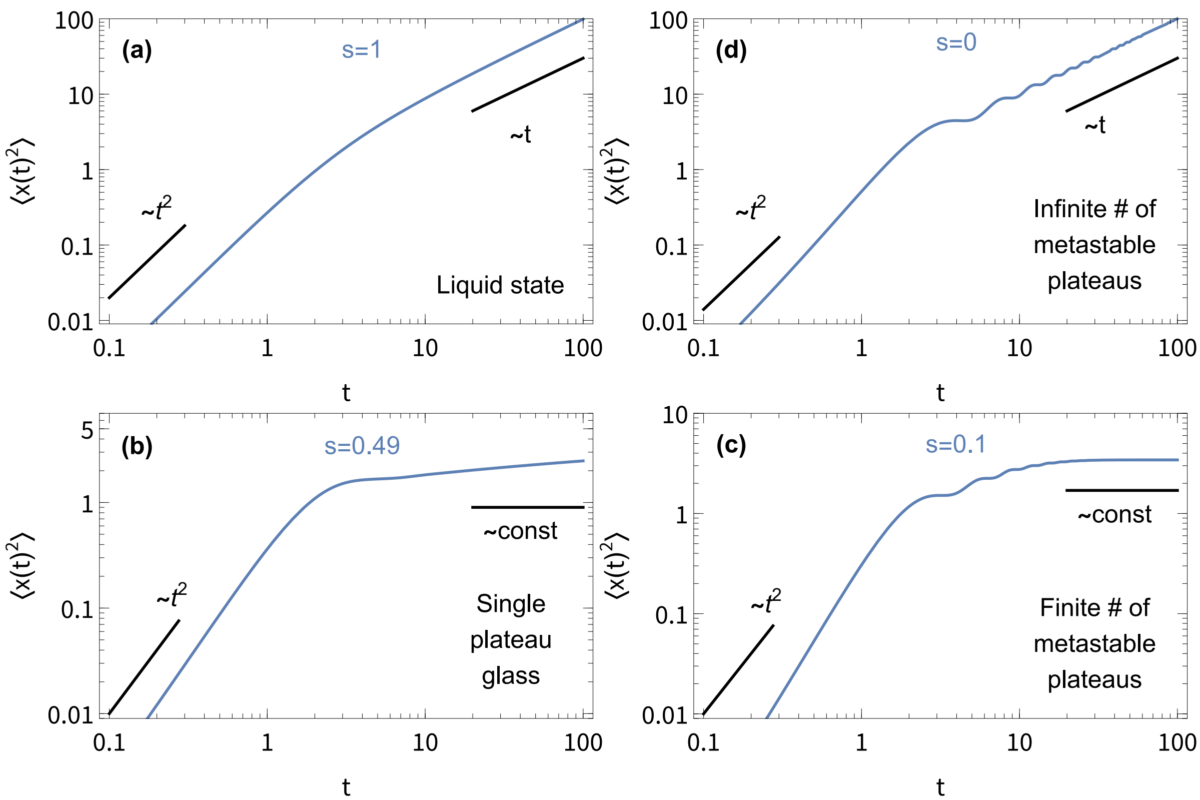

Figure 17: The exact MSD for different values of s. **(a)** A regular Brownian motion. **(b)** A usual glassy behaviour, exhibiting ballistic motion at short times and localisation at longer times. **(c)** An unconventional glass, displaying ballistic motion at short times, but also an intermediate regime with a set of small plateaus, before the long-time plateau sets in. **(d)** A particle in a quadratic potential. Here, the friction term vanishes and an infinite collection of plateaus appear. The overall slope is however finite, reminiscent of a liquid behaviour. The analytical asymptotes for $t \to 0$ and $t \to \infty$ are drawn next to the plots.

glass" phase, proposed by Gardner, is realised, with an infinite number of metastable plateaus and finite average slope ($\sim t$), typical of liquids. This is an asymptotic phase, in which the fractal glass acquires infinite depth [Fig. 17(d)].

Now, we concentrate on the region $0 < s \lesssim 0.1$, which describes a finite-depth fractal glass, reminiscent of the Gardner phase. The evolution of the MSD upon varying s is depicted in Fig. 18. At short times ($0 < t < \pi\sqrt{M/\eta}$), there exists a universal regime, in which all curves collapse into a single one. Afterwards, the small plateaus regime sets in, but the overall slope of the intermediate-time behaviour *increases* as s is reduced, thus showing a gradual transition from an overall glass to liquid phase. At sufficiently long times, there is saturation, except for $s = 0$. This freezing occurs on increasingly longer timescales as s is reduced. More interestingly, the length of these plateaus is constant in time, as promptly visualised in a linear scale plot (inset of Fig. 18). This emergent frequency indicates that we are observing a *time-glass* phase.

The periodicity in the MSD can be calculated with the observation that the period is independent

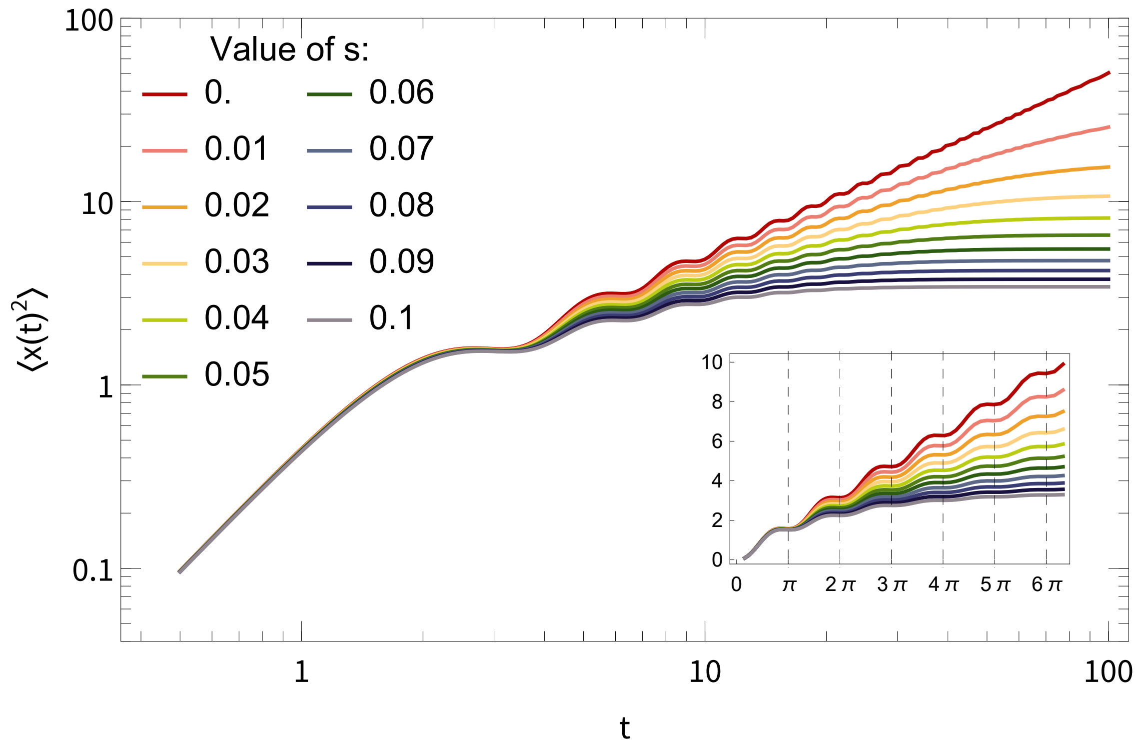

Figure 18: The MSD for several small values of s, as indicated in the legend. The inset shows a linear scale plot to highlight the periodicity in the anomalous glass phase, characterising a time glass.

of s. We can therefore use a simpler model with $s = v_0 = 0$, to get

$$\begin{aligned} \langle x(t)^2 \rangle &= \frac{K}{M^2} \int_0^t \left[\tau E_{2,2} \left(-\frac{\eta}{M} \tau^2 \right) \right]^2 \, d\tau \\ &= \frac{K}{M\eta} \int_0^t \sin^2 \left(\sqrt{\frac{\eta}{M}} \tau \right) \, d\tau \\ &= \frac{K}{2M\eta} \left[t + \frac{1}{2} \sqrt{\frac{M}{\eta}} \sin \left(2 \sqrt{\frac{\eta}{M}} t \right) \right], \end{aligned} \tag{4.15}$$

where the relation between the Mittag-Leffler function and the sine can be seen using their Taylor expansions. This yields a periodicity of $\pi\sqrt{M/\eta}$ in time. For non-zero s, the same period applies only in a finite time-window before freezing.

The position and velocity auto-correlation functions (PACF and VACF, respectively) have been plotted alongside a normalised MSD for several values of s in Fig. 19. Here, we can observe a clear relation between the plateaus in the MSD and the oscillations in the PACF and VACF. Upon lowering s from one, we see small oscillations forming for a short initial period. These oscillations then become larger and remain for longer times, until at $s = 0$ they become a sine function in the harmonic oscillator. We want to highlight the striking similarity in the PACF with Ref. [70], even though their system is different with a coloured noise and external harmonic potential.

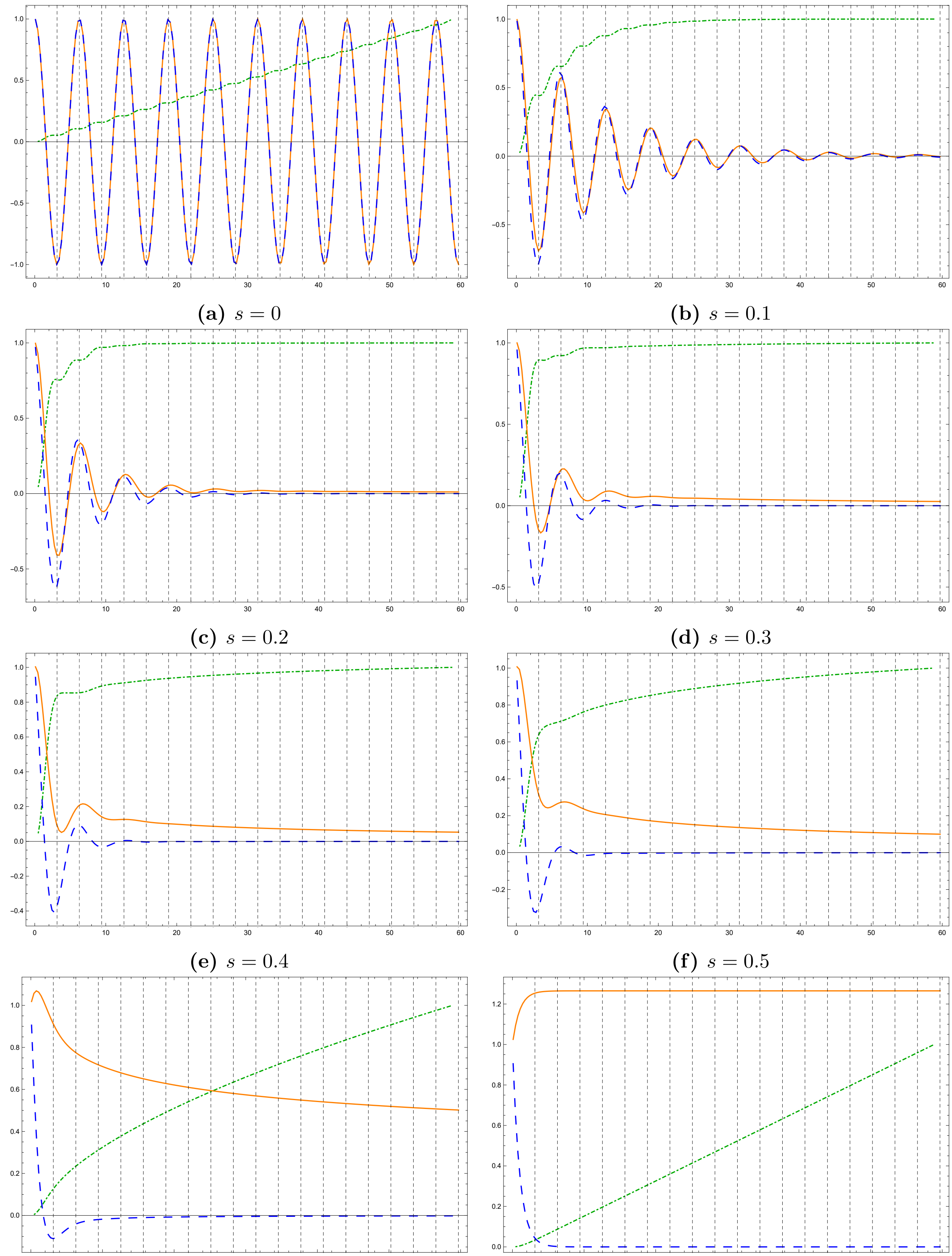

(a) $s = 0$

(b) $s = 0.1$

(c) $s = 0.2$

(d) $s = 0.3$

(e) $s = 0.4$

(f) $s = 0.5$

(g) $s = 0.8$

(h) $s = 1$

Figure 19: Normalised MSD (Green, Dotdashed), PACF (Orange, Line), VACF (Blue, Dashed). The dashed vertical lines are at multiples of the emergent periodicity $\pi\sqrt{M/\eta}$.

The analytical forms of the PACF and VACF for $t_0 \gg (M/\eta)^{s-2}$ are given by

$$\begin{aligned}\frac{\langle x(t_0)x(t_0+t)\rangle}{\langle x(t_0)^2\rangle} &= \frac{K}{M^2\langle x(t_0)^2\rangle}\int_0^{t_0} \tau E_{2-s,2}\left(-\frac{\eta}{M}\tau^{2-s}\right)\times \\ &\quad (t+\tau)E_{2-s,2}\left(-\frac{\eta}{M}(t+\tau)^{2-s}\right)\,\mathrm{d}\tau \end{aligned} \tag{4.16}$$

$$\begin{aligned}\frac{\langle v(t_0)v(t_0+t)\rangle}{\langle v(t_0)^2\rangle} &= \frac{K}{M^2\langle v(t_0)^2\rangle}\int_0^{t_0} \left[\frac{\mathrm{d}}{\mathrm{d}\tau}\tau E_{2-s,2}\left(-\frac{\eta}{M}\tau^{2-s}\right)\right]\times \\ &\quad \left[\frac{\mathrm{d}}{\mathrm{d}(t+\tau)}(t+\tau)E_{2-s,2}\left(-\frac{\eta}{M}(t+\tau)^{2-s}\right)\right]\,\mathrm{d}\tau. \end{aligned} \tag{4.17}$$

Since we have computed the analytical long-time exponent of the MSD, given by t^{2s-1}, one might expect a universality in a rescaling regime. By rescaling the MSD with $t^{1/(2s-1)}$ we would expect a universal linear long-time exponent. However, this is not always the case, as the exponent is negative for $s < 1$. This would thus result in a flip of the time axis[13], making the universal exponent show in the short-time regime for these values of s. We, therefore, rescale with the absolute value $t^{1/|2s-1|}$. This rescaling is presented in Figure 20 for some small s values. We observe that the final saturation of the MSD is retained by this rescaling. Indeed, this is expected since the MSD will be approximately constant in this regime, and a constant function does not change upon rescaling the input.

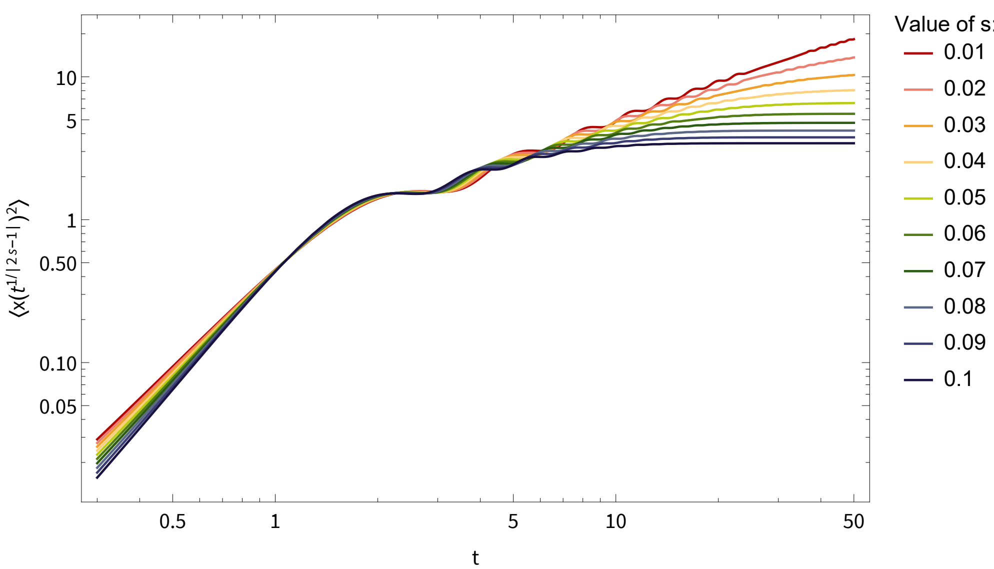

Figure 20: A plot of the MSD rescaled with $t^{1/|2s-1|}$ for several small s values.

4.3 Microscopic model

Now, we will follow the same steps of the Caldeira-Leggett calculation, but using the TLS Bath instead of the harmonic oscillators, to show a microscopic model for the time glass. Therefore, we have to revisit both the computation of the friction term and of the force term, as these are the terms that depend on the spectral function. We will use the same model as Ref. [44], but in a

[13] Similar to $t \to 1/t$.

low-temperature limit, $kT \ll \hbar\Omega$ in combination with the limit $\Omega \to \infty$. Recall that the spectral function of the two-level systems bath is given by

$$J(\omega, T) = \begin{cases} \frac{\pi}{2}\eta\omega^s \tanh\left(\frac{\hbar\omega_j}{2kT}\right) & \text{if } \omega < \Omega \\ 0 & \text{if } \omega > \Omega. \end{cases} \tag{4.18}$$

Taking the limit $kT \ll \hbar\Omega$ will therefore send the tangent hyperbolic to its limiting value of 1. After the limit $\Omega \to \infty$, this results in an effective spectral function given by

$$J(\omega) = \eta(s)\omega^s, \tag{4.19}$$

where we allow η to depend on the value of s. In this way, we aim to produce an effective fractional Langevin equation for the description the of particle.

Starting with the friction term in Eq. (3.31), we insert the new spectral function for the sub-Ohmic case, where $0 < s < 1$, to find

$$\begin{aligned} F_{fr} &= \frac{\mathrm{d}}{\mathrm{d}t}\left\{\frac{2}{\pi}\int_0^t d\tau \int_0^\infty d\omega \frac{J(\omega)}{\omega}\cos[\omega(t-\tau)]q(\tau)\right\} \\ &= \frac{\mathrm{d}}{\mathrm{d}t}\left\{\frac{2\eta(s)}{\pi}\int_0^t d\tau \int_0^\infty d\omega\omega^{s-1}\cos[\omega(t-\tau)]q(\tau)\right\} \\ &= \frac{\mathrm{d}}{\mathrm{d}t}\left\{\frac{2\eta(s)}{\pi}\int_0^\infty d\omega\omega^{s-1}\cos(\omega)\int_0^t d\tau(t-\tau)^{-s}q(\tau)\right\} \\ &= \frac{2\eta(s)}{\pi}\int_0^\infty d\omega\omega^{s-1}\cos(\omega)\frac{\mathrm{d}}{\mathrm{d}t}\int_0^t d\tau(t-\tau)^{-s}q(\tau), \end{aligned} \tag{4.20}$$

where, in the third line, we shifted $\omega \to \omega/(t-\tau)$. Although this shift is only valid for $t \neq \tau$, the expression before the shift has a pole of order s at $t = \tau$, identical to the pole we get after the shift at the boundary $t = \tau$. We therefore conclude that the shift $\omega \to \omega/(t-\tau)$ is valid on the entire domain.

In the last line of Eq. (4.20), we can now recognise a Riemann-Liouville fractional derivative up to the constant from the gamma function. However, assuming that $q(0) = 0$, we know that the Riemann-Liouville derivative is equal to the Caputo derivative and so that

$$F_{fr} = \frac{2\eta(s)}{\pi}\Gamma(1-s)\int_0^\infty d\omega\omega^{s-1}\cos(\omega)\, {}_0^C\mathbf{D}_t^s q(t). \tag{4.21}$$

Focusing on the remaining integral, we expand the cosine into its exponential form and do a reparametrisation $\omega = \pm i\nu$ to see that

$$\begin{aligned} \int_0^\infty \omega^{s-1}\cos(\omega)\ \mathrm{d}\omega &= \frac{1}{2}\int_0^\infty \omega^{s-1}e^{i\omega}\ \mathrm{d}\omega + \frac{1}{2}\int_0^\infty \omega^{s-1}e^{-i\omega}\ \mathrm{d}\omega \\ &= \frac{i^s}{2}\int_0^{-i\infty} \nu^{s-1}e^{-\nu}\ \mathrm{d}\nu + \frac{i^{-s}}{2}\int_0^{i\infty} \nu^{s-1}e^{-\nu}\ \mathrm{d}\nu. \end{aligned} \tag{4.22}$$

From Eq. (4.22), we note that we can make two-quarter circle complex-contour integrations and combine this with the Cauchy-integral theorem to conclude that both integrals are equal to the integral from 0 to ∞ when $s < 1$. We therefore find that

$$\int_0^\infty \omega^{s-1}\cos(\omega)\ \mathrm{d}\omega = \frac{i^s + i^{-s}}{2}\int_0^\infty \nu^{s-1}e^{-\nu}\ \mathrm{d}\nu = \cos\left(\frac{\pi s}{2}\right)\Gamma(s), \tag{4.23}$$

and thus

$$F_{fr} = \frac{2\eta(s)}{\pi}\Gamma(1-s)\Gamma(s)\cos\left(\frac{\pi s}{2}\right) {}_0^C\mathbf{D}_t^s q(t). \tag{4.24}$$

We can further simplify Eq. (4.24) using Euler's reflection formula:

$$\Gamma(s)\Gamma(1-s) = \frac{\pi}{\sin(\pi s)} \quad \forall s \notin \mathbb{Z}. \tag{4.25}$$

To absorb the constants, we now define

$$\eta(s) = \frac{\eta_s \sin(\pi s)}{2\cos\left(\frac{\pi s}{2}\right)} = \eta_s \sin\left(\frac{\pi s}{2}\right), \tag{4.26}$$

such that we have

$$F_{fr} = \eta_s \, {}_0^C\mathbf{D}_t^s q(t). \tag{4.27}$$

The change in spectral function also has consequences for the correlation of the noise term. As we saw in Eq. (3.34), the force is given in microscopic variables by

$$f(t) = \sum_j C_j \left[q_j(0)\cos(\omega_j t) + \frac{\dot{q}_j(0)}{\omega_j}\sin(\omega_j t) \right] \tag{4.28}$$

and, since equipartition breaks down at low temperatures, we assume the following rescaled microscopic correlations:

$$\langle q_j(0)\rangle = \langle \dot{q}_j(0)\rangle = \langle \dot{q}_j(0) q_{j'}(0)\rangle = 0, \tag{4.29}$$

$$\langle q_j(0) q_{j'}(0)\rangle = \frac{k_B T}{m_j \omega_j^{s+1}}\delta_{jj'}, \tag{4.30}$$

$$\langle \dot{q}_j(0) \dot{q}_{j'}(0)\rangle = \frac{k_B T}{m_j \omega_j^{s-1}}\delta_{jj'}. \tag{4.31}$$

We will show that these correlations lead to a white-noise force. We can quickly see that the average force is still zero, but the force squared correlation in this model is now given by

$$\begin{aligned}
\langle f(t) f(t')\rangle &= \left\langle \sum_j C_j \left[q_j(0)\cos(\omega_j t) + \frac{\dot{q}_j(0)}{\omega_j}\sin(\omega_j t)\right] \sum_{j'} C_{j'} \left[q_{j'}(0)\cos(\omega_{j'} t') + \frac{\dot{q}_{j'}(0)}{\omega_{j'}}\sin(\omega_{j'} t')\right] \right\rangle \\
&= \sum_{jj'} C_j C_{j'} \left[\langle q_j(0) q_{j'}(0)\rangle \cos(\omega_j t)\cos(\omega_{j'} t') + \frac{\langle \dot{q}_j(0)\dot{q}_{j'}(0)\rangle}{\omega_j \omega_{j'}}\sin(\omega_j t)\sin(\omega_{j'} t') \right. \\
&\quad \left. + \frac{\langle q_j(0)\dot{q}_{j'}(0)\rangle}{\omega_{j'}}\cos(\omega_j t)\sin(\omega_{j'} t') + \frac{\langle \dot{q}_j(0) q_{j'}(0)\rangle}{\omega_j}\sin(\omega_j t)\cos(\omega_{j'} t') \right] \\
&= \sum_{jj'} C_j C_{j'} \left[\frac{k_B T}{m_j \omega_j^{s+1}}\delta_{jj'}\cos(\omega_j t)\cos(\omega_{j'} t') + \frac{k_B T}{m_j \omega_j \omega_{j'} \omega_j^{s-1}}\delta_{jj'}\sin(\omega_j t)\sin(\omega_{j'} t') \right],
\end{aligned} \tag{4.32}$$

where we have used the linearity in the expectation and plugged in the new expectations for the "oscillators", given by Equations (4.30) and (4.31). Now, using the delta functions and extracting the form of the spectral function, we find

$$\begin{aligned}\langle f(t)f(t')\rangle &= \sum_j C_j^2 \frac{k_B T}{m_j \omega_j^{s+1}} \left[\cos(\omega_j t)\cos(\omega_j t') + \sin(\omega_j t)\sin(\omega_j t')\right] \\ &= k_B T \sum_j \frac{C_j^2}{m_j \omega_j^{s+1}} \cos[\omega_j (t-t')] \\ &= k_B T \int_0^\infty d\omega \sum_j \frac{C_j^2}{m_j \omega_j^{s+1}} \delta(\omega - \omega_j) \cos[\omega_j (t-t')] \\ &= k_B T \frac{2}{\pi} \int_0^\infty d\omega \frac{J(\omega)}{\omega^s} \cos[\omega (t-t')]. \end{aligned} \tag{4.33}$$

Since the low-temperature limit provides an effective $J(\omega) = \eta_s \sin(\pi s/2)\, \omega^s$, we can see that for any s, it only remains left with an integral over the cosine, which provides the effective correlation

$$\langle f(t)f(t')\rangle = 2\eta_s k_B T \sin\left(\frac{\pi s}{2}\right) \delta(t-t'). \tag{4.34}$$

Observe that the limit $s \to 1$ retrieves the familiar formula for Brownian white-noise. However, for $0 < s < 1$, we see that the bath of semi-classical truncated oscillators, with energies rescaled by ω^{1-s}, in a low-temperature limit gives rise to the fractional Langevin equation as its effective description. We have thus found a connection between quantum motion and Caputo fractional derivatives.

5 Applications of the fractional (kinetics) Langevin equation

The original Langevin equation has a second and first order derivative, which we generalised to a second and β order derivative in Chapter 4, changing the friction term to a viscoelastic term. Now, we will also generalise the Newtonian second order derivative to a fractional derivative of order α, which we will call fractional kinetics. Although this lays the interpretation of the external force open, we will see how this even more general fractional-kinetics Langevin equation can still be solved analytically and how it will give rise to many different kinds of systems found in Nature.

5.1 Fractional-kinetics Langevin equation

Suppose that we want to have an even more general equation than the fractional Langevin equation, replacing the second order derivative (kinetic term) with a fractional order derivative, allowing us to put more systems into the same class of equations. We thus consider the fractional-kinetics Langevin equation

$$M\mathbf{D}_t^{\alpha} q(t) + \eta \mathbf{D}_t^{\beta} q(t) = f(t), \tag{5.1}$$

where $f(t)$ is the random "force"[14], and we will assume that $\alpha > \beta \geq 0$ for all the following calculations.

We have already derived the general solution of Equation (5.1) for both Riemann-Liouville and Caputo fractional derivatives in Examples 2.3.11 and 2.3.12. Here, we will do some statistical analysis for static initial conditions, in which case, the choice of definition will not matter and in either case we find the solution

$$q(t) = \frac{1}{M} f(t) * \left[t^{\alpha-1} E_{\alpha-\beta,\alpha}\left(-\frac{\eta}{M} t^{\alpha-\beta}\right)\right]. \tag{5.2}$$

Applying the same statistics on $f(t)$ as in the original fractional Langevin equation allows us to find that

$$\langle q(t) \rangle = 0, \tag{5.3}$$

$$\langle q(t)^2 \rangle = \frac{K}{M^2} \int_0^t \left[\tau^{\alpha-1} E_{\alpha-\beta,\alpha}\left(-\frac{\eta}{M} \tau^{\alpha-\beta}\right)\right]^2 \, d\tau. \tag{5.4}$$

The small t expansion of the MSD is given by

$$\begin{aligned}
\langle q(t)^2 \rangle &= \frac{K}{M^2} \int_0^t \left[\tau^{\alpha-1} E_{\alpha-\beta,\alpha}\left(-\frac{\eta}{M} \tau^{\alpha-\beta}\right)\right]^2 \, d\tau \\
&\approx \frac{K}{M^2} \int_0^t \left[\frac{\tau^{\alpha-1}}{\Gamma(\alpha)} \right]^2 \, d\tau \\
&= \begin{cases} \frac{K}{M^2 \Gamma(\alpha)(2\alpha-1)} \, t^{2\alpha-1} & \text{if } \alpha \neq 1/2, \\ \frac{K}{M^2 \Gamma(\alpha)} \, \ln(t) & \text{if } \alpha = 1/2. \end{cases}
\end{aligned}$$

In particular this implies a negative exponent if $\alpha < 1/2$.

[14]Since we have changed the Newtonian term of $f = ma$, $f(t)$ is in first principle not a force, but we will keep the name "force" to indicate the properties of the function $f(t)$. We can take the $2-\alpha$ derivative of the fractional-kinetics equation to see $\mathbf{D}_t^{2-\alpha} f(t)$ as a force.

The large-time expansion is also similar to the original fractional Langevin equation. There is, however, a new restriction when using Theorem 4.1.1 for the asymptotic behaviour. We need the first index of the Mittag-Leffler function to be between 0 and 2. For this MSD, that means that we need $0 < \alpha - \beta < 2$, or $\beta < \alpha < 2 + \beta$, in order to use Theorem 4.1.1. In that case, however, we find that for $\beta \neq \frac{1}{2}$, $t > t_l \gg 1$ and $\eta/M > 0$, we have

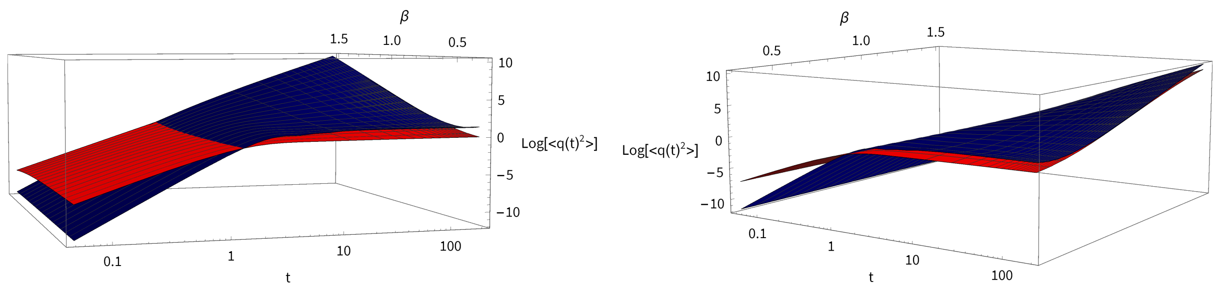

(a) **(b)**

Figure (a,b): Two viewpoints of the MSD with $\alpha = 1.6$ (red) and $\alpha = 2.2$ (blue) and β varying between 0.3 and 1.5.

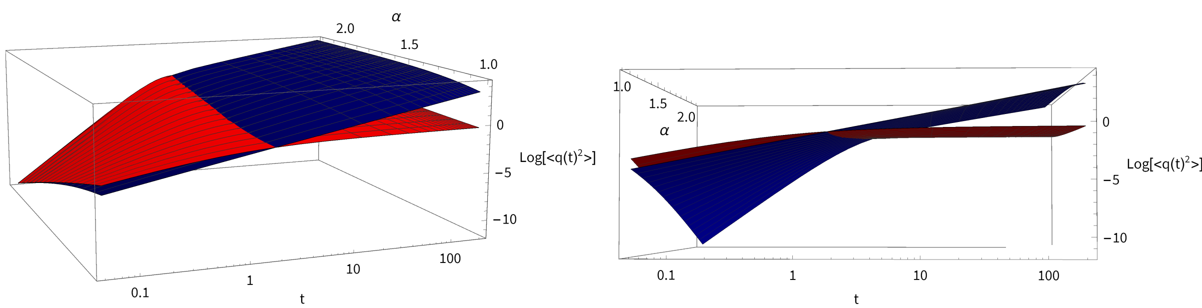

(c) **(d)**

Figure (c,d): Two viewpoints of the MSD with $\beta = 0.3$ (red) and $\beta = 0.9$ (blue) and α varying between 1 and 2.2.

Figure 21: A comparison of the MSD for two choices of derivative orders and the other derivative order varying with $K = \eta = M = 1$. Note that we plot the logarithm of the MSD and the time axis has logarithmic scaling.

$$
\begin{aligned}
\langle q(t)^2\rangle &= \frac{1}{M} f(t) * \left[t^{\alpha-1} E_{\alpha-\beta,\alpha}\left(-\frac{\eta}{M} t^{\alpha-\beta}\right)\right] \\
&= \langle q(t_l)^2\rangle + \frac{K}{M^2}\int_{t_l}^{t} \left[\tau^{\alpha-1} E_{\alpha-\beta,\alpha}\left(-\frac{\eta}{M}\tau^{\alpha-\beta}\right)\right] \, d\tau \\
&\approx \langle q(t_l)^2\rangle + \frac{K}{M^2}\int_{t_l}^{t} \left(-\frac{\tau^{\alpha-1}}{-\frac{\eta}{M}\tau^{\alpha-\beta}\Gamma(\alpha-(\alpha-\beta))}\right)^2 \, d\tau \\
&= \langle q(t_l)^2\rangle + \frac{K}{\eta^2\Gamma(\beta)^2}\int_{t_l}^{t} \tau^{2\beta-2} \, d\tau \\
&= \langle q(t_l)^2\rangle + \frac{K}{(2\beta-1)\eta^2\Gamma(\beta)^2}\left(t^{2\beta-1} - t_l^{2\beta-1}\right) \\
&= \left(\langle q(t_l)^2\rangle - \frac{K t_l^{2\beta-1}}{(2\beta-1)\eta^2\Gamma(\beta)^2}\right) + \frac{K t^{2\beta-1}}{(2\beta-1)\eta^2\Gamma(\beta)^2},
\end{aligned}
$$

while for $\beta = \frac{1}{2}$, we have

$$
\begin{aligned}
\langle q(t)^2\rangle &\approx \langle q(t_l)^2\rangle + \frac{K}{\eta^2\Gamma(1/2)^2}\int_{t_l}^{t} \tau^{-1} \, d\tau \\
&= \langle q(t_l)^2\rangle + \frac{K}{\eta^2\pi}\ln\left(\frac{t}{t_l}\right).
\end{aligned}
$$

Remarkably, we find that this is, up to the extra condition required for the statement to hold, exactly the same formula as for the original fractional Langevin equation. In other words, the long term MSD behaviour is, for $\beta < \alpha < 2+\beta$, independent of α. Combining this with the observation that the short-term behaviour is completely determined by α and independent of β, we get the opportunity to tune both short- and long-term exponents of the MSD simply by tuning the orders of derivatives used in the differential equation. In Figure 21, we can see this property graphically. In 21(a,b), where we have two different α, we can see that the short-term MSD is very different while the long term MSD looks very similar. In Figure 21(c,d), where we have two different β, we can see that the short term MSD looks very similar, while the long term MSD is different. We can also observe this behaviour by looking at the slope in the direction of the varying parameter: In Figure 21(a,b) we see very little change while varying β for small t, whereas we can see a clear change for large t. The opposite holds for Figure 21(c,d).

5.2 Applications to physical systems

The fractional-kinetics Langevin equation (Eq. 5.1) can give rise to many different forms, depending on the choice of α and β. In this Section, we will highlight several areas of physics where sub-cases of this analytically solved equation have been shown to describe some physical system. We begin with the integer-order cases, followed by the fractional Langevin equation with a different type of noise. Next, we compare our analytical solution to some numerical work on the relaxation oscillation equation, where-after we discuss the Bagley-Torvik equation.

Integer cases

Equation (5.1) has two free parameters, α and β, to tune to any pair of real numbers. Beside the main purpose of expanding outside of integer orders, this also allows to encapsulate many different ordinary differential equations into one class of solutions. Some of the most basic physical systems such as Newton's second law, the motion of a harmonic oscillator $m\ddot{x} + kx = F_{ext}$, or Brownian motion using the classical Langevin equation $m\ddot{x}+\eta\dot{x} = F_{ext}$ are all just specific cases of this general equation. Another example includes the Abraham-Lorentz equation to describe the self-radiation reaction of a charged particle (see Ref. [71] for a historic overview on self-radiation descriptions):

$$m\frac{d^2}{dt^2}x - m\tau\frac{d^3}{dt^3}x = F_{ext}, \tag{5.5}$$

where $\tau = 2e^2/3mc^3$ provides a time scale, e is the charge of the particle, c the speed of light, m the mass, and F_{ext} is an external force. For a white-noise force, the MSD has been plotted in Figure 22. Although all these equations have been solved independently, the idea to combine them using the differential orders as continuous parameters seems intriguing. For example, in the fractional Langevin equation we obtained the integer limits of Brownian motion and a driven harmonic oscillator. In the intermediate regime, we found much more structure than from a simple linear interpolation. It would be interesting to try similar fractional transitions to other systems which can fall in the same class according to this fractional derivative scheme.

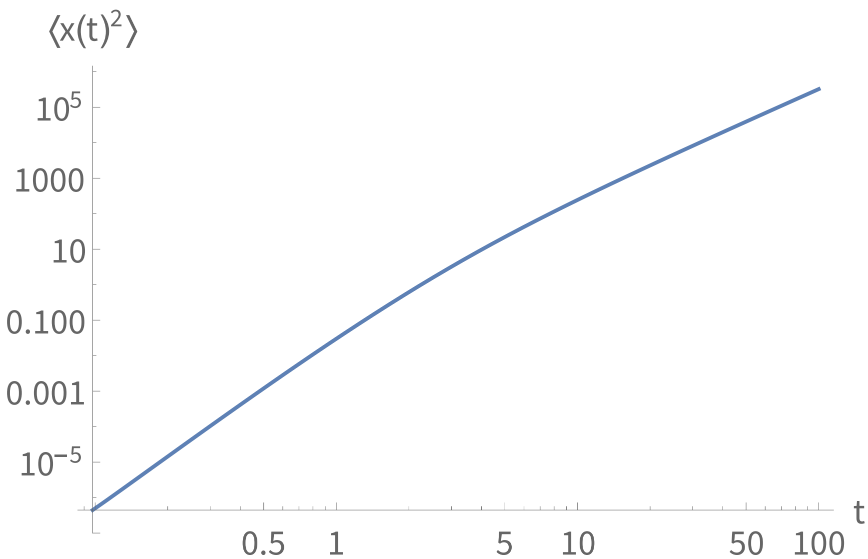

Figure 22: A log-log plot of the MSD for the Abraham-Lorentz equation, subjected to a white-noise force, with all zero initial conditions. The short-time exponent is t^5 and the long-time exponent is t^3.

Fractional Langevin equation with coloured noise

In this thesis, we have mostly been describing the fractional Langevin equation with a white-noise force. However, much attention has been given to the same equation with coloured noise [72–76], *i.e.*,

$$\langle f(t)f(t')\rangle = K(t-t')^{-\beta}. \tag{5.6}$$

This coloured noise depends on the order of the fractional derivative. The reasoning behind this choice comes from the fluctuation-dissipation theorem, which relates the thermodynamic fluctuations to the dissipation constant, thus allowing to describe systems at higher temperatures. Note that the solution of the fractional Langevin equation is identical in either case, since the change will only show up once the statistics play a role. We can compare many results of our work with this coloured noise, simply by dimensional analysis. Since the dimension of a delta function is equal to the inverse of its input, the dimensional difference between white noise and coloured noise is an order of $t^{1-\beta}$. Hence, the exponent of quantities such as the MSD will change from $2\beta - 1$ to just β with coloured noise. An important implication of this is that this means that the fractional Langevin equation shows only regular sub-diffusion for $\beta < 1$, without any saturation in the MSD. This is also a direct proof for why the coloured noise cannot describe a time glass. This system has, however, been linked to a microscopic model of a tracer particle in a one-dimensional many-particle system with a general two-body interaction potential [73]. In Ref. [74], the solution of the coloured-noise fractional Langevin equation is also compared with experiments in Ref. [77] with protein molecules.

Comparison with numerical work on the relaxation-oscillation equation

In this thesis, we have only focused on analytical results. However, numerical tools have been of great use for many applications. During this thesis, Dr. Varese S. Timóteo from Universidade Estadual de Campinas (UNICAMP) visited the group of Prof. Morais Smith. During this time, we had a discussion on fractional derivative equations. Dr. Timoteo had recently looked into this topic and utilised numerical techniques from Podlubny [25, Ch.8] to solve the relaxation-oscillation equation

$$ {}^{RL}_{0}\mathbf{D}^{\alpha}_{t} x(t) + Ax(t) = f(t), \tag{5.7}$$

with $1 < \alpha \leq 2$, $f(t)$ any function, and $x(0) = x'(0) = 0$, which has also been discussed in Refs. [78, 79]. Since this equation also fits within the scope of the fractional-kinetics Langevin equation, we can directly compare the numerical result with the analytical result derived in Example 2.3.11. For this, we have chosen two functions to compare to, namely, $f(t) = \sin(t)\sin(2t)$ and a white noise, and we have compared these two functions in the equation

$$ {}^{RL}_{0}\mathbf{D}^{3/2}_{t} x(t) + 2x(t) = f(t). \tag{5.8}$$

The two solutions of this equation have been plotted in Figure 23. The results for the numerical solution are 1000 points interpolated, while the analytical results are 100 dots. We can see a clear agreement between numerical and analytical values, but what is interesting is that the numerical solution evaluates around 90 times faster in Mathematica than the analytical solution with the white noise, although it is only a factor of 6 for the sine like function. This long evaluation time is due to the integral in the analytical solution. This requires a numerical integral for each point, thus resulting in 100 numerical integrals for a single plot. In comparison, the numerical methods change the problem into a linear algebra problem, which can be evaluated very quickly. The drawback, however, is that the precision becomes more difficult at larger t, as errors might accumulate. In contrast, the numerical evaluation of the analytical solution does not accumulate errors, as each point is evaluated independently, thus only acquiring errors from the numerical integration which allows to check the accumulation errors from the numerical methods. Furthermore, if we were to do some statistical analysis in the white-noise case, this would require many evaluations of the numerical solution, which will still not yield reliable long-time result simply averaging over the iterations, while we can simply apply the statistics directly on the analytical solution and retrieve exact results.

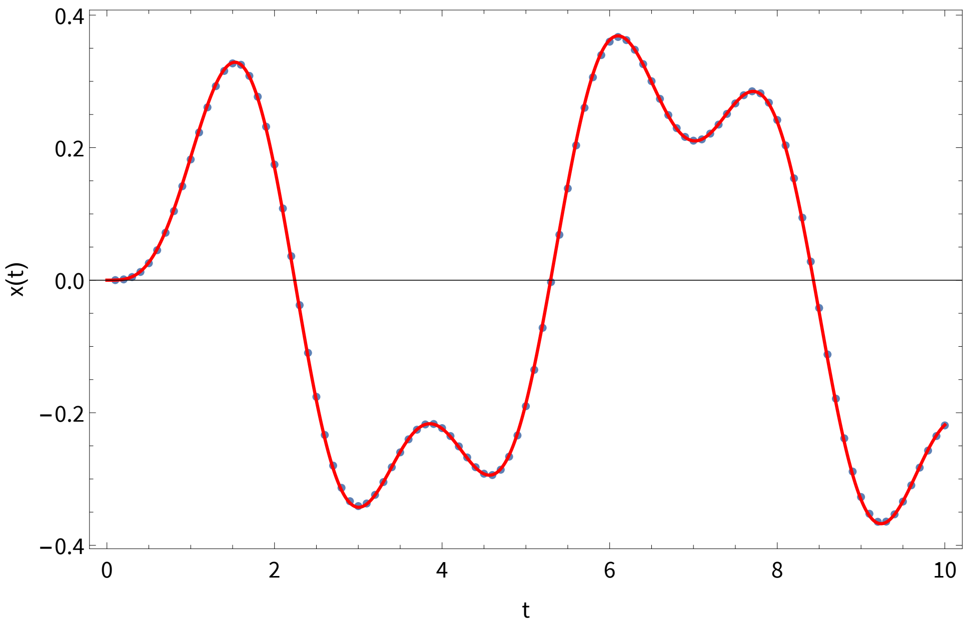

(a) $f(t) = \sin(t)\sin(2t)$

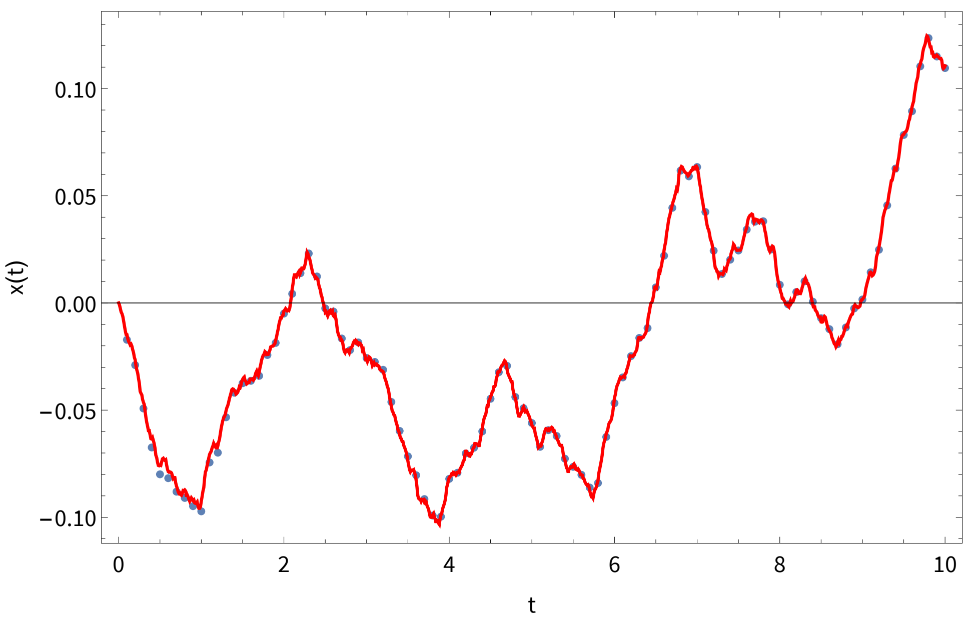

(b) $f(t)$ = randomly generated white noise

Figure 23: A comparison of our analytical solution (100 blue dots), obtained by using Laplace transforms, to the numerical solution (1000 points interpolated red line) for the first 10 units of t, obtained by Timóteo [80] using the numerical methods in Podlubny [25, Ch.8], of Eq. (5.8) with $f(t)$ indicated below the figures.

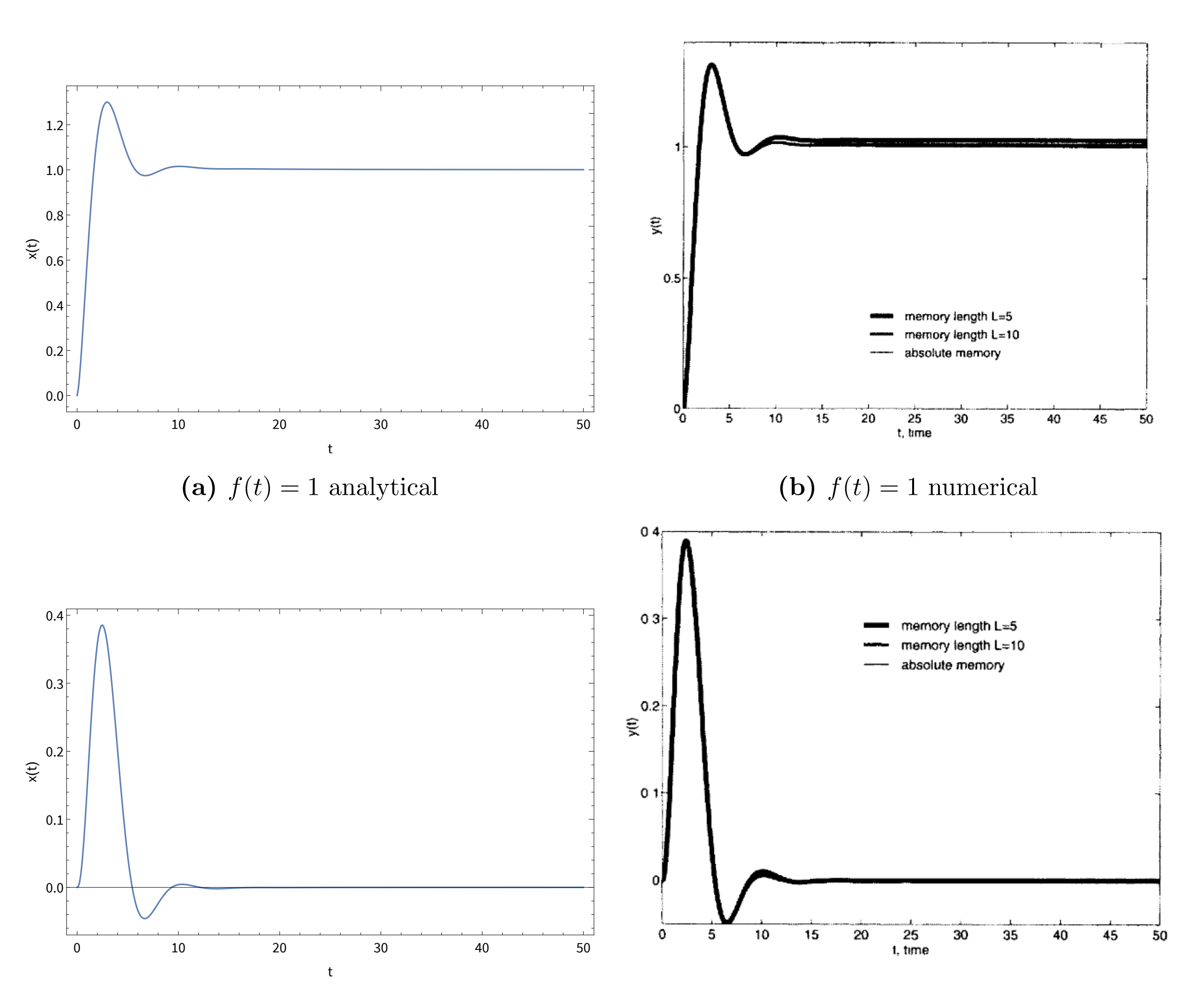

(a) $f(t) = 1$ analytical

(b) $f(t) = 1$ numerical

(c) $f(t) = te^{-t}$ analytical

(d) $f(t) = te^{-t}$ numerical

Figure 24: Analytical (left) and numerical (right) solutions of Eq. (5.9) with $f(t)$ indicated below each plot. The right figures are extracted from Ref [25, Sec. 8.4] where the numerical solutions are presented using a short-memory principle.

We can go further into a numerical comparison with Podlubny [25, Sec. 8.4], where numerical solutions using the "Short-Memory" principle are provided, which means that effectively the long tail of the memory kernel is neglected. In Ref. [25], numerical solutions to the equation

$$ {}^{RL}_{0}\mathbf{D}_t^{3/2} x(t) + x(t) = f(t), \quad \text{with } x(0) = x'(0) = 0 \tag{5.9} $$

are given for four different functions $f(t)$. Ref. [25], however, only compares the short-memory principle with other numerical results and shows how the shorter memories retain a reasonable amount of accuracy while computing much faster. In Figures 24 and 25, we show the analytical solutions to these problems beside the numerical solutions obtained by Ref [25]. In particular, we can see that Figures 24a, 24c, and 25c agree very well with the numerical solutions from Ref [25]. However, Figure 25a is quite different from the numerical solutions presented by Ref. [25], shown in Figure 25b. This might be due to a problem with the numerical methods or even a simple typo in

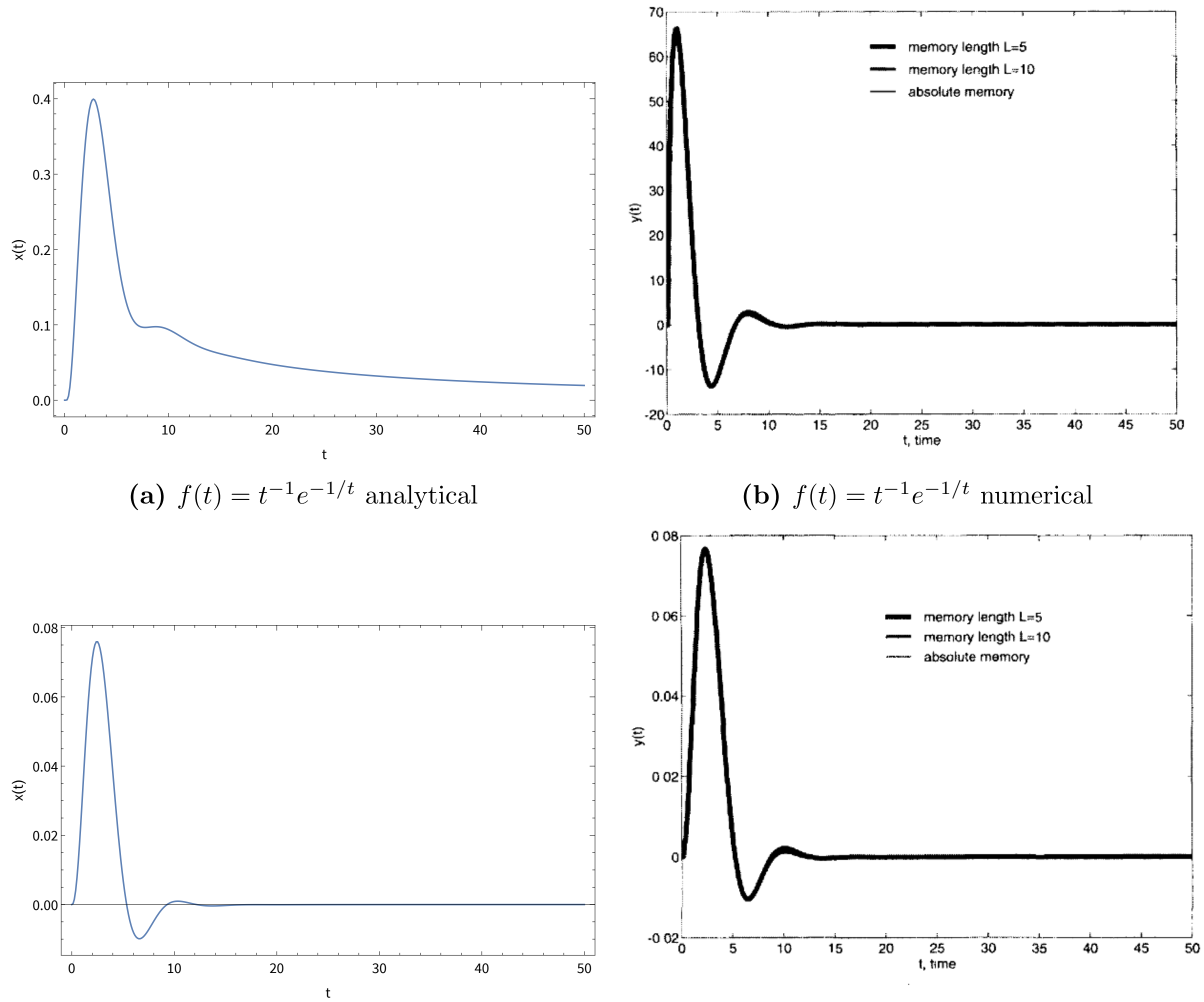

(a) $f(t) = t^{-1}e^{-1/t}$ analytical

(b) $f(t) = t^{-1}e^{-1/t}$ numerical

(c) $f(t) = e^{-t}\sin(0.2t)$ analytical

(d) $f(t) = e^{-t}\sin(0.2t)$ numerical

Figure 25: Analytical (left) and numerical (right) solutions of Eq. (5.9) with $f(t)$ indicated below each plot. The right figures are extracted from Ref [25, Sec. 8.4] where the numerical solutions are presented using a short-memory principle. Note that Fig. **(a)** shows quite different behaviour from Fig. **(b)**.

his formula, since changing the function from $f(t) = t^{-1}e^{-1/t}$ into $f(t) = t^{-1}e^{-t}$ already provides more similar results.

Bagley-Torvik equation

The Bagley-Torvik equation was first introduced in Ref. [81], where they show that the motion of a rigid plate immersed in a Newtonian fluid and connected to a massless spring of stiffness C connected to a fixed point is described by the equation

$$A\ddot{x}(t) + B\,{}_0^C\mathbf{D}_t^{3/2}x(t) + Cx(t) = f(t), \tag{5.10}$$

where $f(t)$ is an external force, A is the mass of the plate, and B is related to the shear stress of the fluid. The fractional derivative arises from the collective behaviour of the fluid caused by the shear stress. Although the analytical solution has been found in terms of an infinite series in Ref. [82] and much numerical work has been done by Diethelm and Ford [83], we can connect some of the limiting cases to the fractional-kinetics Langevin equation. For this, we have three interesting limits. Setting the mass A of the plate to zero, we retrieve a particular case of the relaxation-oscillation equation with $\alpha = 3/2$. If the shear stress of the liquid becomes zero ($B = 0$), then we find the driven harmonic oscillator, while, if we omit the spring connected to the plate ($C = 0$), then we find a particular super-diffusive case of the fractional Langevin equation with $\beta = 3/2$.

6 Conclusion

Fractional derivatives have been fascinating scientists ever since the discovery of calculus. Here, we have provided an introduction into this field, with an extensive description of many relevant properties. We have presented five of the most used definitions: Riemann-Liouville, Liouville, Grünwald-Letnikov, Caputo, and Weyl, and have shown how they can be different or related. In particular, we have discussed several different solution methods for fractional differential equations, involving Fourier transformations, Laplace transformations, and fractional power series, where we have proven that any smooth function admits a fractional power series expansion. We have then compared the solutions of fractional differential equations given a different choice of fractional derivative and found that small differences, such as the derivative order or a sign of a constant, can give very different relations between the various definitions.

Next, we talked about several quantum many-body systems, beginning with classical Brownian motion and its relation to a particle coupled to many harmonic oscillators in the context of the Caldeira-Leggett model, and showed how a two-level systems bath can change some of the results in that model such as the spectral function. We have also given an overview of glasses, both normal and in the Gardner phase, and briefly talked about time crystals, all very useful for putting time glasses into context.

One of the main contributions of this thesis is the theoretical description of time glasses. Recently conjectured, these periodic glassy properties are shown to emerge from the analytical solution of the fractional Langevin equation in the regime $0 < s < 0.1$, where the mean square displacement shows several intermediate plateaus before there is a total saturation. These intermediate plateaus occur periodically, thus characterising the time glass. We have shown how the phenomenological fractional Langevin equation is related to a two-level systems bath coupled to a semi-classical system, thus establishing the relation between a fractional derivative and a sub-Ohmic system.

Finally, we have investigated the fractional-kinetics Langevin equation and have shown several existing physics theories, with both ordinary- and fractional derivatives, which can all be described as limiting cases of this fractional differential equation, for which we derived the analytical solution. Here, we also compare our analytical solution to some results obtained by numerical methods.

As an outlook, it would be interesting to extend these results to other types of equations with friction terms, as e.g. the Landau-Lifshitz-Gilbert equation describing magnetism, or to include non-linear potentials in the fractional Langevin equation

References

[1] Dorothy V. Schrader. 'The Newton-Leibniz controversy concerning the discovery of the calculus'. In: *The Mathematics Teacher* 55.5 (1962), pp. 385–396.

[2] Rudolf Hilfer et al. 'Threefold introduction to fractional derivatives'. In: *Anomalous transport: Foundations and applications* (2008), pp. 17–73.

[3] Leonhard Euler. 'De progressionibus transcendentibus seu quarum termini generales algebraice dari nequeunt'. In: *Commentarii academiae scientiarum Petropolitanae* (1738), pp. 36–57.

[4] Jean B. J. baron Fourier. *Théorie analytique de la chaleur*. F. Didot, 1822.

[5] Joseph Liouville. *Mémoire sur quelques questions de géométrie et de mécanique, et sur un nouveau genre de calcul pour résoudre ces questions*. 1832.

[6] Igor Podlubny, Richard L. Magin and Iryna Trymorush. 'Niels Henrik Abel and the birth of fractional calculus'. In: *Fractional Calculus and Applied Analysis* 20.5 (2017), pp. 1068–1075.

[7] Niels H. Abel. 'Oplösning af et par opgaver ved hjelp af bestemte integraler'. In: *Magazin for naturvidenskaberne* 2.55 (1823), p. 2.

[8] Bernhard Riemann. 'Versuch einer allgemeinen auffassung der integration und differentiation,(Januar 1847)'. In: *Bernhard Riemann's gesammelte mathematische Werke und wissenschaftlicher Nachlass* (1953), p. 353.

[9] Anton K. Grunwald. 'Uber" begrente" Derivationen und deren Anwedung'. In: *Zangew Math und Phys* 12 (1867), pp. 441–480.

[10] Michele Caputo. *Elasticita e dissipazione*. Zanichelli, 1969.

[11] HongGuang Sun et al. 'A new collection of real world applications of fractional calculus in science and engineering'. In: *Communications in Nonlinear Science and Numerical Simulation* 64 (2018), pp. 213–231.

[12] Arkadii Chikrii and Ivan Matychyn. 'Riemann–Liouville, Caputo, and Sequential Fractional Derivatives in Differential Games'. In: *Advances in Dynamic Games: Theory, Applications, and Numerical Methods for Differential and Stochastic Games*. Ed. by Michèle Breton and Krzysztof Szajowski. Boston: Birkhäuser Boston, 2011, pp. 61–81.

[13] Rudolf Hilfer et al. *Applications of fractional calculus in physics*. Vol. 35. 12. World scientific Singapore, 2000.

[14] Trifce Sandev and Živorad Tomovski. *Fractional Equations and Models: Theory and Applications*. Vol. 61. Springer Nature, 2019.

[15] Andrea Ninarello, Ludovic Berthier and Daniele Coslovich. 'Models and algorithms for the next generation of glass transition studies'. In: *Physical Review X* 7.2 (2017), p. 021039.

[16] Samuel S. Schoenholz et al. 'A structural approach to relaxation in glassy liquids'. In: *Nature Physics* 12.5 (2016), pp. 469–471.

[17] Giulio Biroli and Jean-Philippe Bouchaud. 'The random first-order transition theory of glasses: A critical assessment'. In: *Ch.2 Structural Glasses and Supercooled Liquids: Theory, Experiment, and Applications* (2012), pp. 31–113.

[18] Elisabeth Gardner. 'Spin glasses with p-spin interactions'. In: *Nuclear Physics B* 257 (1985), pp. 747–765.

[19] Patrick Charbonneau et al. 'Glass and jamming transitions: From exact results to finite-dimensional descriptions'. In: *Annual Review of Condensed Matter Physics* 8 (2017), pp. 265–288.

[20] Patrick Charbonneau et al. 'Fractal free energy landscapes in structural glasses'. In: *Nature communications* 5.1 (2014), pp. 1–6.

[21] Frank Wilczek. 'Quantum time crystals'. In: *Physical Review Letters* 109.16 (2012), p. 160401.

[22] Jiehang Zhang et al. 'Observation of a discrete time crystal'. In: *Nature* 543.7644 (2017), pp. 217–220.

[23] Frank Wilczek. 'Crystals in time'. In: *Scientific American* 321.5 (2019), pp. 28–35.

[24] José Tenreiro Machado. 'A Review of Definitions for Fractional Derivatives and Integral'. In: *Mathematical Problems in Engineering* (June 2014), pp. 1–6.

[25] Igor Podlubny. *Fractional differential equations: an introduction to fractional derivatives, fractional differential equations, to methods of their solution and some of their applications.* Vol. 198. Elsevier, 1998.

[26] Stefan G. Samko, Anatoly A. Kilbas, Oleg I Marichev et al. *Fractional integrals and derivatives.* Vol. 1. Gordon and Breach Science Publishers, Yverdon Yverdon-les-Bains, Switzerland, 1993.

[27] Kai Diethelm. *The analysis of fractional differential equations: An application-oriented exposition using differential operators of Caputo type.* Springer Science & Business Media, 2010.

[28] Anatolii A. Kilbas, Hari M. Srivastava and Juan J. Trujillo. *Theory and applications of fractional differential equations.* Vol. 204. Elsevier Science Limited, 2006.

[29] Keith Oldham and Jerome Spanier. *The fractional calculus theory and applications of differentiation and integration to arbitrary order.* Vol. 111. Elsevier, 1974.

[30] Manuel D. Ortigueira. *Fractional calculus for scientists and engineers.* Vol. 84. Springer Science & Business Media, 2011.

[31] Eric W. Weisstein. 'Leibniz integral rule'. In: *https://mathworld.wolfram.com/* (2003).

[32] Tomas Kisela. 'Fractional Differential Equations and Their Applications'. MA thesis. BRNO University of Technology, Aug. 2008.

[33] Christopher L. MacDonald et al. 'Efficient computation of the Grünwald–Letnikov fractional diffusion derivative using adaptive time step memory'. In: *Journal of Computational Physics* 297 (2015), pp. 221–236.

[34] Marc Weilbeer. *Efficient numerical methods for fractional differential equations and their analytical background.* Papierflieger, 2005.

[35] Roberto Barrio. 'Performance of the Taylor series method for ODEs/DAEs'. In: *Applied Mathematics and Computation* 163.2 (2005), pp. 525–545.

[36] James R. Scott. 'Solving ODE initial value problems with implicit Taylor series methods'. In: (2000).

[37] Ahmad El-Ajou et al. 'New results on fractional power series: theories and applications'. In: *Entropy* 15.12 (2013), pp. 5305–5323.

[38] Amir O Caldeira. *An introduction to macroscopic quantum phenomena and quantum dissipation.* Cambridge University Press, 2014.

[39] Amir O. Caldeira, Antonio H. Castro Neto and T. Oliveira de Carvalho. 'Dissipative quantum systems modeled by a two-level-reservoir coupling'. In: *Physical Review B* 48.18 (1993), p. 13974.

[40] Amir O Caldeira and Anthony J. Leggett. 'Path integral approach to quantum Brownian motion'. In: *Physica A: Statistical mechanics and its Applications* 121.3 (1983), pp. 587–616.

[41] Amir O Caldeira and Anthony J. Leggett. 'Quantum Tunneling in a Dissipative System'. In: *Annals of physics* 149 (1983), pp. 374–456.

[42] AO Caldeira and Anthony J. Leggett. 'Influence of damping on quantum interference: An exactly soluble model'. In: *Physical Review A* 31.2 (1985), p. 1059.

[43] Ulrich Weiss. *Quantum dissipative systems*. Vol. 13. World scientific, 2012.

[44] Armando Villares Ferrer and Cristiane Morais Smith. 'Dynamical localization of a particle coupled to a two-level system thermal reservoir'. In: *Physical Review B* 76.21 (2007), p. 214303.

[45] Alfred Shapere and Frank Wilczek. 'Classical time crystals'. In: *Physical Review Letters* 109.16 (2012), p. 160402.

[46] Jana Tóthová et al. 'Langevin theory of anomalous Brownian motion made simple'. In: *European journal of physics* 32.3 (2011), p. 645.

[47] Stephen J Blundell and Katherine M Blundell. *Concepts in thermal physics*. Oxford University Press, 2009.

[48] Armando Villares Ferrer, Amir O. Caldeira and C Morais Smith. 'Optical conductivity of charge carriers interacting with a two-level systems reservoir'. In: *Physical Review B* 74.18 (2006), p. 184304.

[49] Ralf Bulla, Ning-Hua Tong and Matthias Vojta. 'Numerical renormalization group for bosonic systems and application to the sub-ohmic spin-boson model'. In: *Physical Review Letters* 91.17 (2003), p. 170601.

[50] Liesbeth M. C. Janssen. 'Mode-coupling theory of the glass transition: A primer'. In: *Frontiers in Physics* 6 (2018), p. 97.

[51] Pablo G. Debenedetti and Frank H. Stillinger. 'Supercooled liquids and the glass transition'. In: *Nature* 410.6825 (2001), pp. 259–267.

[52] Leticia F. Cugliandolo and Jorge Kurchan. 'On the out-of-equilibrium relaxation of the Sherrington-Kirkpatrick model'. In: *Journal of Physics A: Mathematical and General* 27.17 (1994), p. 5749.

[53] Liesbeth M. C. Janssen and David R. Reichman. 'Microscopic dynamics of supercooled liquids from first principles'. In: *Physical Review Letters* 115.20 (2015), p. 205701.

[54] Giulio B. J. P. Biroli et al. 'Thermodynamic signature of growing amorphous order in glass-forming liquids'. In: *Nature Physics* 4.10 (2008), pp. 771–775.

[55] Ludovic Berthier et al. 'Gardner physics in amorphous solids and beyond'. In: *The Journal of chemical physics* 151.1 (2019), p. 010901.

[56] Qinyi Liao and Ludovic Berthier. 'Hierarchical landscape of hard disk glasses'. In: *PRX* 9.1 (2019), p. 011049.

[57] James S Langer. 'Theories of glass formation and the glass transition'. In: *Reports on Progress in Physics* 77.4 (2014), p. 042501.

[58] Zamaan Raza, Björn Alling and Igor A. Abrikosov. 'Computer simulations of glasses: the potential energy landscape'. In: *Journal of Physics: Condensed Matter* 27.29 (2015), p. 293201.

[59] Antoine Seguin and Olivier Dauchot. 'Experimental evidence of the Gardner phase in a granular glass'. In: *Physical Review Letters* 117.22 (2016), p. 228001.

[60] Andrew Hammond and Eric Corwin. 'Direct observation of the Gardner/marginal glass transition within a colloidal glass'. In: *American Physical Society* (2019), K58–007.

[61] Haruki Watanabe and Masaki Oshikawa. 'Absence of Quantum Time Crystals'. In: *Physical Review Letters* 114 (25 June 2015), p. 251603.

[62] Patrick Bruno. 'Impossibility of spontaneously rotating time crystals: a no-go theorem'. In: *Physical Review Letters* 111.7 (2013), p. 070402.

[63] Jared Rovny, Robert L. Blum and Sean E. Barrett. 'Observation of discrete-time-crystal signatures in an ordered dipolar many-body system'. In: *Physical Review Letters* 120.18 (2018), p. 180603.

[64] Bikun Li et al. 'Discrete time crystal in the gradient-field Heisenberg model'. In: *Physical Review B* 101.11 (2020), p. 115303.

[65] Norman Y Yao et al. 'Classical discrete time crystals'. In: *Nature Physics* (2020), pp. 1–10.

[66] Robin C. Verstraten, Rodrigo F. Ozela and Cristiane Morais Smith. *Time Glass: A Fractional Calculus Approach*. 2020. arXiv: `2006.08786 [cond-mat.stat-mech]`.

[67] Guido Boffetta and Igor M. Sokolov. 'Relative dispersion in fully developed turbulence: the Richardson's law and intermittency corrections'. In: *Physical Review Letters* 88.9 (2002), p. 094501.

[68] JinRong Wang, Yong Zhou and D. O'Regan. 'A note on asymptotic behaviour of Mittag–Leffler functions'. In: *Integral Transforms and Special Functions* 29.2 (2018), pp. 81–94.

[69] Rudolf Gorenflo et al. *Mittag-Leffler functions, related topics and applications*. Vol. 2. Springer, 2014.

[70] Stanislav Burov and Eli Barkai. 'Critical exponent of the fractional Langevin equation'. In: *Physical Review Letters* 100.7 (2008), p. 070601.

[71] Kirk T. McDonald. *On the History of the Radiation Reaction*. 2017.

[72] Eric Lutz. 'Fractional langevin equation'. In: *Fractional Dynamics: Recent Advances*. World Scientific, 2012, pp. 285–305.

[73] Ludvig Lizana et al. 'Foundation of fractional Langevin equation: harmonization of a many-body problem'. In: *Physical Review E* 81.5 (2010), p. 051118.

[74] Stanislav Burov and Eli Barkai. 'Fractional Langevin equation: Overdamped, underdamped, and critical behaviors'. In: *Physical Review E* 78.3 (2008), p. 031112.

[75] Ralf Metzler and Joseph Klafter. 'The random walk's guide to anomalous diffusion: a fractional dynamics approach'. In: *Physics Reports* 339.1 (2000), pp. 1–77.

[76] Thomas Vojta, Sarah Skinner and Ralf Metzler. 'Probability density of the fractional Langevin equation with reflecting walls'. In: *Physical Review E* 100.4 (2019), p. 042142.

[77] Samuel C. Kou and X. Sunney Xie. 'Generalized Langevin equation with fractional Gaussian noise: subdiffusion within a single protein molecule'. In: *Physical Review Letters* 93.18 (2004), p. 180603.

[78] Alain Oustaloup. 'From fractality to non integer derivation : A fundamental idea for a new process control strategy'. In: Nov. 2006, pp. 53–64.

[79] Francesco Mainardi. ‘Fractional relaxation-oscillation and fractional diffusion-wave phenomena’. In: *Chaos, Solitons & Fractals* 7.9 (1996), pp. 1461–1477.

[80] Varese S. Timóteo. [Private communication].

[81] Peter J. Torvik and Ronald L. Bagley. ‘On the appearance of the fractional derivative in the behavior of real materials’. In: *Journal of Applied Mechanics* 51.2 (1984).

[82] S. Saha Ray and R. K. Bera. ‘Analytical solution of the Bagley Torvik equation by Adomian decomposition method’. In: *Applied Mathematics and Computation* 168.1 (2005), pp. 398–410.

[83] Kai Diethelm and J. Ford. ‘Numerical solution of the Bagley-Torvik equation’. In: *BIT Numerical Mathematics* 42.3 (2002), pp. 490–507.